

~~CONFIDENTIAL~~

88

Copy
RM E51D30

#68 17986

NACA

note-1

RESEARCH MEMORANDUM

ANALYSIS OF THE LIQUID-METAL TURBOJET CYCLE FOR
PROPULSION OF NUCLEAR POWERED AIRCRAFT

By William W. Wachtl and Frank E. Rom

Lewis Flight Propulsion Laboratory
Cleveland, Ohio

CLASSIFICATION CHANGE
IFIED EFFECTIVE JUNE 12, 1983
AUTHORITY NASA 101-4 BY J. J. CARROLL

~~CONFIDENTIAL~~

NATIONAL ADVISORY COMMITTEE
FOR AERONAUTICS

WASHINGTON
November 19, 1951
Reclassified October 16, 1961

~~CONFIDENTIAL~~

NACA RM E51D30

XEROX
MICROFILM

GIN
100

DECLASSIFIED

NACA RM E51D30

NATIONAL ADVISORY COMMITTEE FOR AERONAUTICS

RESEARCH MEMORANDUM

ANALYSIS OF THE LIQUID-METAL TURBOJET CYCLE FOR
PROPULSION OF NUCLEAR POWERED AIRCRAFT

By William W. Wachtl and Frank E. Rom

SUMMARY

17986

An analysis of the nuclear powered liquid-metal turbojet cycle is presented for a wide range of engine operating conditions at flight Mach numbers of 0.9 and 1.5, and at altitudes of 30,000 and 50,000 feet.

The method of analysis and working charts are presented to facilitate investigations beyond the scope of this report.

The thrust per engine plus heat exchanger weight is optimized at the four flight conditions for heat exchanger inlet Mach number, compressor pressure ratio, and turbine-inlet temperature for a range of liquid-metal-to-air heat exchanger effective wall temperatures.

Airplane gross weight and reactor heat release is presented for typical values of airplane lift-drag ratio, structure to gross weight ratio, and sum of reactor, shield, payload, and auxiliary weights. The effect of varying these assumptions and of including nacelle drag is shown along with the effect of flight conditions.

INTRODUCTION

Analyses are being made at the NACA Lewis laboratory to determine the characteristics of various aircraft propulsion systems utilizing nuclear energy. A study of the direct-air turbojet cycle was made in reference 1 and additional results of this study are presented in references 2 and 3. A preliminary comparison of the direct air, helium, and liquid-metal turbojet cycles is made in reference 3.

The present report gives an analysis of the design point performance of nuclear powered liquid-metal turbojet engines. The variables considered are turbine-inlet temperature, compressor pressure ratio, liquid-metal-to-air heat exchanger wall temperature, heat exchanger air inlet Mach number, altitude, and flight speed. The compressor pressure ratio, heat exchanger inlet Mach number, and turbine-inlet temperature were optimized for maximum engine net thrust per engine plus heat exchanger weight at several values of heat exchanger effective wall temperature. It is shown that for fixed values of airplane lift-drag ratio, and structure to gross weight ratio, the thrust per engine plus heat exchanger weight is the most important parameter in determining gross weight. Inasmuch as this parameter is so important, and because of the uncertainty in the lift-drag ratio attainable at supersonic speeds, in shield and auxiliary weights, and in allowable reactor heat release rates, engine performance is emphasized in this report. However, curves are presented which enable rapid determination of airplane gross weight for any set of shield and auxiliary weights, payload, structure to gross weight ratio, and airplane lift-drag assumptions. In addition, curves of heat input per pound of air and net thrust per pound of air per second are presented to enable the determination of reactor heat release necessary to operate the required turbojet engines.

Airplane gross weight and reactor heat release are calculated for several flight conditions for various engine operating conditions. Typical values of shield, auxiliary equipment, and payload weights, and aerodynamic assumptions were selected to facilitate these calculations. The effect of varying the assumptions necessary to calculate gross weight and reactor heat release from engine data is presented. In addition, the effect of varying flight conditions upon gross weight and reactor heat release is also indicated.

SYMBOLS

The following symbols are used in this report:

- A area, ft^2
- c_p specific heat at constant pressure, $\text{Btu/lb } ^\circ\text{R}$
- C_D drag coefficient
- C_v nozzle velocity coefficient
- d hydraulic diameter of tubes, ft
- D drag, lb

DECLASSIFIED

NACA RM E51D30

3

f free flow ratio, flow area divided by frontal area

F thrust, lb

g acceleration due to gravity, ft/sec²

h enthalpy, Btu/lb

Δh air enthalpy change, Btu/lb

J 778 ft-lb/Btu

k thermal conductivity, Btu/sec ft² °R/ft

l tube length, ft

L lift, lb

M Mach number

p static pressure, lb/ft²

P total pressure, lb/ft²

q dynamic pressure, $\frac{\rho_a V_a^2}{2g}$, lb/ft²

Q reactor heat release rate, Btu/sec

T total temperature, °R

ΔT total temperature change, °R

U over-all heat transfer coefficient, Btu/sec ft² °R

v reactor volume, ft³

V velocity, ft/sec

w weight flow, lb/sec

W weight, lb

δ ratio of total pressure to NACA standard sea level static pressure,
 $\frac{P}{2116}$

η efficiency

0317122A.030

4

NACA RM E51D30

γ ratio of specific heats
 μ viscosity, lb/ft-sec
 ρ density, lb/ft³
 θ ratio of total temperature to NACA standard sea level static temperature, $\frac{T}{519}$

Subscripts:

a air flow
c compressor
e engine
f frontal
g gross
j jet
K shield + reactor + payload + auxiliary
l liquid metal
n net
N nacelle
r reactor
m reactor maximum wall
s structure
t turbine
T engine plus heat exchanger
w exchanger effective wall
x exchanger

- y reactor-wall-to-liquid metal
- ∞ small stage
- 0 free stream
- 1 compressor inlet
- 2 compressor outlet
- 2' inlet to heat exchanger (in tubes)
- 3 turbine inlet
- 4 turbine outlet

DESCRIPTION OF THE CYCLE

A schematic diagram of the liquid-metal turbojet cycle is shown in figure 1. It is a binary system incorporating a closed liquid cycle and an open air cycle. A nuclear reactor is used as the heat source, and a heat exchanger replaces the standard engine combustion chamber.

The liquid-metal coolant is pumped through the reactor where it is heated by contact with walls of the reactor flow passages. From the reactor the liquid metal flows through the heat exchanger where it gives up energy to the air; it is then ducted back to the reactor thus completing its cycle.

Air enters the diffuser of the turbojet engine, is compressed by the compressor, and then passes through the heat exchanger taking heat from the liquid metal. This hot compressed air expands through the turbine which extracts the required energy to run the compressor. The air then expands through the exhaust nozzle to provide the propulsive thrust.

ASSUMPTIONS

Engine component efficiencies. - In the present analysis the efficiencies assumed for the engine components are, insofar as possible representative of the best current practice. The values used are as follows:

Compressor small-stage efficiency,	0.88
Turbine adiabatic efficiency,	.90
Exhaust nozzle velocity coefficient (full expansion),	.97

The inlet diffuser characteristics are shown in figure 2 where the ratio of actual to theoretical total pressure is plotted against flight Mach number. The subsonic portion of the curve assumes a 0.08 q_0 loss in dynamic pressure, and the supersonic portion was obtained from reference 4.

Engine weight. - The engine weight per pound of corrected air flow is shown in figure 3 as a function of compressor pressure ratio. The curve was obtained from an NACA weight analysis of turbojet engines and includes all engine components except the combustion chambers. The air flow per unit compressor frontal area is assumed to be 25 pounds per second per square foot corrected to static sea level conditions and is assumed to be independent of engine size for this analysis.

Heat exchanger. - The liquid-metal-to-air heat exchanger is assumed to be of the tubular counterflow type with air flowing through the tubes, and liquid metal flowing in the spaces between the tubes. The weight is computed assuming that the tubes are made of stainless steel having an internal diameter of 0.25 inch and a wall thickness of 0.01 inch, and that the space around the tubes is filled with lithium. The weight of the shell, headers and baffles is included. The exchanger free flow factor A_a/A_f is 0.65. The exchanger is assumed to have a constant effective wall temperature. The exchanger l/d expressed in the parameter $\left[\left(\frac{A_a \mu_w}{w_a d} \right)^{0.2} \left(\frac{1}{d} \right) \right]_x$ (from reference 5) is shown in figure 4 as a

function of air inlet temperature, air outlet temperature, and exchanger effective wall temperature. The heat exchanger air pressure drop expressed as the ratio of the outlet total pressure to air inlet total pressure is shown in figure 5. The pressure ratio is plotted as a function of air inlet temperature, air outlet temperature, and exchanger effective wall temperature for air inlet Mach numbers of 0.12, 0.16, and 0.20 which cover the range of values investigated.

The assumption of an effective wall temperature greatly simplifies heat transfer calculations with no loss in accuracy. Only a negligible error in heat exchanger pressure ratio is introduced by this assumption.

Reactor maximum wall temperature. - The reactor maximum wall temperature is computed by making the following assumptions: (1) the heat exchanger effective wall temperature is equal to the average of the inlet and outlet liquid-metal temperature; (2) that the difference

between the reactor wall temperature and liquid-metal temperatures is constant; and (3) that the liquid-metal temperature rise is fixed for each flight condition so that the liquid-metal velocity is 15 feet per second at optimum engine conditions.

Reactor, shield, and auxiliary weights. - A fixed value of 190,000 pounds is assumed for W_K , the sum of the reactor, shield assembly, payload, and auxiliary weights (pumps, piping, chemical fuel, etc.). This weight was arbitrarily assumed in order to calculate typical airplane gross weights from the engine data. Assuming a fixed value of W_K allows a wide latitude of weight distributions among the components of W_K . Inasmuch as gross weight is a direct function of W_K , the gross weight for any other desired value of W_K can easily be found. The effect of selecting different fixed values of W_K is shown later in the report.

For any given reactor size, reference 6 indicates a negligible variation of shield weight with reactor heat release Q . Since this is true and since the payload and auxiliary weight are relatively fixed, no variation of W_K with Q is considered.

Airplane assumptions. - The structure to gross weight ratio W_s/W_g , of the airplane in general is assumed to be 0.35 for the gross weight computations. The airplane design L/D , exclusive of nacelles, is assumed a function of Mach number as follows:

Mach number	L/D
0.9	18
1.5	9
2.0	5.5

Variation of structure to gross weight ratio W_s/W_g , and L/D from the above values is considered later in the report.

Nacelle drag D_N , is generally considered to be zero, however, in cases where D_N is included, the effect is shown for the following range of drag coefficients:

Subsonic $C_{D,N}$,	0 to 0.08
Supersonic $C_{D,N}$,	0 to 0.4

The air flow per unit nacelle frontal area, corrected to static sea level conditions is assumed to be 15 pounds per second per square foot

compared to 25 pounds per second per square foot of compressor frontal area. This assumption accounts for structure space.

METHODS

The turbojet cycle as presented in this analysis is optimized for maximum net thrust per engine plus exchanger weight. It is shown in the following discussion that this parameter gives the minimum airplane gross weight for fixed values of airplane L/D , structure to gross weight ratio W_s/W_g , and the sum of reactor, shield assembly, payload and auxiliary weights W_K .

Weight Balance

The gross weight of an airplane is equal to the sum of all the component weights.

$$W_g = W_K + W_s + W_e + W_x \quad (1)$$

These weights can be separated into two groups: (1) weights relatively independent of gross weight; and (2) weights dependent upon gross weight. The first group consists of the sum of reactor, shield assembly, payload, and auxiliary weight W_K , where the auxiliary weight includes such items as the control equipment, pumps, piping, and auxiliary fuel required for thrust augmentation. Group two consists of the aircraft structure weight, engine weight, and heat exchanger weight $W_s + W_e + W_x$.

The structure weight is given by

$$W_s = \left(\frac{W_s}{W_g} \right) W_g \quad (2)$$

The engine weight plus heat exchanger weight is

$$W_e + W_x = W_T = \frac{W_g}{\frac{F_n}{W_T} \times \frac{L}{D}} \quad (3)$$

where

$$F_n = F_j - \frac{w_a V_0}{g} - D_N \quad (4)$$

Combining equations (1), (2), and (3)

$$W_g = \frac{W_K}{1 - \frac{W_s}{W_g} - \frac{1}{\left(\frac{F_n}{W_T}\right) \times \frac{L}{D}}} \quad (5)$$

Inspection of equation (5) shows that the gross weight is a minimum when the net thrust per engine plus exchanger is a maximum for fixed values of W_K , W_s/W_g , and L/D , consequently a study of engine performance is sufficient for evaluating a given cycle in a nuclear powered airplane. The analysis presented in this report optimizes F_n/W_T and is therefore not restricted by particular weight and airplane assumptions.

Cycle Analysis

The performance of the turbojet cycle with a heat exchanger in lieu of the conventional burners is calculated for a range of flight and engine variables in order to obtain optimum engine performance. The flight conditions investigated are flight Mach numbers of 0.9 and 1.5 at altitudes of 30,000 and 50,000 feet. The compressor pressure ratio is varied from 2 to 15; the turbine-inlet temperature from 1200° to 2300° R; the heat exchanger effective wall temperature from 1400° to 2600° R; and the heat exchanger inlet Mach numbers from 0.12 to 0.20.

The stations in the cycle are numbered according to the diagram in figure 1.

Calculation of net thrust per pound of air per second, F_n/w_a . - The compressor inlet temperature T_1 , and pressure P_1 , were determined at the assumed flight conditions and corresponding diffuser pressure ratio P_1/P_0 (fig. 2). The enthalpies at each station and the temperature rise through the compressor corresponding to the selected pressure ratio, were determined from the thermodynamic property tables and methods presented in reference 7. The compressor work per pound of air is then

$$\Delta h_c = h_2 - h_1, \text{ Btu/lb air}$$

The compressor outlet temperature T_2 , and pressure P_2 , are identical to the heat exchanger inlet temperature T_2' , and pressure P_2' . Knowing the heat exchanger inlet temperature, and with assumed values of inlet Mach number M_2' , heat exchanger effective wall temperature T_w ,

and turbine-inlet temperature T_3 , the heat exchanger pressure ratio P_3/P_2 , is found from figure 5. The turbine work is equal to the compressor work, so the turbine exit enthalpy is

$$h_4 = h_3 - \Delta h_c, \text{ Btu/lb air}$$

The turbine outlet temperature and the turbine pressure ratio are found by the charts and methods of reference 7. The tail-pipe pressure ratio is then

$$\frac{P_4}{P_0} = \frac{P_4}{P_3} \times \frac{P_3}{P_2} \times \frac{P_2}{P_1} \times \frac{P_1}{P_0} \times \frac{P_0}{P_0}$$

The jet thrust per pound of air F_j/w_a , is a function of tail-pipe pressure ratio and the square root of the tail-pipe temperature, and is obtained from the following equation for a complete expansion process.

$$\frac{F_j}{w_a} = C_v \sqrt{\frac{2Jc_p T_4}{g} \left[1 - \left(\frac{P_0}{P_4} \right) \right]^{\frac{\gamma-1}{\gamma}}}$$

The net thrust per pound of air F_n/w_a , is obtained by dividing equation (4) by w_a

$$\frac{F_n}{w_a} = \frac{F_j}{w_a} - \frac{V_0}{g} - \frac{D_N}{w_a} \quad (6)$$

Where the nacelle drag per pound of air per second D_N/w_a is defined by

$$\frac{D_N}{w_a} = C_{D,N} q \left(\frac{A_f \delta_0}{w_a \sqrt{\theta_0}} \right)_N \frac{\sqrt{\theta_0}}{\delta_0} \quad (7)$$

where $\left(\frac{w_a \sqrt{\theta_0}}{A_f \delta_0} \right)_N$ is the corrected air flow per unit nacelle

frontal area (15 lb/sec-sq ft). The effect of nacelle drag is not included in the general engine analysis, but is introduced later in the discussion to show the effects on airplane performance.

The preceding methods were used to calculate a set of generalized performance charts which were used in the actual analysis. These charts have been included in appendix A.

DECLASSIFIED

Engine plus heat exchanger weight. - The weight of the turbojet engine less combustors per pound of air per second W_e/w_a , is found from figure 3 at the desired compressor pressure ratio. The heat exchanger weight per pound of air per second is a function of the exchanger air flow per unit area $(w_a/A_a)_x$ and the exchanger $1/d$ as given by

$$\frac{W_x}{w_a} = 1.9 \left(\frac{A_a}{w_a} \times \frac{1}{d} \right)_x \quad (8)$$

where the constant 1.9 is evaluated from the assumption of stainless steel tubes, with lithium filling the spaces between the tubes.

The exchanger air flow per unit flow area is found from the exchanger inlet conditions P_2' , T_2' , and M_2' . The heat exchanger $1/d$ is found from the parameter, $\left[\left(\frac{A_a}{w_a} \frac{\mu_w}{d} \right)^{0.2} \left(\frac{1}{d} \right) \right]_x$ shown in figure 4. The hydraulic diameter is assigned and the viscosity μ_w , is evaluated at the effective wall temperature T_w . The engine plus exchanger weight per pound of air per second W_T/w_a , is then the sum of W_e/w_a and W_x/w_a .

Thrust per pound of engine plus exchanger. - The thrust per pound of engine plus exchanger is calculated from the net thrust and engine weight per pound of air per second.

$$\frac{F_n}{W_T} = \frac{F_n/w_a}{W_T/w_a} \quad (9)$$

The F_n/W_T is plotted as a function of turbine-inlet temperature, heat exchanger inlet Mach number and compressor pressure ratio for all the flight conditions considered.

Heat input. - The heat input to the turbojet is found by subtracting the enthalpy at the compressor outlet h_2 , from the enthalpy at the turbine inlet h_3 .

$$\Delta h_x = h_3 - h_2, \text{ Btu/lb air}$$

Airplane gross weight. - The method of determining engine performance in terms of F_n/w_a , F_n/W_T , and Δh_x has been given. In order to

DECLASSIFIED

translate this engine data to airplane performance, certain assumptions regarding airplane lift drag L/D , structure to gross weight ratio W_s/W_g , and the sum of shield, reactor, payload, and auxiliary weight W_K , must be made. If values are assigned to these quantities, equation (5) can be used to calculate airplane gross weight. Figure 6 has been prepared from equation (5) so that W_g can be found more conveniently. W_g/W_K is plotted as a function of thrust per engine plus exchanger weight F_n/W_T , for a range of L/D and for W_s/W_g equal to 0.35. The airplane gross weight is found by multiplying the ordinate evaluated at the design F_n/W_T and L/D by the assigned value of W_K .

Engine air flow. - The air flow required for a given airplane is found from the gross weight W_g , L/D , and net thrust per pound of air per second F_n/w_a , by the relation

$$w_a = \frac{W_g}{\frac{L}{D} \times \frac{F_n}{w_a}} \quad (10)$$

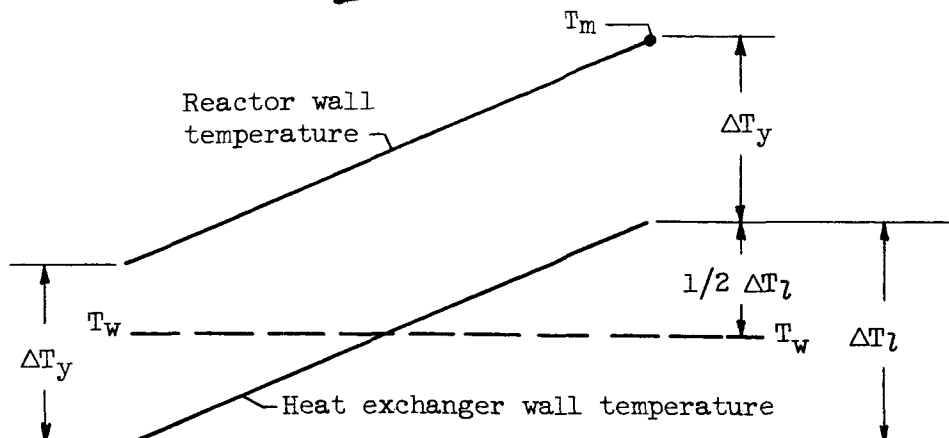
Reactor Calculations

Heat release. - The heat release rate required from the reactor, neglecting losses, is obtained by multiplying the enthalpy rise per pound of air through the heat exchanger by the engine air flow

$$Q = \Delta h_x w_a, \text{ Btu/sec} \quad (11)$$

Inasmuch as the heat losses in piping and heat required for running the pumps and auxiliaries are chiefly a function of the individual installation, no attempt was made to include these requirements in the heat release curves of this analysis. In order to account for these quantities, the heat release required of the reactor must be increased accordingly.

Reactor maximum wall temperature. - The reactor maximum wall temperature is determined by the liquid-metal temperature rise through the reactor ΔT_l , the average liquid-metal temperature (assumed to be T_w), and the reactor-wall-to-liquid-metal temperature difference ΔT_y .



In determining reactor maximum wall temperature T_m , the heat exchanger effective wall temperature T_w , is assumed to be the average liquid-metal temperature. A constant temperature difference based on the assumptions of constant heat generation along the reactor length is assumed between the reactor wall and liquid metal. The equation for calculating the maximum reactor wall temperature is then

$$T_m = T_w + 1/2 \Delta T_l + \Delta T_y \quad (12)$$

where

$$\Delta T_l = \frac{Q}{(\rho V c_p)_l (f A_f)_r}$$

and

$$\Delta T_y = \frac{Q}{4 U_l \left(\frac{1}{d} f A_f \right)_r}$$

where from reference 8,

$$U_l = \frac{k_l}{d_r} \left[7 + 0.025 \left(\frac{\rho V d_r c_p}{k} \right)_l^{0.8} \right]$$

Equation (12) then becomes

$$T_m = T_w + \frac{1}{2} \left(\frac{Q}{f A_f} \right)_r \left[\frac{1}{(\rho V c_p)_l} + \frac{1}{2 U_l \left(\frac{1}{d} \right)_r} \right] \quad (13)$$

For each flight condition, the liquid-metal temperature rise is held constant at a value which gives a liquid-metal velocity of 15 feet per second at the optimum compressor pressure ratio and turbine-inlet temperature.

RESULTS AND DISCUSSION

The performance of the liquid-metal nuclear-powered turbojet cycle is presented by first discussing engine performance and the effect of design variables on engine performance. The engine performance is emphasized in this report, however, a discussion of the performance of the airplane-engine combination in terms of airplane gross weight and reactor heat release is also considered. The remainder of the discussion is concerned with the effect of changing airplane and weight assumptions on airplane gross weight and reactor heat release.

Engine Performance

The net thrust per engine plus heat exchanger weight of the turbojet engine is optimized for exchanger inlet Mach number, compressor pressure ratio, and turbine-inlet temperature for a range of heat exchanger effective wall temperatures. The data are presented for altitudes of 30,000 and 50,000 feet, and for flight Mach numbers of 0.9 and 1.5. In addition, net thrust per pound of air per second and air enthalpy rise through the heat exchanger are shown for the corresponding engine and flight conditions to completely specify engine performance.

Heat exchanger inlet Mach number. - The effect of heat exchanger air inlet Mach number on thrust per engine plus heat exchanger weight is illustrated in figures 7(a) and 7(b) for an altitude of 30,000 feet and at flight Mach numbers of 0.9 and 1.5, respectively. For each assumed value of heat exchanger effective wall temperature and turbine-inlet temperature there is a value of inlet Mach number which gives maximum F_n/W_T . For a fixed value of T_3 , low inlet Mach number gives low pressure drop and consequently higher thrust, but also high exchanger weight due to the large frontal area required. High inlet Mach numbers result in high pressure drop reducing the engine thrust, but also giving low exchanger weight due to the smaller frontal area. Consequently, a heat exchanger inlet Mach number which gives a maximum value of thrust per pound of engine plus exchanger weight is expected. The optimum (i.e. maximum) values of F_n/W_T are indicated in both figures by cross marks.

The optimum inlet Mach numbers range from about 0.14 to about 0.18 for all the compressor pressure ratios, turbine-inlet temperatures, and exchanger wall temperatures shown for the flight Mach number of 0.9. For the flight Mach number of 1.5 shown in figure 7(b) the optimum inlet Mach numbers range from about 0.14 to about 0.22. Curves similar

DECLASSIFIED

to these were plotted for all the flight conditions and engine operating variables considered to determine the optimum exchanger inlet Mach number for each condition and all the values fell within the ranges shown on the figures.

Optimum compressor pressure ratio. - The net thrust per engine plus heat exchanger weight for various values of exchanger effective wall temperature, turbine-inlet temperature, and for optimum inlet Mach number is shown as a function of compressor pressure ratio in figures 8 to 11. The data are presented at altitudes of 30,000 and 50,000 feet and for flight Mach numbers of 0.9 and 1.5. The corresponding values of thrust per pound of air per second are also shown. The solid lines represent constant T_3 , and the dashed lines are the envelope curves for maximum F_n/W_T at any pressure ratio. These figures indicate that for each exchanger wall temperature and turbine-inlet temperature there is an optimum compressor pressure ratio. For all the heat exchanger and turbine-inlet temperature combinations shown the optimum pressure ratio varies from about 3 to 8 for both altitudes at a flight Mach number of 0.9. At a flight Mach number of 1.5 the optimum compressor pressure ratio varies from about 2.5 to 6 for both altitudes.

Optimum turbine-inlet temperature. - For each assumed heat exchanger effective wall temperature T_w , there is a value of turbine-inlet temperature which gives the maximum F_n/W_T . The thrust per pound of air per second is increased by increasing the turbine-inlet temperature T_3 , however, the exchanger pressure drop is also increased due to the higher exchanger l/d required to obtain the higher T_3 for a given T_w . This increased pressure drop with increasing l/d will eventually counterbalance the increase in thrust due to the increased turbine-inlet temperature. In addition, the exchanger weight increases due to the larger l/d , and consequently there exists an optimum turbine-inlet temperature.

As observed in figures 8 to 11, the best turbine-inlet temperature is closer to the heat exchanger effective wall temperature T_w , at lower values of T_w than at the higher values of T_w .

Enthalpy rise through heat exchanger. - The enthalpy rise per unit air flow through the heat exchanger corresponding to the thrust per engine plus exchanger weight is shown at the four flight conditions in figures 12(a) to 12(d). The enthalpy rise is given as a function of compressor pressure ratio for a range of turbine-inlet temperatures. These curves are included at this point to completely define engine performance, and thus conveniently group all the engine data necessary for gross weight and heat release calculations together.

Effect of heat exchanger effective wall temperature on optimum engine performance. - The performance of the liquid-metal nuclear-powered turbojet engine is summarized in figures 13(a) to 13(d). Maximum thrust per engine plus exchanger weight F_N/W_T is plotted against the heat exchanger effective wall temperature T_w . The corresponding values of net thrust per pound of air per second F_N/w_a , heat addition to the air Δh_x , optimum compressor pressure ratio P_2/P_1 , optimum turbine-inlet temperature T_3 , and difference between the exchanger effective wall temperature and optimum turbine-inlet temperature $T_w - T_3$ are also shown. For any T_w , the optimum engine performance is readily obtained from these curves.

The optimum P_2/P_1 at altitudes of 30,000 and 50,000 feet for optimum turbine-inlet temperature varies from 4 to 7.5 for a flight Mach number of 0.9, and from 2.5 to 5.5 for a Mach number of 1.5.

The temperature difference $T_w - T_3$ varies from 150° to 250° R for a Mach number of 0.9 for a range of T_w from 1600° to 2400° R. At a Mach number of 1.5, $T_w - T_3$ varies from 150° to 350° R for a range of T_w from 1600° to 2600° R.

The optimum heat exchanger inlet Mach number M_2' at optimum P_2/P_1 and T_3 varies from 0.15 to 0.16 at a Mach number of 0.9, and varies from 0.18 to 0.19 at a Mach number of 1.5. No noticeable trends with T_w were apparent, consequently no plot of optimum M_2' against T_w is included.

Effect of engine and exchanger weight on optimum thrust per pound of engine and exchanger. - At a given value of heat exchanger effective wall temperature the optimum compressor pressure ratio, heat exchanger inlet Mach number, and turbine-inlet temperature for maximum thrust per pound of engine plus exchanger is not affected by the engine weight assumption if the relative variation of engine weight with compressor pressure ratio remains unchanged from that given by figure 3.

The optimum compressor pressure ratio, heat exchanger inlet Mach number, and turbine-inlet temperature are also not affected by the heat exchanger weight assumption (equation 8) as long as the exchanger weight is assumed to vary directly with air flow area and length diameter ratio of the passages. These changes in heat exchanger and engine weight assumptions would change the magnitude of F_N/W_T but would not change the optimum P_2/P_1 , M_2' , or T_3 .

DECLASSIFIED

Airplane Performance

The airplane performance for the liquid-metal turbojet is shown in figures 14 to 17 in terms of airplane gross weight and reactor heat release. For all the figures presented the structure to gross weight ratio is assumed to be 0.35. The airplane lift-drag ratios at the flight Mach numbers of 0.9 and 1.5 are 18 and 9, respectively. The sum of the shield, reactor, payload, and auxiliary weights is assumed to be 190,000 pounds. The reactor liquid-metal velocity is 15 feet per second for all the optimum conditions shown.

Effect of compressor pressure ratio and turbine-inlet temperature. -

The effect of compressor pressure ratio and turbine-inlet temperature upon airplane gross weight and reactor heat release is shown in figures 14(a) to 14(d) for flight Mach numbers of 0.9 and 1.5 at altitudes of 30,000 and 50,000 feet. The heat exchanger effective wall temperature is 2000° R in all cases, and the turbine-inlet temperature varies from 1500° to 1900° R. The reactor wall temperature corresponding to the 2000° R heat exchanger effective wall temperature is given in each case.

The liquid-metal velocity V_l , in figures 14(a) to 14(d) is 15 feet per second at the optimum compressor pressure ratio (minimum gross weight). This V_l together with the reactor heat release Q at these optimum conditions determines the reactor maximum wall temperature T_m , for the fixed 2000° R heat exchanger effective wall temperature (equation 13). For the off-optimum P_2/P_1 and T_3 , V_l is varied ± 3 feet per second in order to maintain $T_m - T_w$ constant.

Airplane gross weight and reactor heat release for a flight Mach number of 0.9 at altitudes of 30,000 and 50,000 feet are shown in figures 14(a) and 14(b). The curves indicate that over the temperature and pressure ratio range considered, the airplane gross weight is insensitive to T_3 and P_2/P_1 at 30,000 feet (fig. 14(a)) but it is somewhat more sensitive at 50,000 feet (fig. 13(b)). This is true because for the combination of the design L/D of 18 and the F_n/W_T obtained, the airplane gross weight is relatively independent of F_n/W_T as indicated in figure 6 except for very low values of F_n/W_T . The thrust per engine plus exchanger weight is higher at 30,000 feet than at 50,000 feet and so gross weight is expected to be less sensitive to compressor pressure ratio and turbine-inlet temperature at the lower altitude. The minimum reactor heat release occurs at a compressor pressure ratio which is higher than the pressure ratio which gives minimum gross weight. For both parts (a) and (b) of figure 14 the reactor heat release is about equal, consequently the same temperature

difference (50° R) exists between the reactor maximum wall temperature and T_w .

Parts (c) and (d) of figure 14 present the performance of the airplane at a Mach number of 1.5 for altitudes of 30,000 and 50,000 feet. The curves indicate that even at the higher flight Mach number (with lower L/D) the airplane gross weight is insensitive to T_3 and P_2/P_1 at 30,000 feet altitude. This is due to the high thrust per engine plus exchanger weight at this Mach number which makes the airplane gross weight relatively insensitive to variations in F_n/W_T as indicated in figure 6. At the higher altitude (fig. 14(d)) the gross weight is more sensitive to T_3 and P_2/P_1 because of the lower values of F_n/W_T . The minimum reactor heat release occurs at a higher pressure ratio than the minimum gross weight as was the case at the lower Mach numbers. The temperature difference $T_m - T_w$, is higher than for a Mach number of 0.9 because of the higher engine air flow required and consequently greater reactor heat release necessary at a Mach number of 1.5. At an altitude of 30,000 feet (fig. 14(c)), $T_m - T_w$ is 100° R, and at an altitude of 50,000 feet (fig. 14(d)), $T_m - T_w$ is 150° R.

Effect of reactor wall temperature. - The effect of reactor wall temperature on airplane gross weight, reactor heat release, and heat exchanger effective wall temperature for optimum heat exchanger inlet Mach number, optimum compressor pressure ratio, and optimum turbine-inlet temperature is shown in figures 15(a) to 15(c). The flight conditions shown are the same as have been considered previously.

The airplane gross weight increases at an increasing rate as the reactor wall temperature is reduced (fig. 15(a)). This rate of increase is not significant, however, until a wall temperature of 1600° R is reached for both flight Mach numbers at 30,000 feet altitude. At 50,000 feet and a Mach number of 0.9, W_g is insensitive to T_m as low as 1800° R, and at a Mach number of 1.5, W_g is insensitive to T_m as low as 2000° R. In general, lower altitudes and lower Mach numbers require lower reactor maximum wall temperatures for a given gross weight. For example, at a gross weight of 400,000 pounds, the required reactor maximum wall temperature is 1180° R at 30,000 feet altitude and 0.9 Mach number. The same gross weight requires a T_m of 1520° R at 50,000 feet altitude for the same Mach number. For a flight Mach number of 1.5 T_m is 1420° R at 30,000 feet and 1880° R at 50,000 feet.

As is shown in figure 15(b), the reactor heat release corresponding to minimum gross weight is relatively unaffected by decreasing T_m until a value is reached at each flight condition where the reactor

heat release increases very rapidly. This is to be expected because the gross weight also increases very rapidly in the same range of reactor maximum wall temperatures.

The heat exchanger effective wall temperature T_w is shown as a function of T_m in figure 15(c), so that the engine performance (fig. 13) corresponding to the airplane performance shown in figures 15(a) and 15(b) can be determined.

From the foregoing figures and equations, a table has been prepared and presented in appendix B which gives a more detailed listing of component weights and reactor, engine, and heat exchanger variables than has been shown. The table is prepared at the four flight conditions for a heat exchanger effective wall temperature of 2000°R and a turbine-inlet temperature of 1700°R .

Effect of flight conditions. - The effect of flight Mach number and altitude on airplane gross weight and reactor heat release is presented in figures 16 and 17. The curves are calculated for a heat exchanger effective wall temperature of 2400°R , turbine-inlet temperature of 2000°R , compressor pressure ratio of 5, and optimum heat exchanger inlet Mach number.

The altitude effect on gross weight and reactor heat release is shown in figure 16 for flight Mach numbers of 0.9 and 1.5. The gross weight and reactor heat release are relatively insensitive to altitude from 0 to 35,000 feet. Above 35,000 feet the reactor heat release and gross weight increases very rapidly.

The effect of flight Mach number on airplane gross weight and reactor heat release is shown in figure 17 for altitudes of 30,000 and 50,000 feet. The gross weight is relatively independent of Mach number, however, the reactor heat release increases quite rapidly with Mach number chiefly because of the rapid decrease in airplane L/D .

Effect of Varying Assumptions

The previous analysis is based on fixed assumed values of the sum of the shield, reactor, payload, and auxiliary weight, airplane lift-drag ratio, and structure to gross weight ratio. In addition, all the engine installations were assumed to be of the submerged type which neglect the effect of nacelle drag. The magnitude of the effect of taking into account different values of these assumptions and considering nacelle drag on airplane gross weight and reactor heat release is shown in figures 18 to 21 for two turbine-inlet temperatures. The effect of reactor diameter on unit heat release is shown in figure 22.

Effect of sum of shield, payload, and auxiliary weight. - The effect of varying W_K on airplane gross weight and reactor heat release is presented in figure 18 for an altitude of 50,000 feet and a Mach number of 0.9. The vertical dashed line indicates the constant 190,000 pound value of W_K assumed in the previous analysis. The curves for two engines are presented; one engine having a heat exchanger effective wall temperature of 2000°R and a turbine-inlet temperature of 1700°R ; the other engine having a T_w of 2400°R , and a T_3 of 2000°R (T_m depends on W_g and Q). The optimum values of compressor pressure ratio and heat exchanger inlet Mach number are used. The airplane gross weight varies directly with the value of W_K as has been discussed and shown previously in equation (7). The required reactor heat release also varies directly with W_K inasmuch as Q varies directly with W_g at a given engine operating point.

Effect of structure to gross weight ratio. - The effect of varying the structure to gross weight ratio W_s/W_g , on airplane gross weight and reactor heat release is presented in figure 19 for the same engine and flight conditions shown in the previous figure. For a reduction in W_s/W_g of 0.35 to 0.30 (14.2 percent) the gross weight and reactor heat release decrease about 9.0 percent. The vertical dashed line represents the W_s/W_g of 0.35 used in the previous analysis.

Effect of airplane lift-drag ratio. - The effect of varying the airplane design point lift-drag ratio on airplane gross weight and reactor heat release is shown in figures 20(a) and 20(b) for flight Mach numbers of 0.9 and 1.5 at an altitude of 50,000 feet for the same engine conditions as in the previous figures. At a flight Mach number of 0.9 reducing the L/D from 18 to about 10 causes a relatively small increase in gross weight. Reducing the L/D further results in a very rapid increase in gross weight. The level of cycle temperature operation has a small effect on gross weight at high L/D values, but this effect becomes large at values of L/D below about 10. Reactor heat release is more sensitive to reduction in L/D and increases quite rapidly with reduction in L/D . The level of cycle temperature operation has practically no effect upon heat release over the range of L/D shown. At a flight Mach number of 1.5, figure 20(b), reducing the L/D from 9 increases the gross weight rapidly. Increasing the L/D from 9, however, causes a relatively small reduction in gross weight. This small effect of L/D upon gross weight at values above 9 is due to the higher thrust per engine weight at a flight Mach number of 1.5. As in the case of the flight Mach number of 0.9, the reactor heat release is more sensitive to changes in L/D than is gross weight.

Effect of nacelle drag. - The effect of engine nacelle drag on airplane gross weight as a function of reactor maximum wall temperature is presented in figures 21(a) and 21(b) for flight Mach numbers of 0.9 and 1.5, respectively at an altitude of 50,000 feet. The turbine-inlet temperature, heat exchanger inlet Mach number, and compressor pressure ratio are optimum. The coefficient of nacelle drag $C_{D,N}$ was selected to include a range of nacelle drag values at both Mach numbers. The coefficient includes the wave and friction drag at a Mach number of 1.5.

At a flight Mach number of 0.9 a nacelle having a drag coefficient of 0.08, which is a reasonable value at this flight condition, increases the gross weight less than 10 percent for reactor maximum wall temperatures as low as 1500° R. This effect increases rapidly for temperatures below 1500° R.

At a flight Mach number of 1.5, nacelle drag becomes very important as is shown in figure 21(b) which indicates that neglecting nacelle drag can be very misleading. The solid lines represent constant $C_{D,N}$, and the dashed lines represent constant heat exchanger effective wall temperatures. For a 500,000 pound airplane the reactor maximum wall temperature must be increased from about 1600° to 2200° R if the nacelle drag coefficient is increased from 0 to 0.2, which is a reasonable value of $C_{D,N}$ at this flight condition. For a fixed airplane gross weight the nacelle drag reduces airplane lift-drag ratio. Consequently, the engine must operate at a higher temperature to overcome the increased drag. The following table lists L/D and T_w against $C_{D,N}$ for one design point airplane.

M_0	Altitude (ft)	W_g (lb)	$C_{D,N}$	T_w ($^{\circ}$ R)	F_n	L/D
1.5	50,000	372,000	0	2000	41,400	9(design)
			.2	2430	56,500	6.58
			.4	2800	71,500	5.2

Effect of reactor size. - In the previous analysis and discussion no specific assumptions have been made regarding reactor size or shield weight. The sum of the weight of reactor, shield, payload, and auxiliary equipment was arbitrarily assumed. Figure 22 is presented in order to show the effect of reactor size on reactor unit heat release Q/v , and airplane gross weight. The reactor diameter was varied from 2.0 to 5.0 feet, maintaining the length to diameter ratio of the reactor at 1.0.

An integral (wrap around) shield was assumed with a constant 2.5 foot thickness and a specific gravity of 8.0. The gross weight required to carry the shield and a 30,000 pound payload plus auxiliary weight is plotted against the reactor unit heat release in Btu per second per cubic inch of reactor. The heat exchanger effective wall temperature is 2000° R, and the compressor pressure ratio, heat exchanger inlet Mach number, and turbine-inlet temperature are optimum.

Reducing the reactor size below 2.5 feet does not materially change the gross weight, but the reactor unit heat release increases rapidly. Increasing the reactor size above 3.5 feet causes a rapid increase in gross weight while the reactor unit heat release is not so greatly affected. At low reactor diameters the unit heat release is much greater for the 1.5 flight Mach number than for 0.9 Mach number, however, this difference decreases for larger reactors.

SUMMARY OF RESULTS

An analysis of the nuclear powered liquid-metal turbojet cycle is presented for a wide range of engine operating conditions and for several flight conditions. The following results were obtained from the investigations:

1. For optimum compressor pressure ratio and turbine-inlet temperature, the optimum heat exchanger inlet Mach number ranges from 0.15 to 0.16 for a flight Mach number of 0.9 and heat exchanger effective wall temperatures of 1400° to 2600° R. For a flight Mach number of 1.5, the optimum heat exchanger inlet Mach number varies from 0.18 to 0.19 for heat exchanger effective wall temperatures of 1200° to 2600° R.
2. The optimum compressor pressure ratio at optimum turbine-inlet temperature varies from about 4.0 to 7.5 at altitudes of 30,000 and 50,000 feet at a flight Mach number of 0.9, for heat exchanger effective wall temperatures of 1400° to 2600° R. At a flight Mach number of 1.5, the optimum compressor pressure ratio varies from 2.5 to 5.5 for heat exchanger effective wall temperatures from 1600° to 2600° R.
3. The difference between the heat exchanger effective wall temperature and the turbine-inlet temperature $T_w - T_3$, varies from 150° to 250° R for a flight Mach number of 0.9 for a range of T_w from

DECLASSIFIED

1600° to 2400° R. For a flight Mach number of 1.5, $T_w - T_3$ varies from 150° R to 350° R for a range of T_w from 1600° to 2600° R.

4. Engine and exchanger weight assumptions change the magnitude of thrust per engine plus exchanger weight, but do not affect the values of compressor pressure ratio, heat exchanger inlet Mach number, and turbine-inlet temperature which give maximum thrust per engine plus exchanger weight, provided that the engine weight is changed proportionally at all pressure ratios and that the exchanger weight is assumed to vary directly with air flow area and length-diameter ratio of the flow passages.

5. Airplane gross weight at an altitude of 30,000 feet and Mach numbers of 0.9 and 1.5 is relatively insensitive to reactor maximum wall temperatures as low as 1600° R. At 50,000 feet altitude and 0.9 Mach number, the airplane is insensitive to T_m as low as 1800° R and at a Mach number of 1.5, W_g is insensitive to T_m as low as 2000° R.

6. Airplane gross weight is relatively insensitive to flight Mach number, but reactor heat release increases rapidly with increasing flight Mach number. Both airplane gross weight and reactor heat release are insensitive to altitude below 35,000 feet, but increase rapidly with increasing altitude above 35,000 feet.

7. For a flight Mach number of 1.5 at 50,000 feet altitude, nacelle drag becomes very significant. For a 500,000 pound airplane the reactor maximum wall temperature must be increased from 1600° to 2200° R if a nacelle drag coefficient of 0.2 is taken into account.

Lewis Flight Propulsion Laboratory,
National Advisory Committee for Aeronautics,
Cleveland, Ohio

APPENDIX A

Engine operating data was calculated and prepared in the form of charts to aid in the analysis. The data is presented on a corrected basis and includes compressor outlet temperature, turbine pressure ratio, turbine outlet temperature, and engine net thrust per pound of air per second neglecting nacelle drag.

Figure 22 shows corrected compressor outlet temperature as a function of compressor pressure ratio. Figures 23 and 24 show turbine pressure ratio and corrected outlet temperature as a function of corrected turbine-inlet temperature for a range of compressor pressure ratios.

Figures 25(a) to 25(j) show the corrected engine net thrust per pound of air per second for a range of corrected turbine-inlet temperatures as a function of pressure ratio across the heat exchanger. Parts (a) to (f) show the corrected net thrust per pound of air per second for a flight Mach number of 0.9 at compressor pressure ratios of 1, 3, 5, 10, and 15. Parts (g) to (j) show the corrected net thrust per pound of air per second at the same pressure ratios for a flight Mach number of 1.5.

DECLASSIFIED

APPENDIX B

A table of weights, sizes, and operating variables of the components of the nuclear powered liquid-metal turbojet airplane is presented for Mach numbers of 0.9 and 1.5 at altitudes of 30,000 and 50,000 feet. The engine in all cases is operating with a heat exchanger effective wall temperature of 2000° R and turbine-inlet temperature of 1700° R. The heat exchanger inlet Mach number is optimum and the compressor pressure ratio is close to optimum.

03171220 1030

Flight condition				
Design altitude	30,000	50,000	30,000	50,000
Flight Mach number	0.9	0.9	1.5	1.5
Design point L/D	18	18	9	9
Operating point				
Heat exchanger wall temperature, °R	2000	2000	2000	2000
Turbine-inlet temperature, °R	1700	1700	1700	1700
Compressor pressure ratio	5	5	3.5	3.5
Component weights, lb				
Reactor shield, payload, aux. eq.	190,000	190,000	190,000	190,000
Engine	11,100	27,000	13,900	37,500
Heat exchangers	4,000	8,300	5,900	13,700
Airplane structure	110,400	126,700	113,000	129,800
Airplane gross weight	315,500	352,000	322,800	371,000
Reactor				
Heat release, Btu/sec	105,000	117,000	248,000	280,000
Maximum wall temperature, °R	2050	2050	2100	2150
Lithium temperature in, °R	1954	1952	1910	1862
Lithium temperature out, °R	2046	2048	2090	2138
Lithium velocity, ft/sec	15.6	16.8	18.8	13.8
Engine				
Net thrust per engine plus exchanger weight, lb/lb	1.17	0.506	1.82	0.803
Net thrust per air flow, lb/lb air/sec	38.2	40.6	30.2	32.7
Total engine air flow, lb/sec	457	492	1180	1267
Net engine thrust, lb	17,500	20,100	35,800	41,200
Compressor frontal area, ft ²	37	100	49	133
Heat exchanger				
Lithium temperature in, °R	2046	2048	2090	2138
Lithium temperature out, °R	1954	1952	1910	1862
Air inlet Mach number	0.162	0.16	0.19	0.18
Air inlet temperature, °R	804	766	886	845
Air outlet temperature, °R	1700	1700	1700	1700
Air enthalpy rise, Btu/lb air	230	238	210	221
Core frontal area, ft ²	26	71	38	111

DECLASSIFIED

REFERENCES

1. Doyle, Ronald B.: Calculated Performance of Nuclear Turbojet Powered Airplane at Flight Mach Number of 0.9. NACA RM E50B23, 1950.
2. Humble, L. V., Wachtl, W. W., and Doyle, R. B.: Preliminary Analysis of Three Cycles for Nuclear Propulsion of Aircraft. NACA RM E50H24, 1950.
3. Doyle, R. B.: Calculated Performance of a Direct-Air Nuclear Turbojet-Powered Airplane Using a Split-Flow Reactor and a Separated-Type Shield. NACA RM E50K06, 1950.
4. Anon.: NACA Conference on Aircraft Propulsion Systems Research, Jan. 18-19, 1950.
5. Pinkel, Benjamin, Noyes, Robert N., and Valerino, Michael F.: Method for Determining Pressure Drop of Air Flowing Through Constant-Area Passages for Arbitrary Heat-Input Distributions. NACA TN 2186, 1950.
6. Report of the Technical Advisory Board, ANP 52, Aug. 4, 1950.
7. English, Robert E., and Wachtl, William W.: Charts of Thermodynamic Properties of Air and Combustion Products from 300° to 3500° R. NACA TN 2071, 1950.
8. Lyon, Richard N.: Forced Convection Heat Transfer Theory and Experiments with Liquid Metals. ORNL 361, Aug. 1949.

0371220 1030

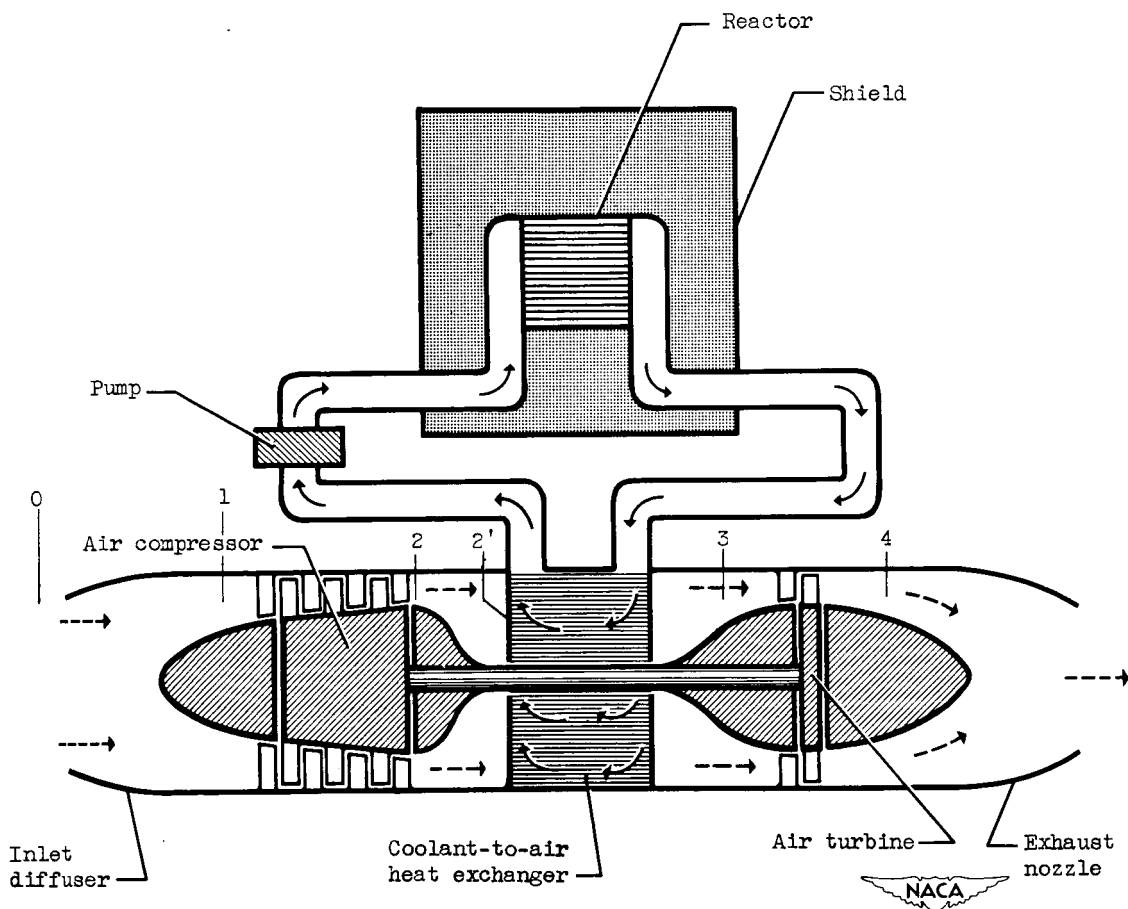


Figure 1. - Schematic diagram of a liquid-metal nuclear powered turbojet engine.

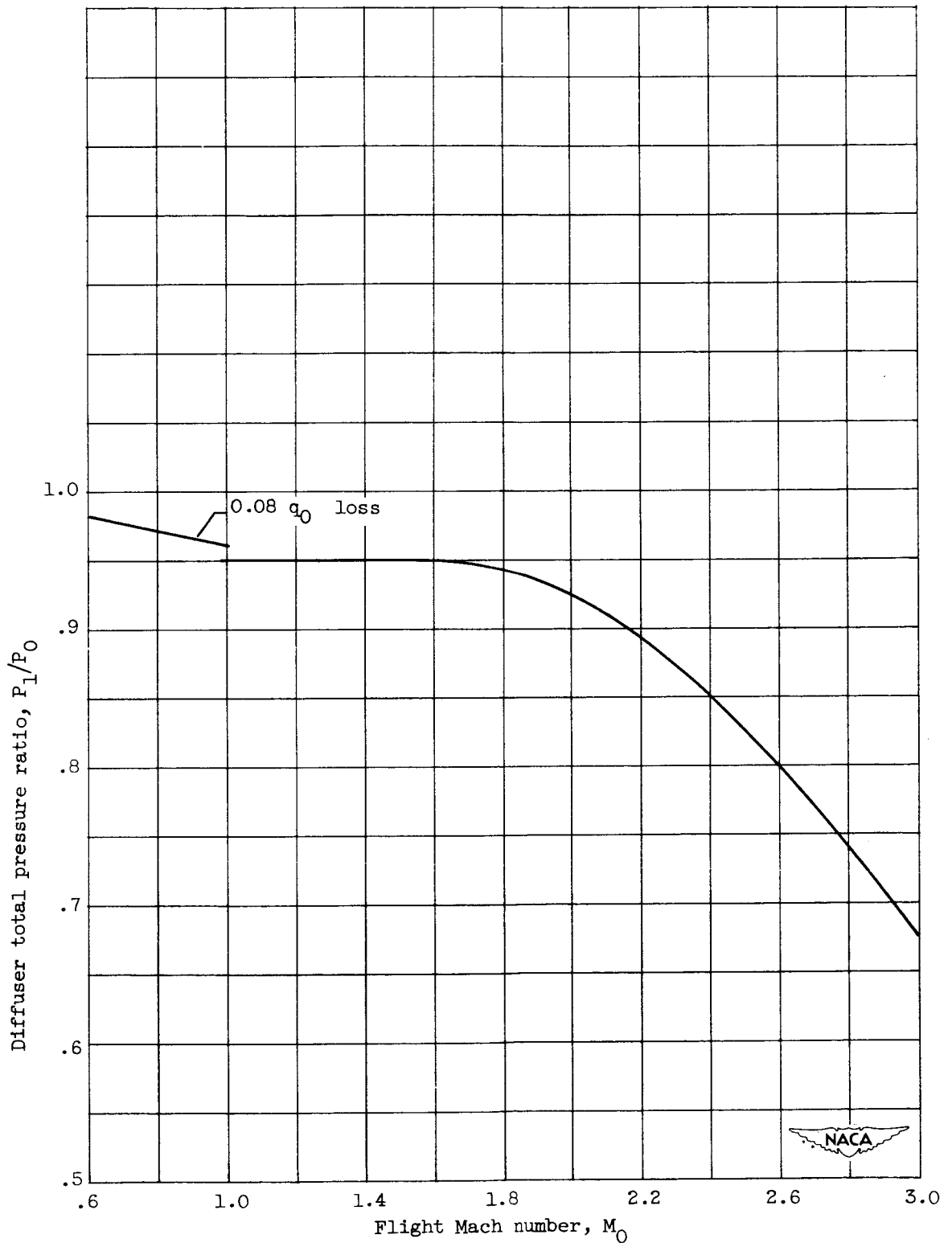


Figure 2. - Diffuser total pressure ratio as a function of flight Mach number.

0371228.1030

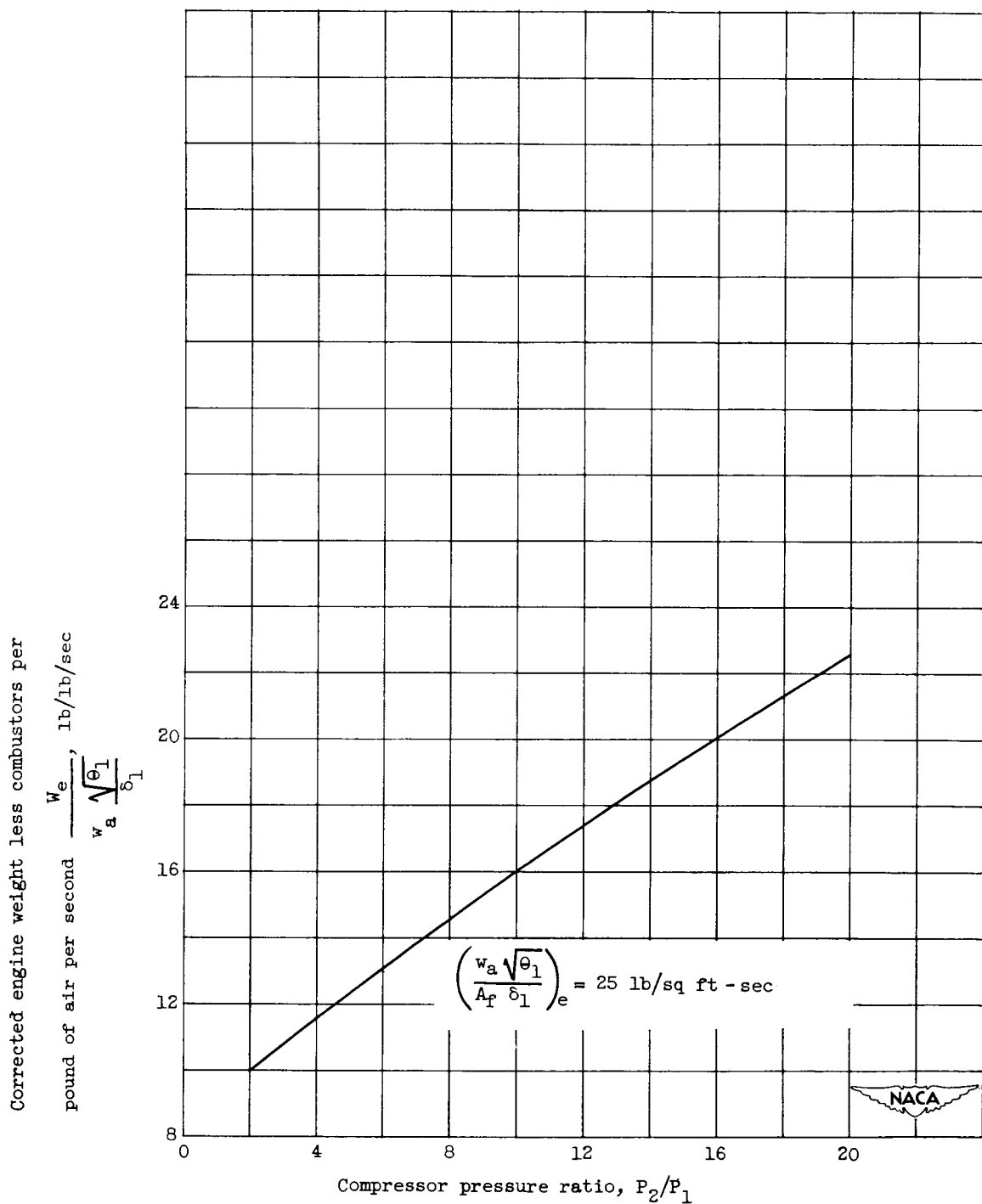


Figure 3. - Corrected specific engine weight as a function of compressor pressure ratio.

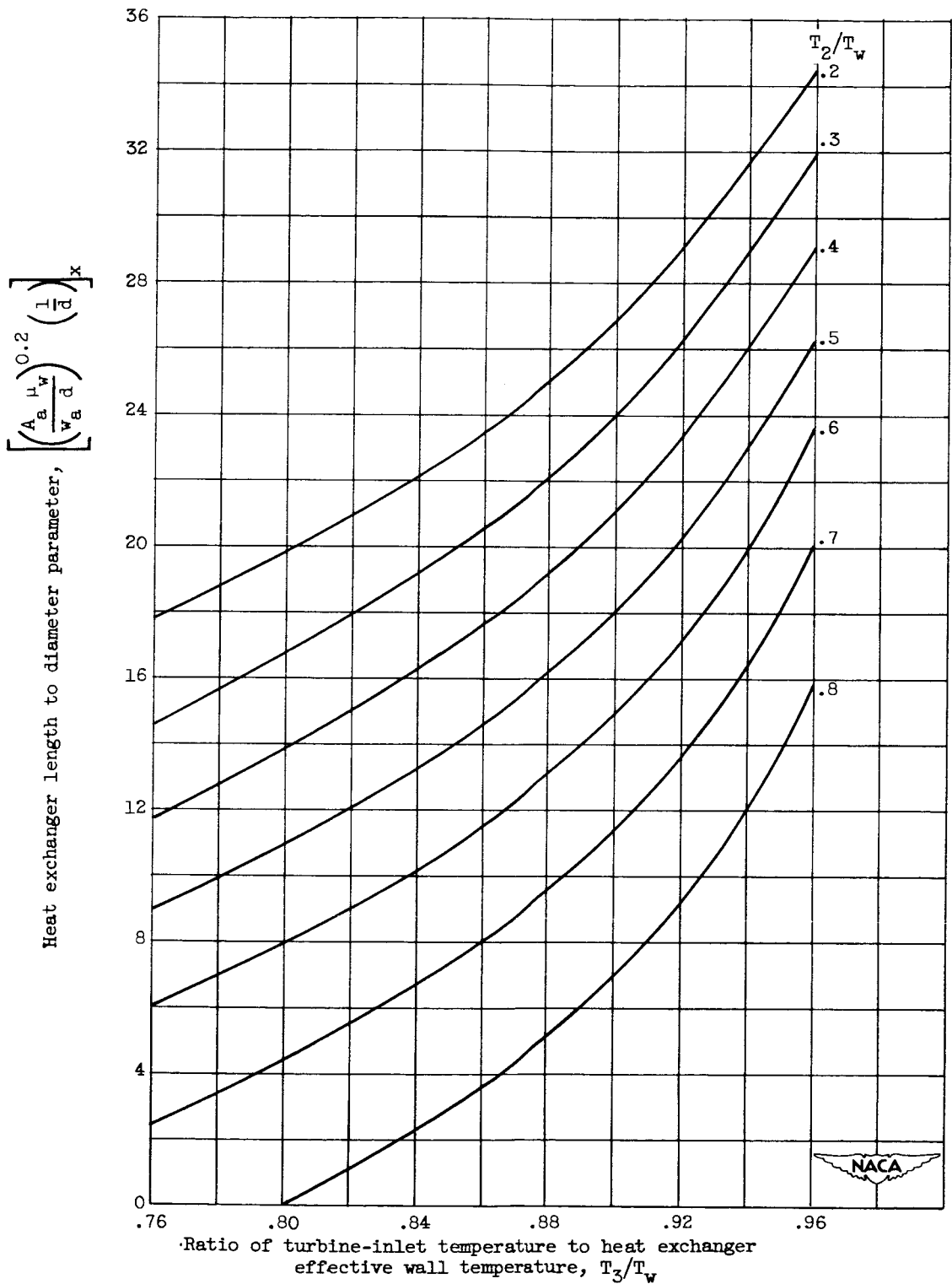
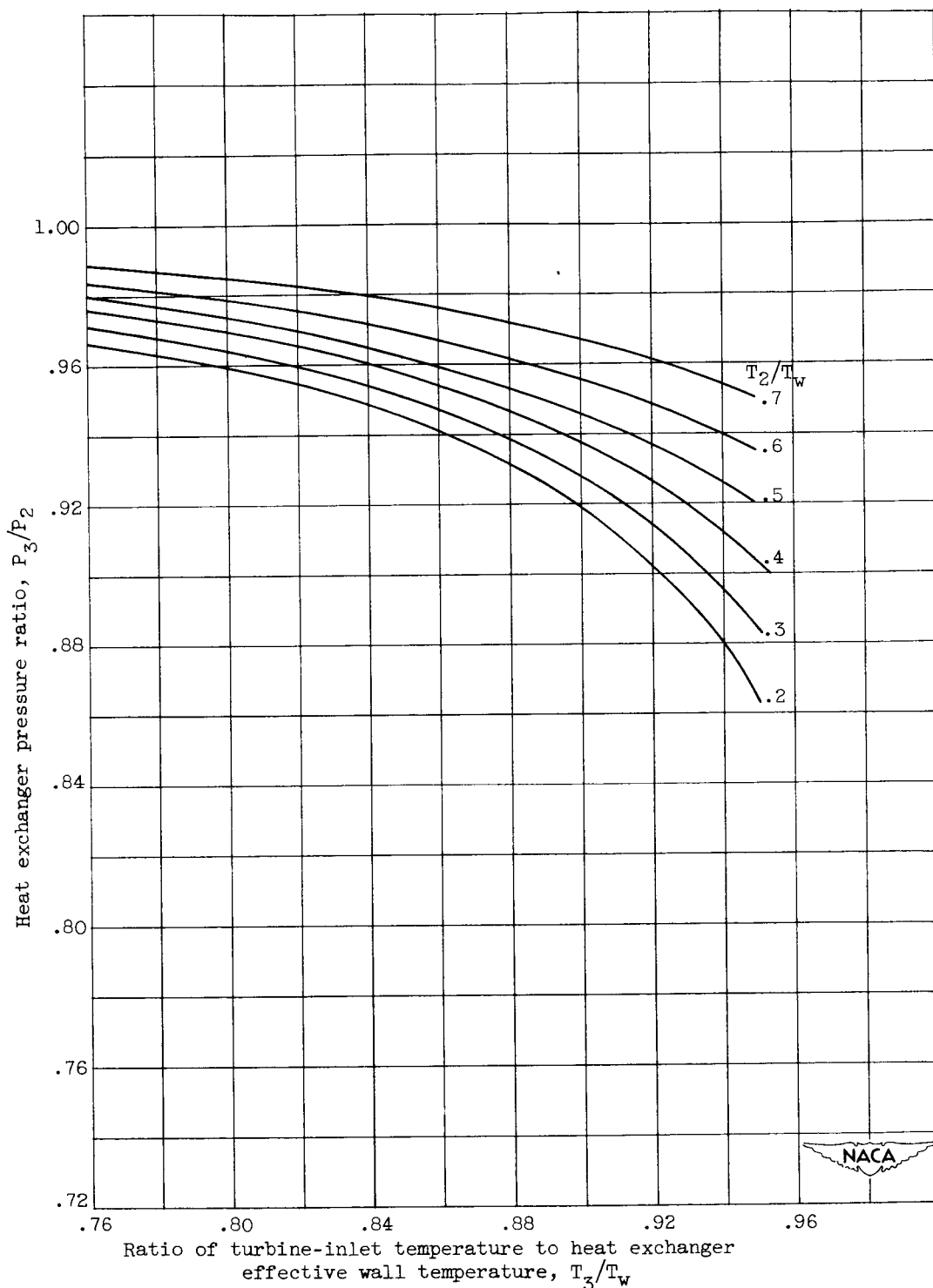


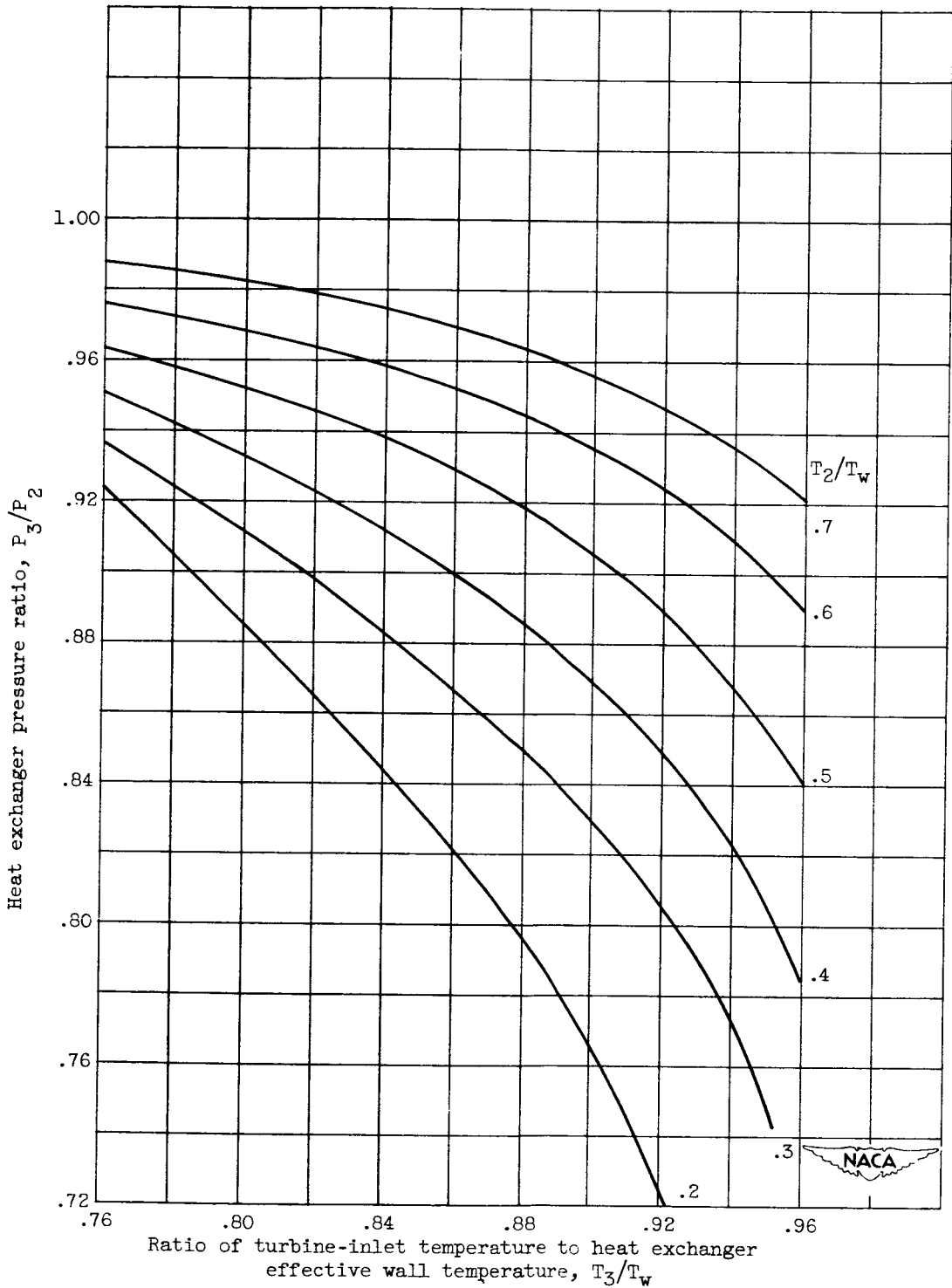
Figure 4. - Length to diameter parameter of heat exchanger tubes as a function of exchanger-inlet air temperature, effective wall temperature, and exit air temperature.

0371228.1030



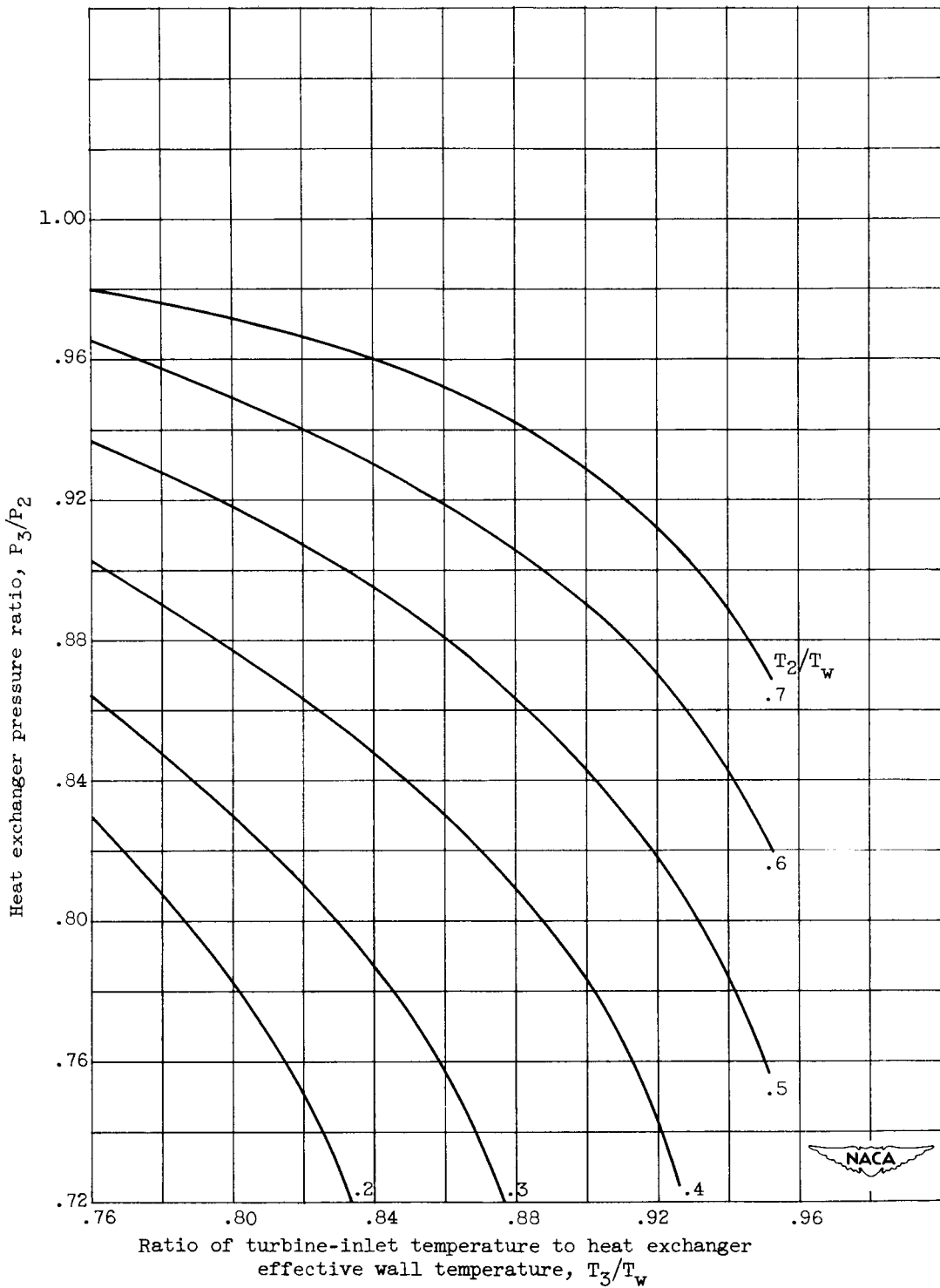
(a) Exchanger-inlet Mach number, 0.12.

Figure 5. - Heat exchanger pressure ratio as a function of exchanger-inlet air temperature, effective wall temperature, and exit air temperature.



(b) Exchanger-inlet Mach number, 0.16.

Figure 5. - Continued. Heat exchanger pressure ratio as a function of exchanger-inlet air temperature, effective wall temperature, and exit air temperature.



(c) Exchanger-inlet Mach number, 0.20.

Figure 5. - Concluded. Heat exchanger pressure ratio as a function of exchanger-inlet air temperature, effective wall temperature, and exit air temperature.

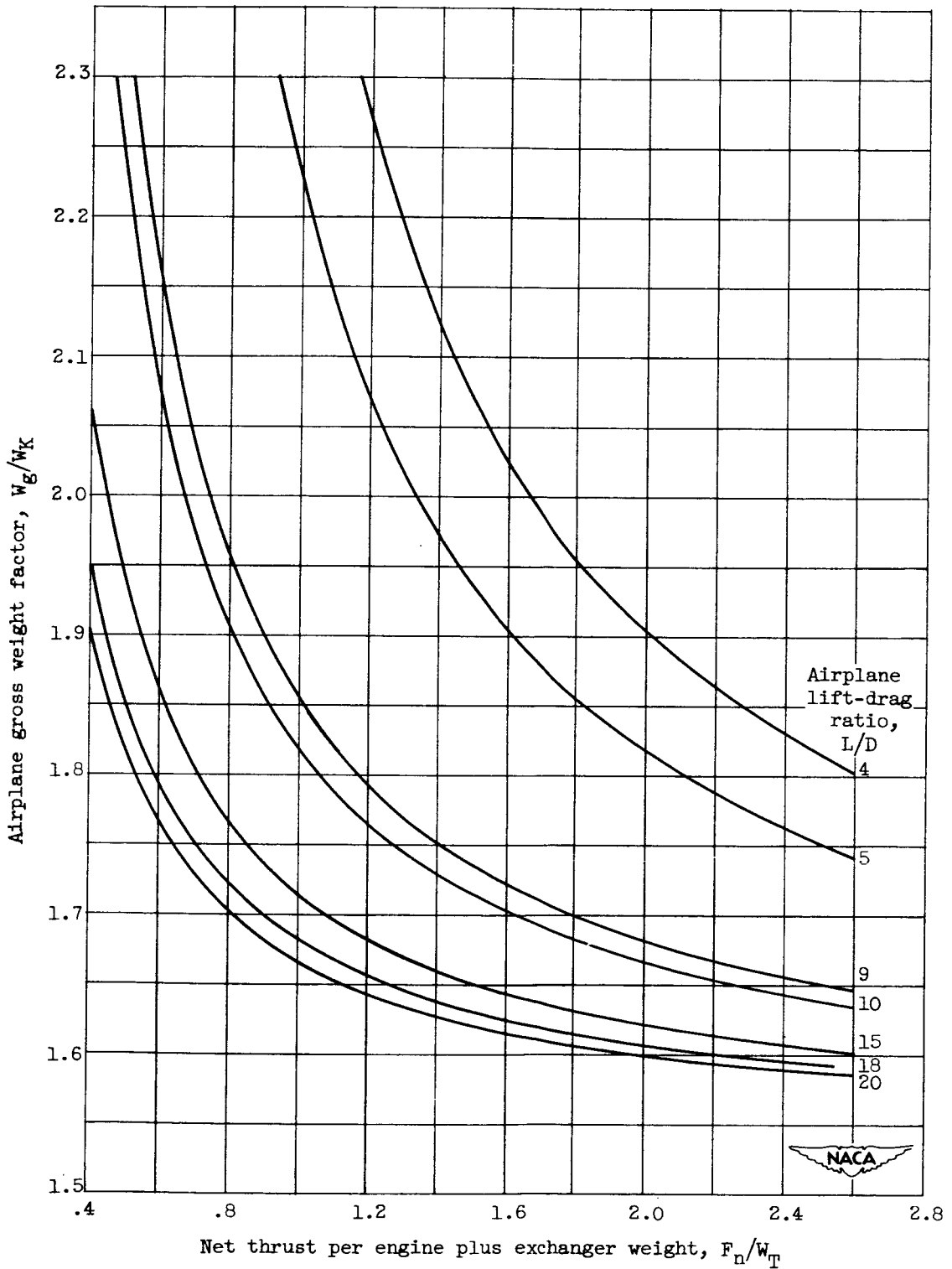
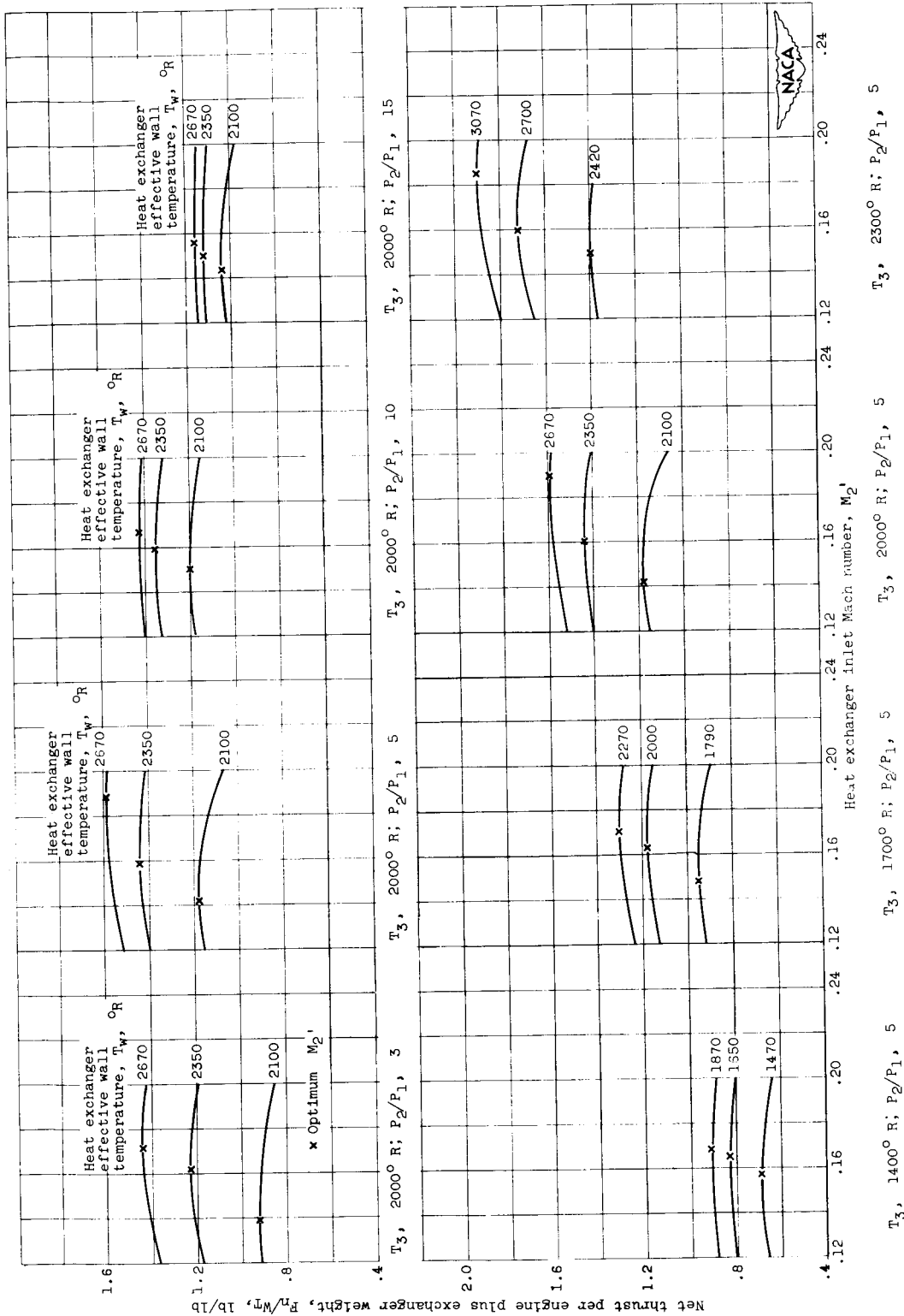


Figure 6. - Airplane gross weight factor as a function of net thrust per engine plus exchanger weight and airplane lift-drag ratio.



(a) Flight Mach number, 0.9.

Figure 7. - Net thrust per engine plus exchanger weight as a function of heat exchanger-inlet Mach number for various values of compressor pressure ratio, turbine-inlet temperature, and heat exchanger effective wall temperature. Altitude, 30,000 feet.

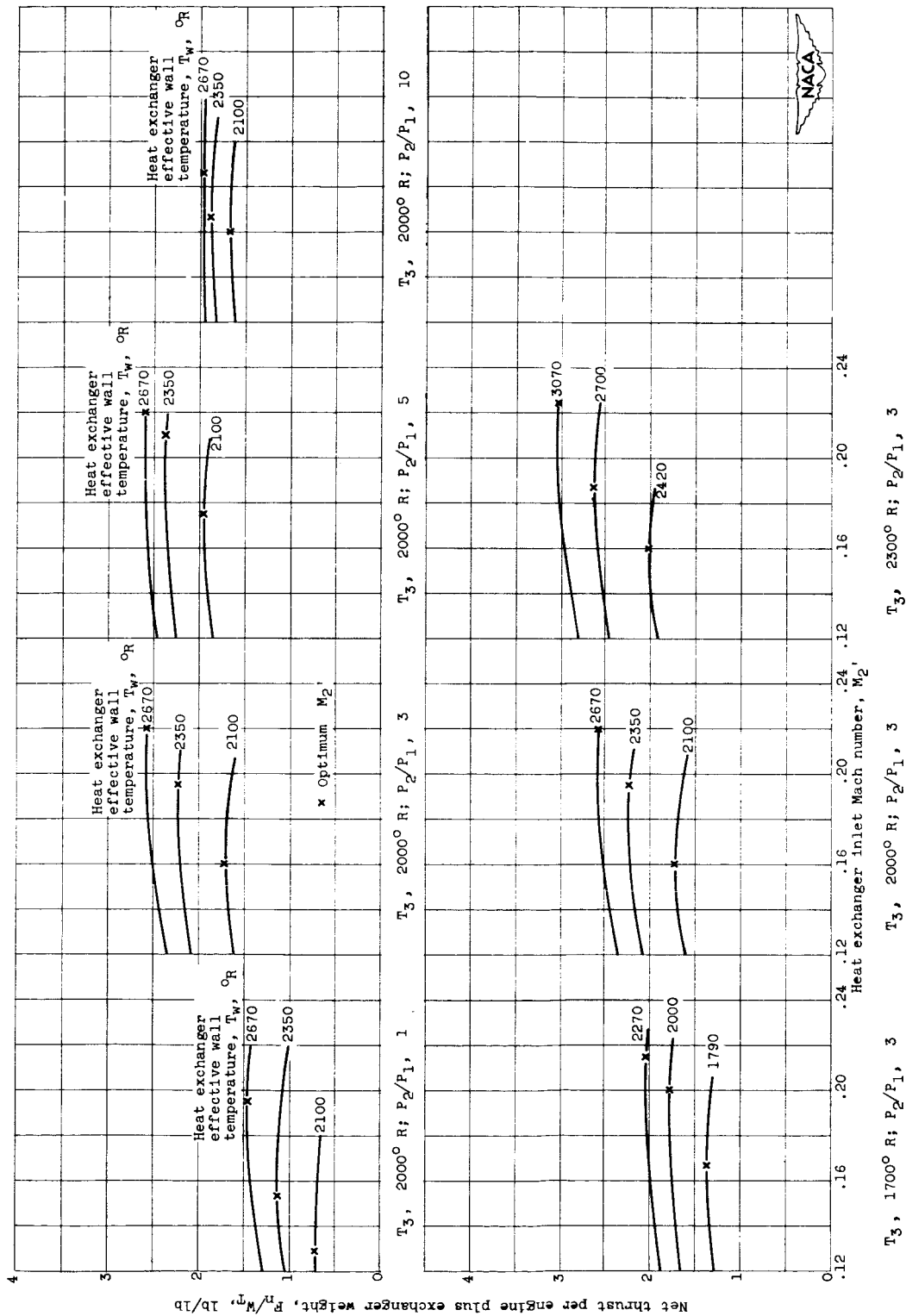


Figure 7. - Concluded. Net thrust per engine plus exchanger weight as a function of heat exchanger-inlet Mach number for various values of compressor pressure ratio, turbine-inlet temperature, and heat exchanger effective wall temperature. Altitude, 30,000 feet.

(b) Flight Mach number, 1.5.

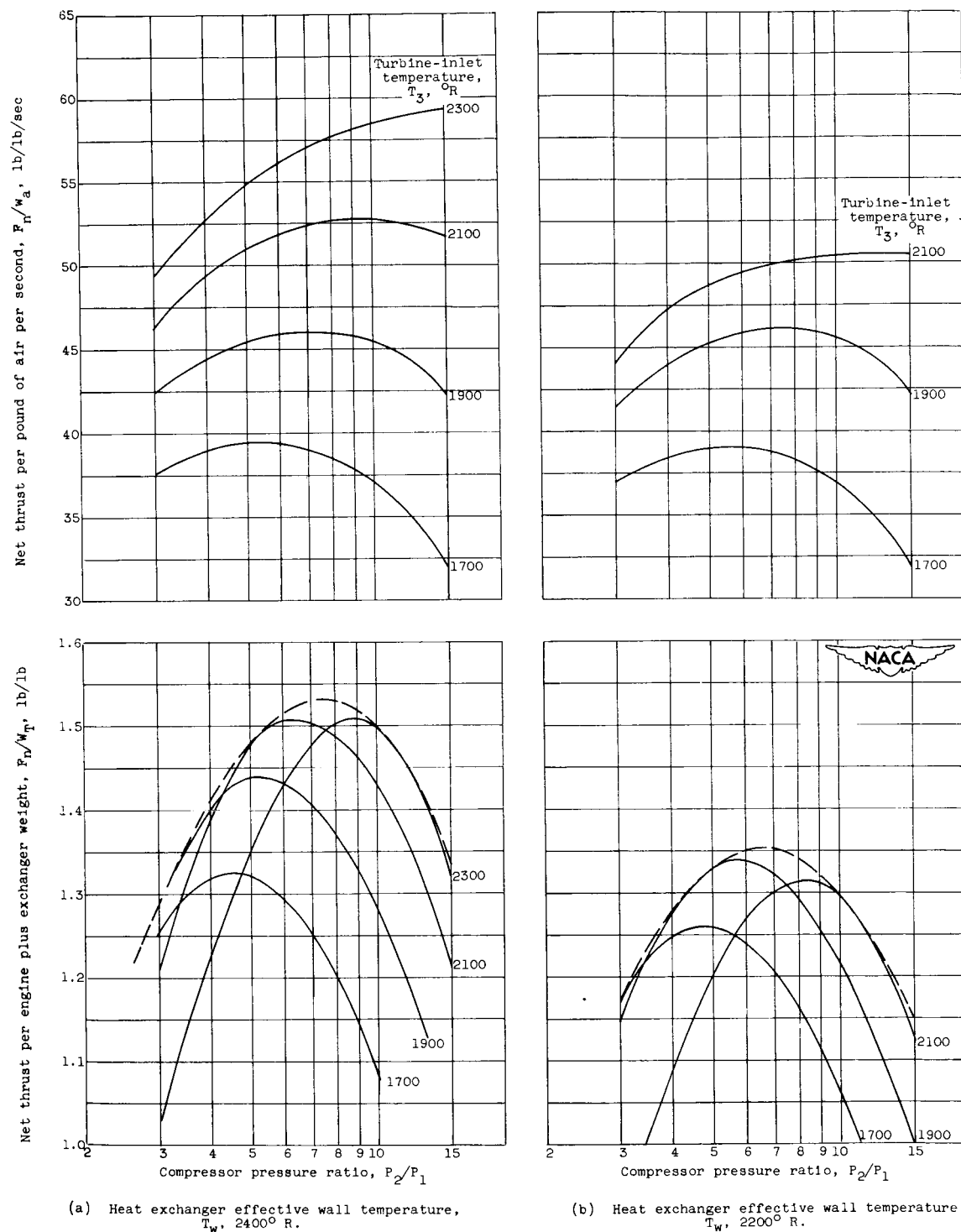


Figure 8. - Net thrust per engine plus exchanger weight and net thrust per pound of air per second as functions of P_2/P_1 , T_w , and T_3 . Optimum, M_2 ; altitude, 30,000 feet; flight Mach number 0.9.

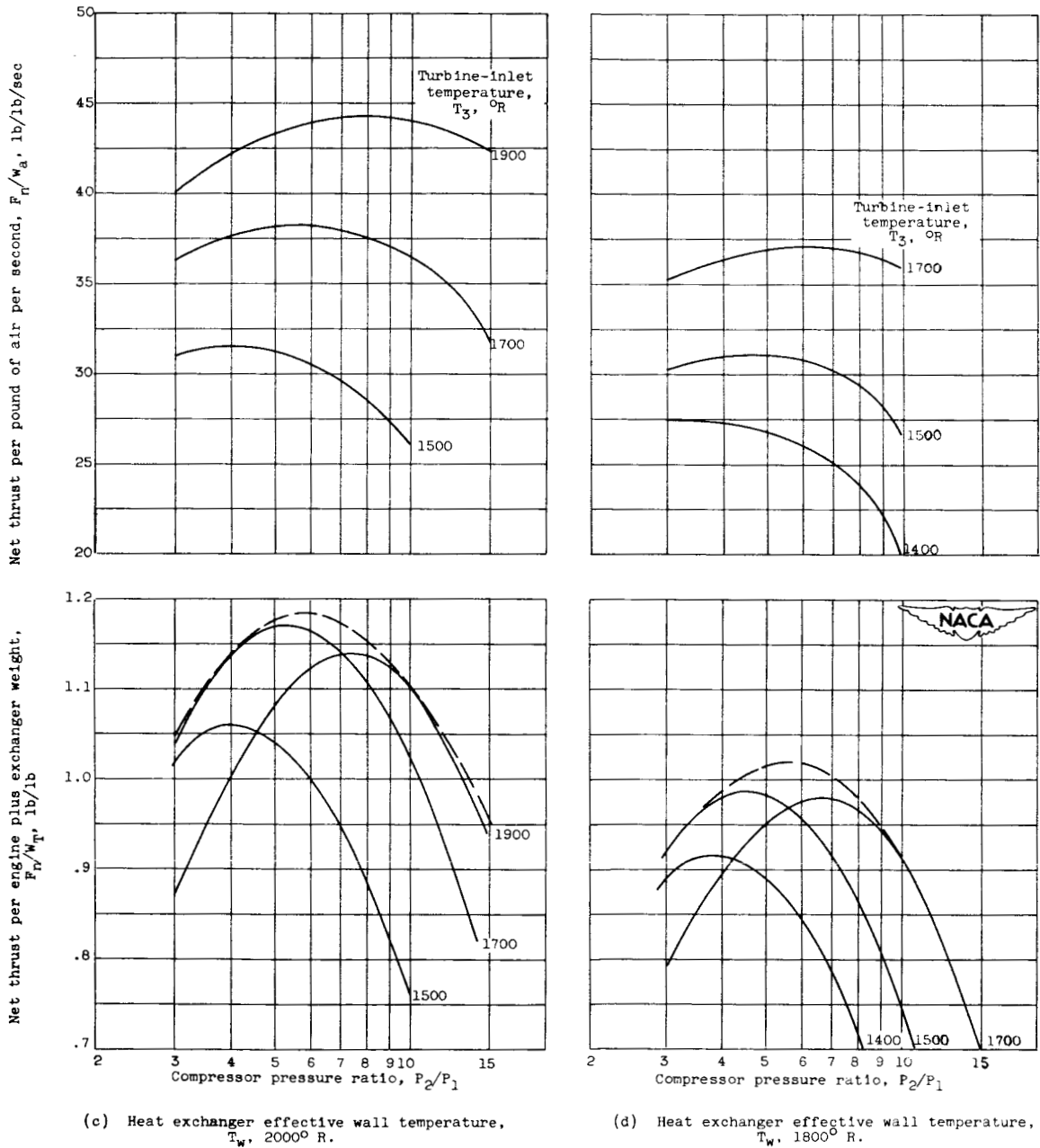
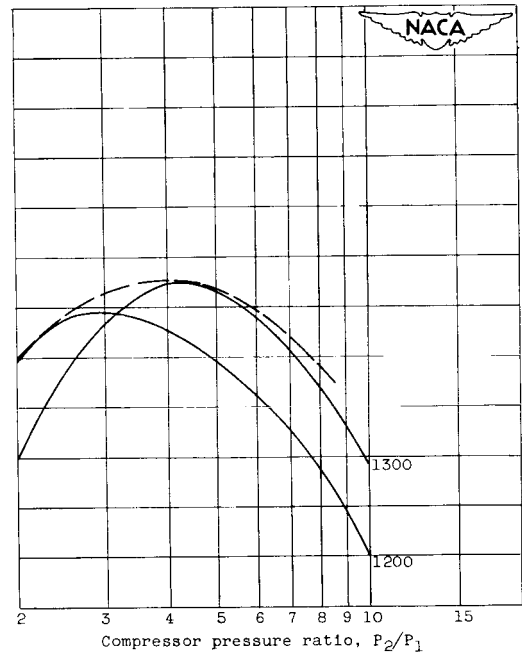
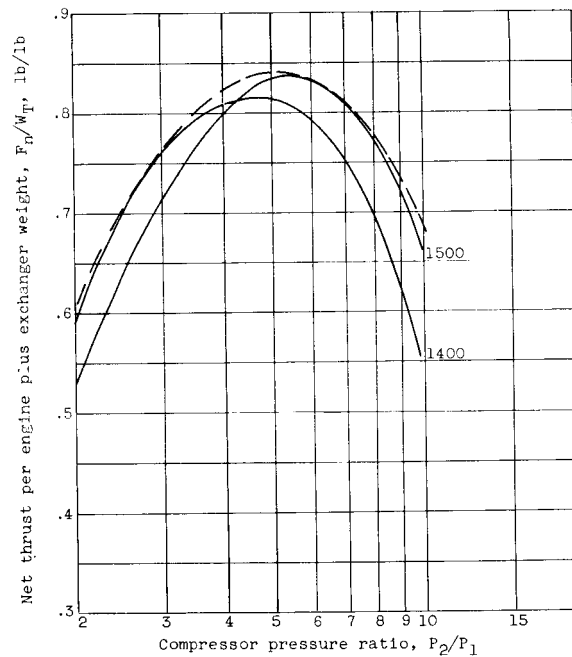
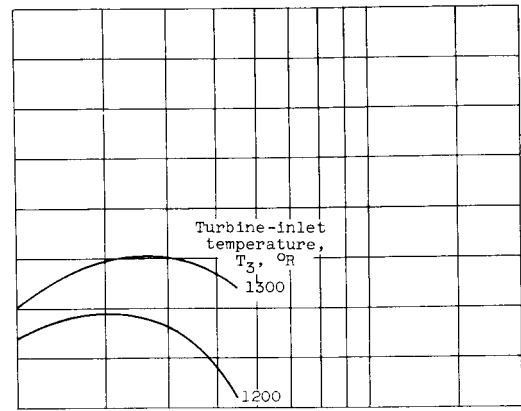
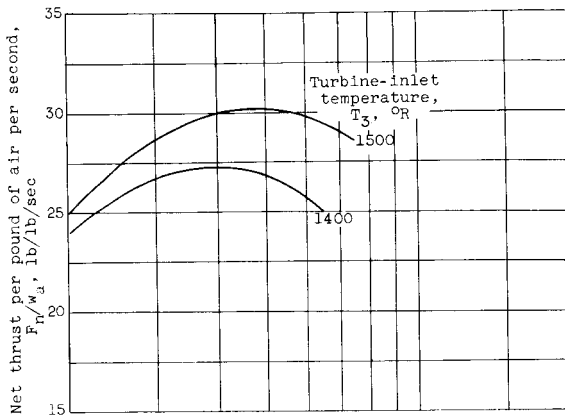


Figure 8. - Continued. Net thrust per engine plus exchanger weight and net thrust per pound of air per second as functions of P_2/P_1 , T_w , and T_3 . Optimum, M_2' ; altitude, 30,000 feet; flight Mach number 0.9.



(e) Heat exchanger effective wall temperature, T_w , 1600° R.

(f) Heat exchanger effective wall temperature, T_w , 1400° R.

Figure 8. - Concluded. Net thrust per engine plus exchanger weight and net thrust per pound of air per second as functions of P_2/P_1 , T_w , and T_3 . Optimum, M_2 ; altitude, 30,000 feet; flight Mach number 0.9.

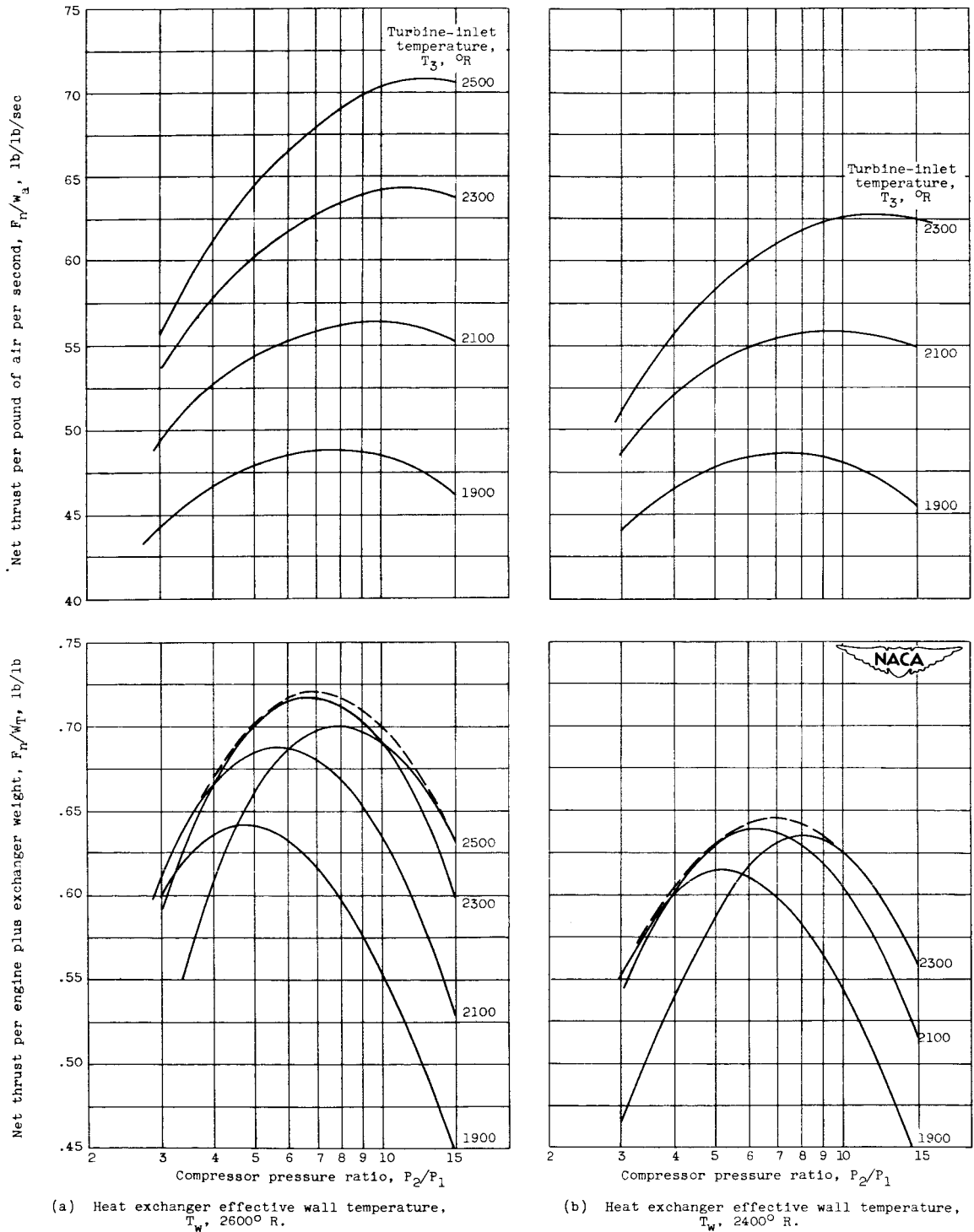
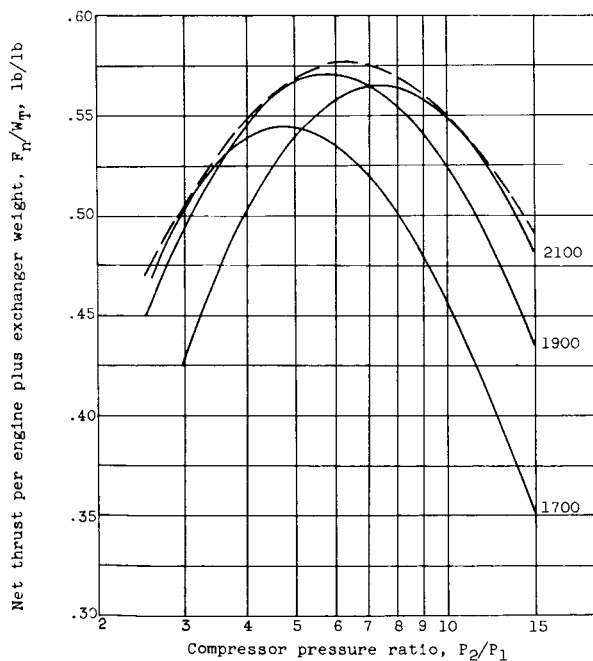
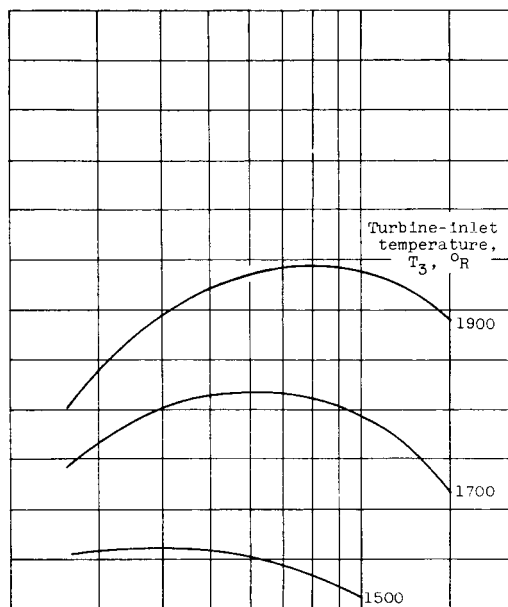
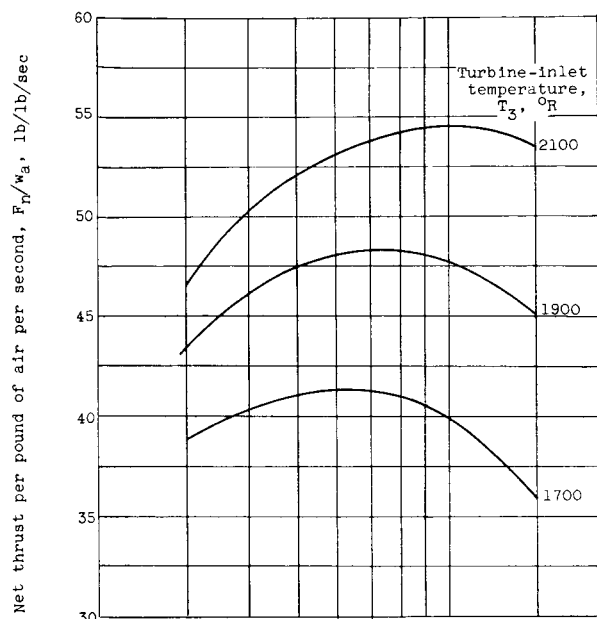
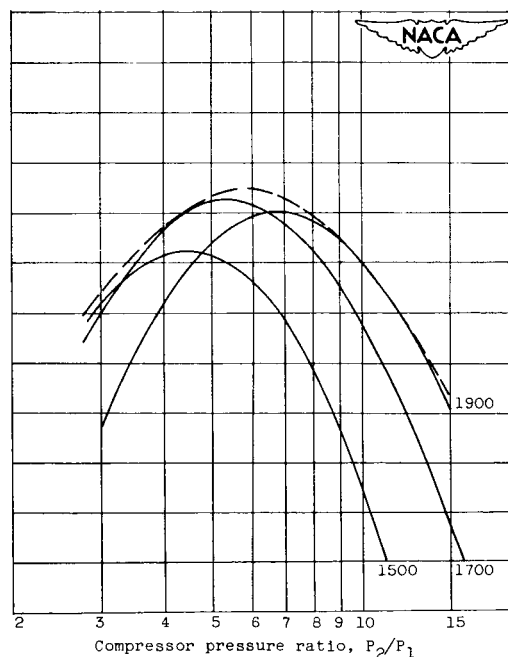


Figure 9. - Net thrust per engine plus exchanger weight and net thrust per pound of air per second as functions of P_2/P_1 , T_w , and T_3 . Optimum, M_2 ; altitude, 50,000 feet; flight Mach number, 0.9.

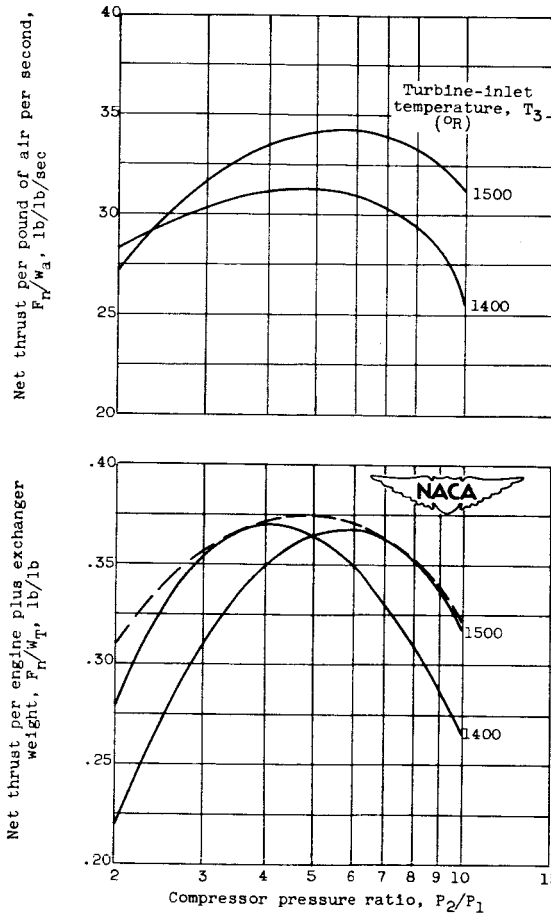


(c) Heat exchanger effective wall temperature, T_w , 2200° R.



(d) Heat exchanger effective wall temperature, T_w , 2000° R.

Figure 9. - Continued. Net thrust per engine plus exchanger weight and net thrust per pound of air per second as functions of P_2/P_1 , T_w , and T_3 . Optimum, M_2' ; altitude, 50,000 feet; flight Mach number, 0.9.



(e) Heat exchanger effective wall temperature, T_w , 1600 °R.

Figure 9. - Concluded. Net thrust per engine plus exchanger weight and net thrust per pound of air per second as functions of P_2/P_1 , T_w , and T_3 . Optimum, M_2' ; altitude, 50,000 feet; flight Mach number, 0.9.

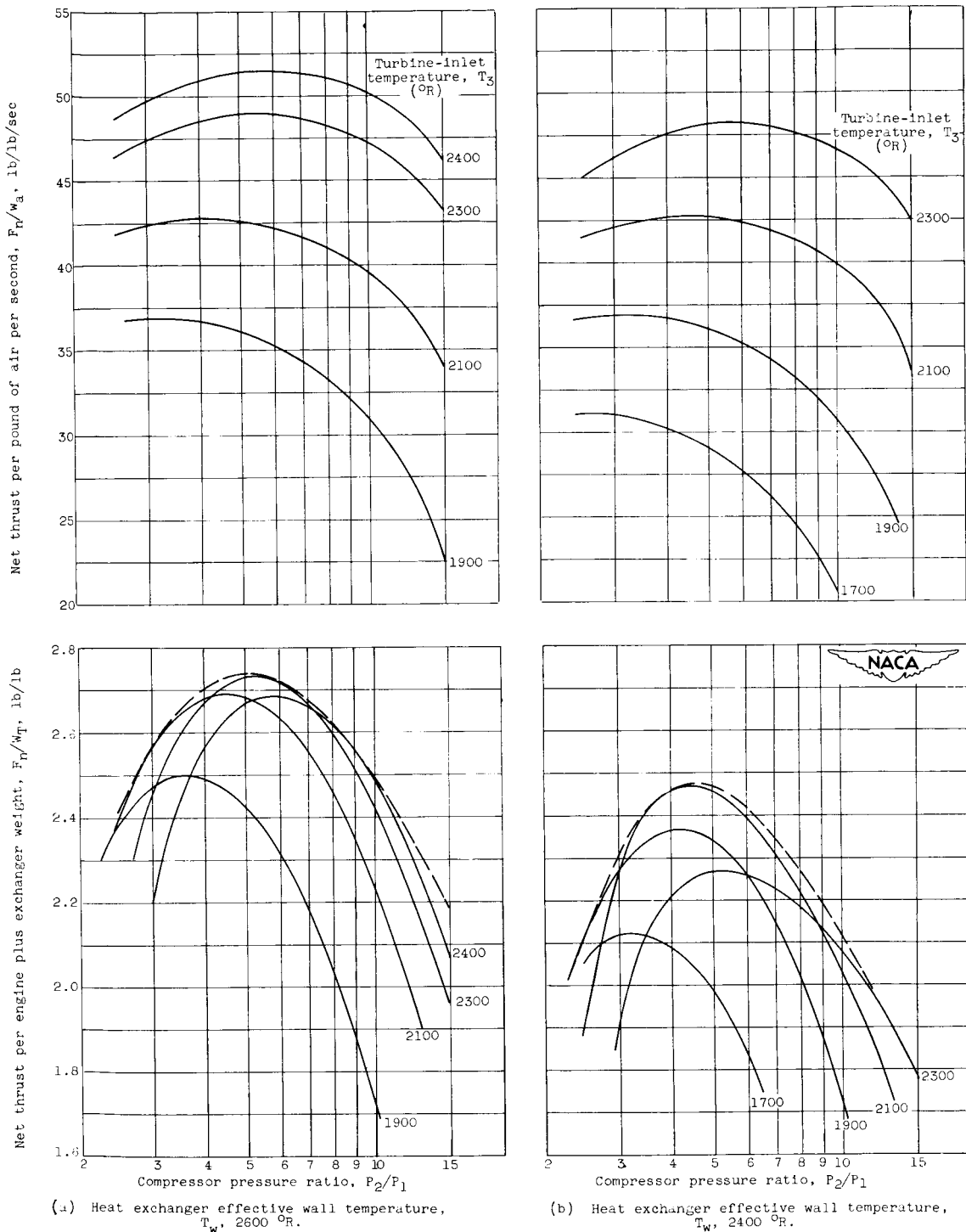


Figure 10. - Net thrust per engine plus exchanger weight and net thrust per pound of air per second as functions of P_2/P_1 , T_w , and T_3 . Optimum M_2 ; altitude 30,000 feet; flight Mach number, 1.5.

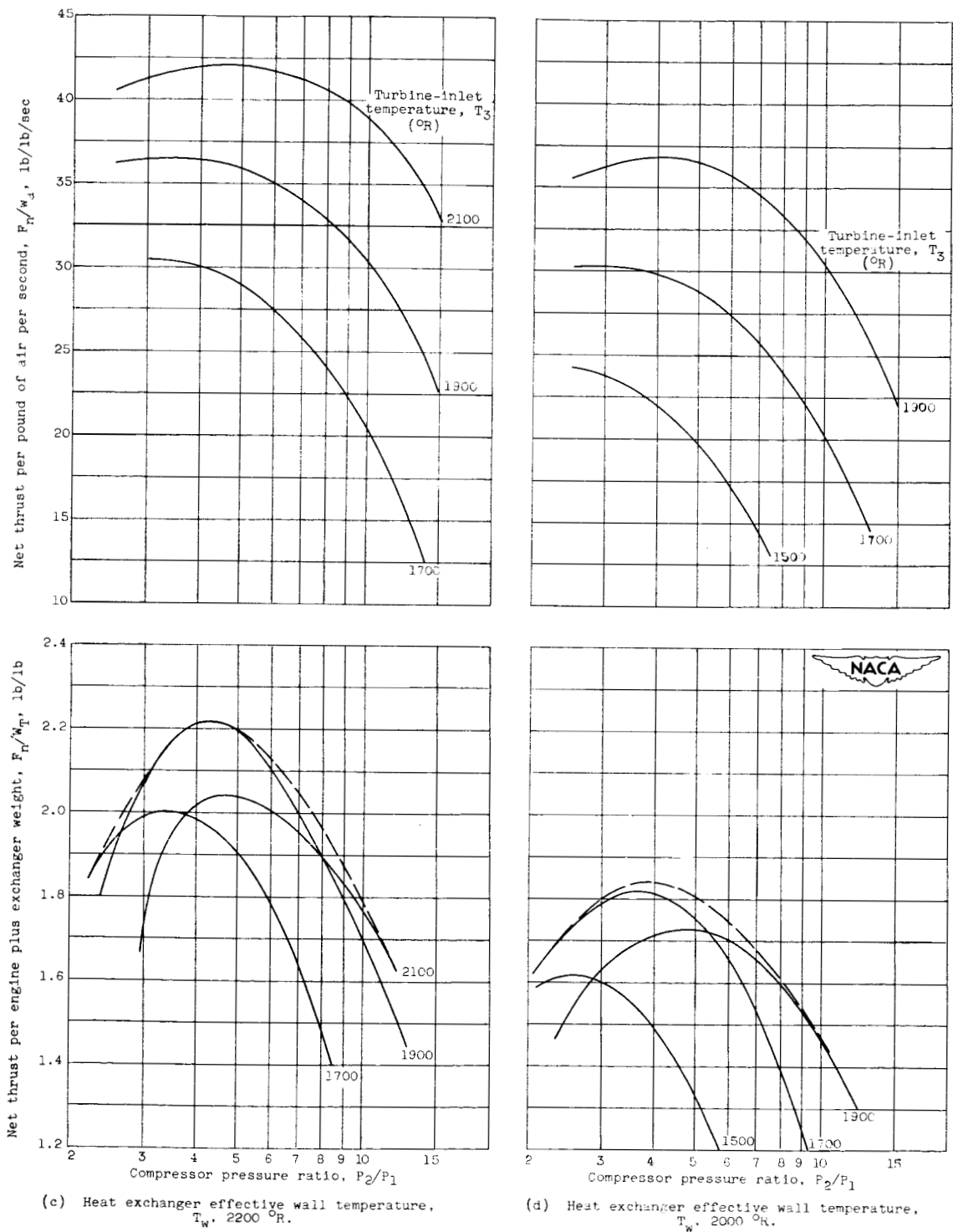
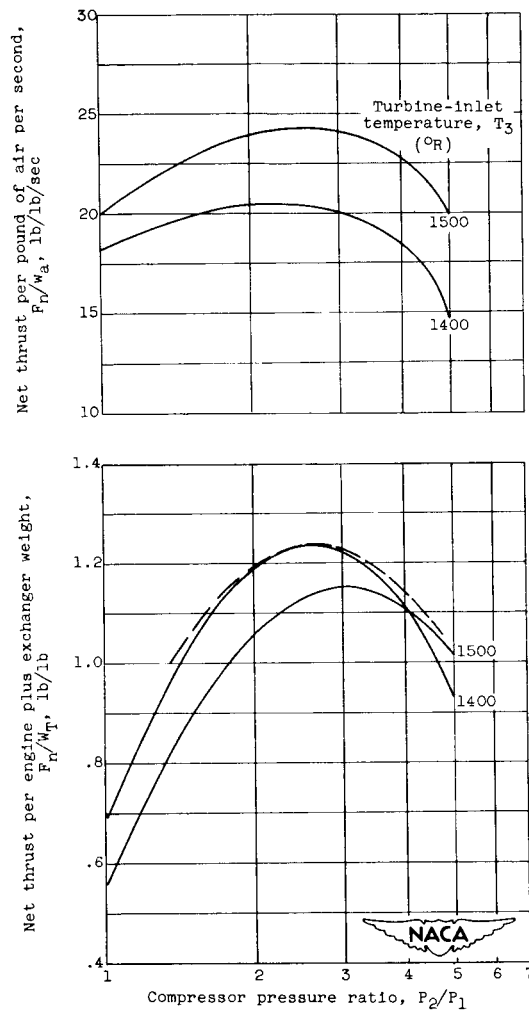


Figure 10. - Continued. Net thrust per engine plus exchanger weight and net thrust per pound of air per second as functions of P_2/P_1 , T_w , and T_3 . Optimum M_2' ; altitude 30,000 feet; flight Mach number, 1.5.



(e) Heat exchanger effective wall temperature, T_w , 1600 °R.

Figure 10. - Concluded. Net thrust per engine plus exchanger weight and net thrust per pound of air per second as functions of P_2/P_1 , T_w , and T_3 . Optimum M_2 ; altitude 30,000 feet; flight Mach number, 1.5.

DECLASSIFIED

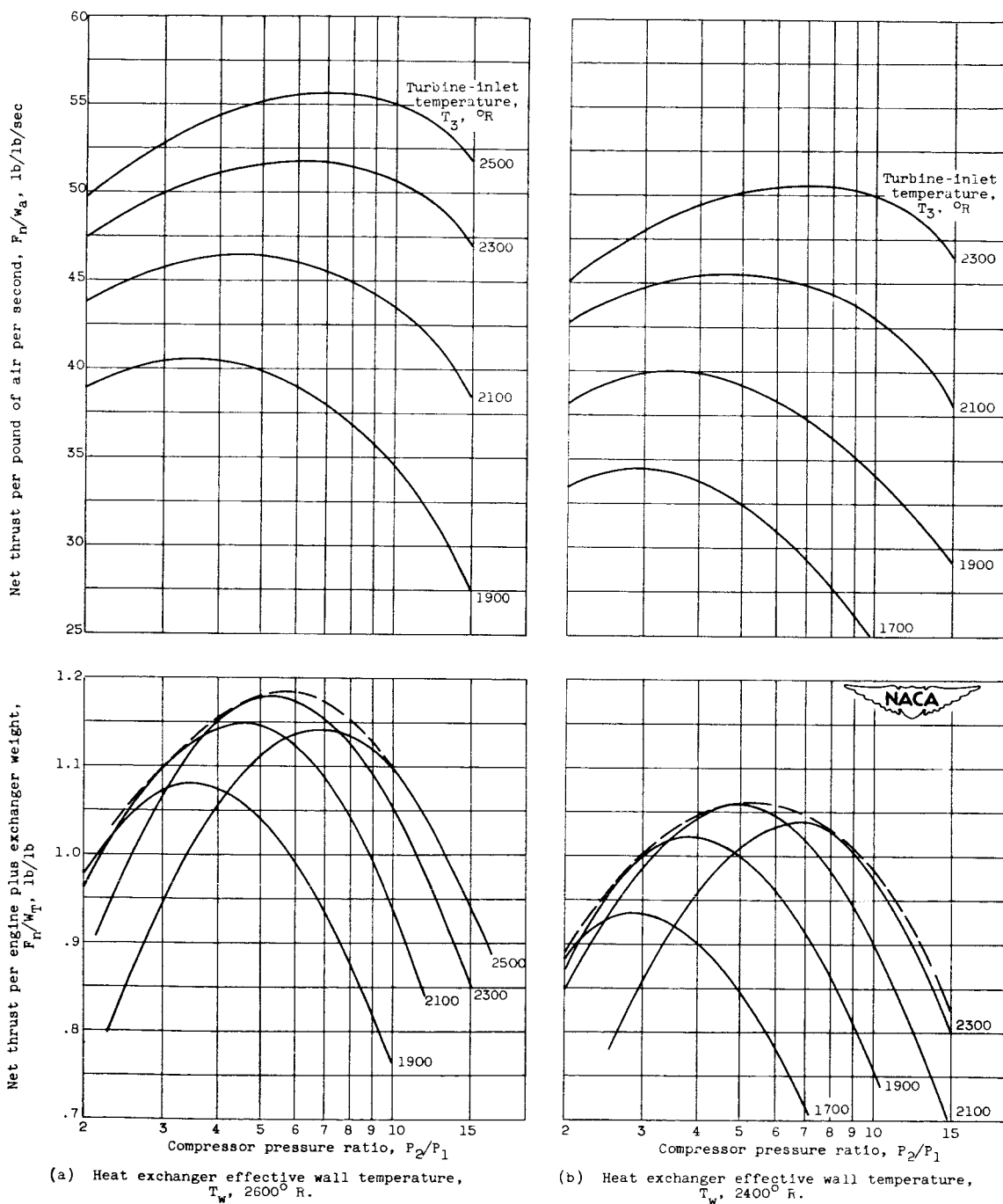
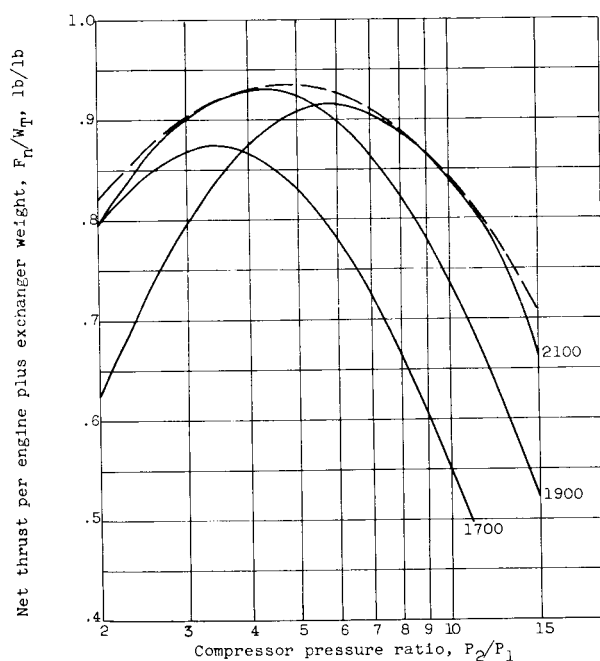
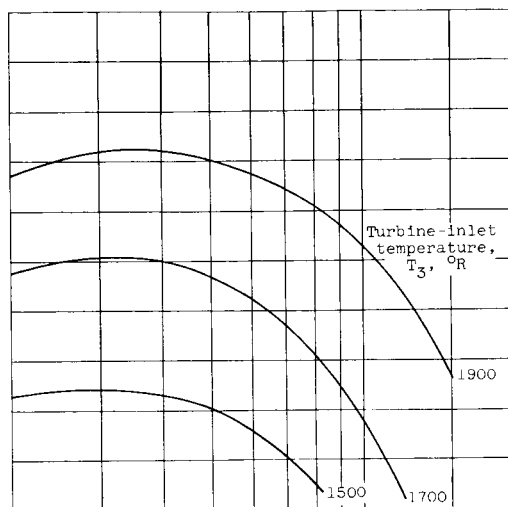
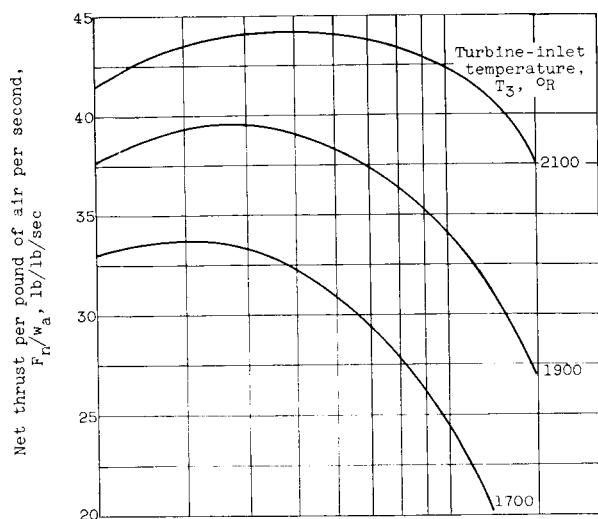
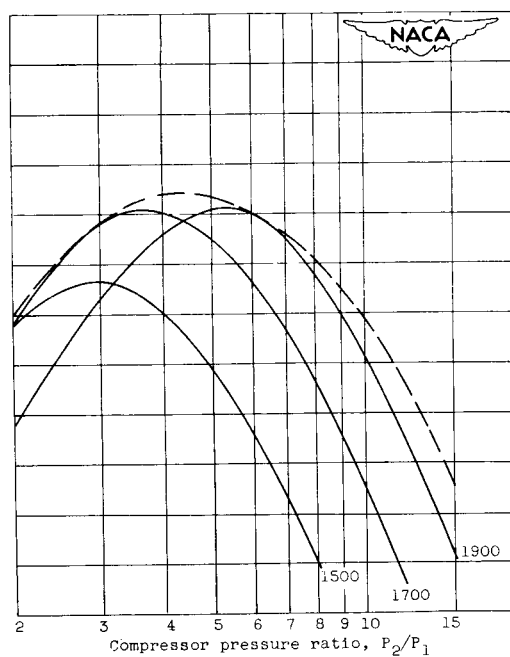


Figure 11. - Net thrust per engine plus exchanger weight and net thrust per pound of air per second as functions of P_2/P_1 , T_w , and T_3 . Optimum M_2 ; altitude, 50,000 feet; flight Mach number, 1.5.

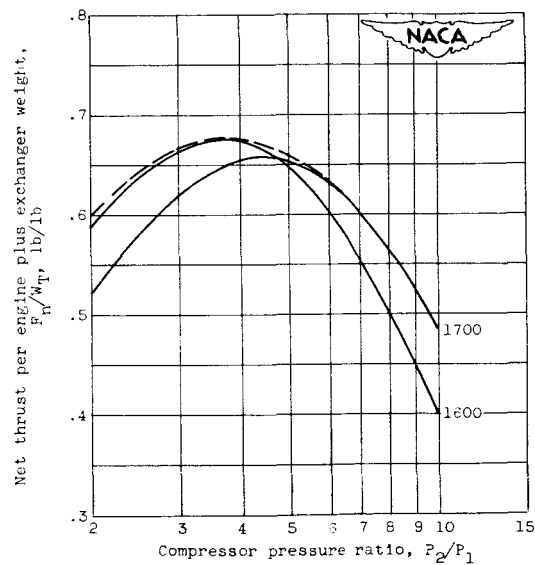
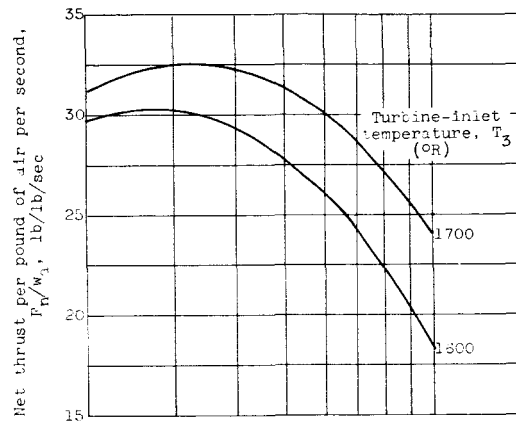


(c) Heat exchanger effective wall temperature, T_w , 2200° R.



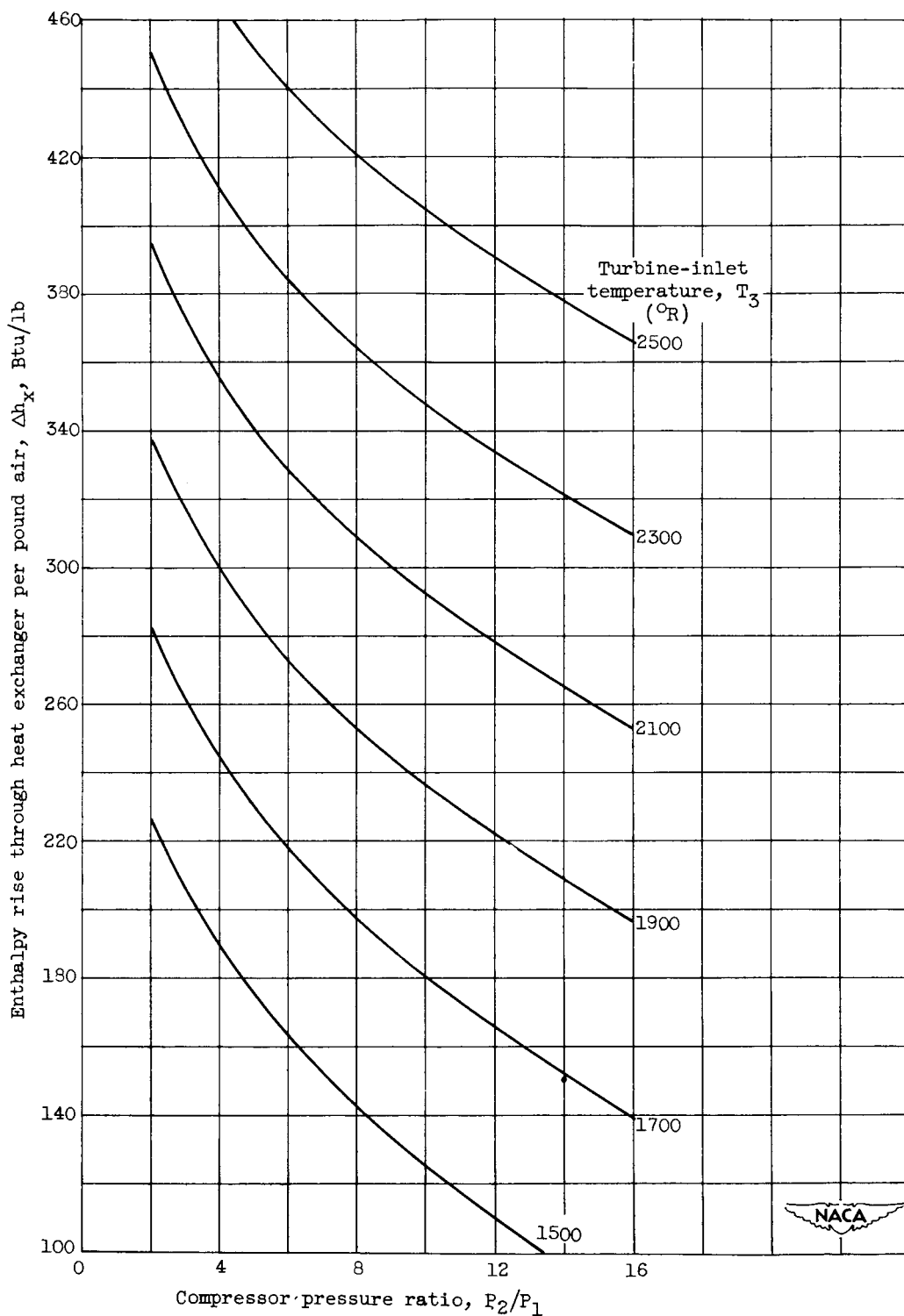
(d) Heat exchanger effective wall temperature, T_w , 2000° R.

Figure 11. - Continued. Net thrust per engine plus exchanger weight and net thrust per pound of air per second as functions of P_2/P_1 , T_w , and T_3 . Optimum M_2 ; altitude, 50,000 feet; flight Mach number, 1.5.



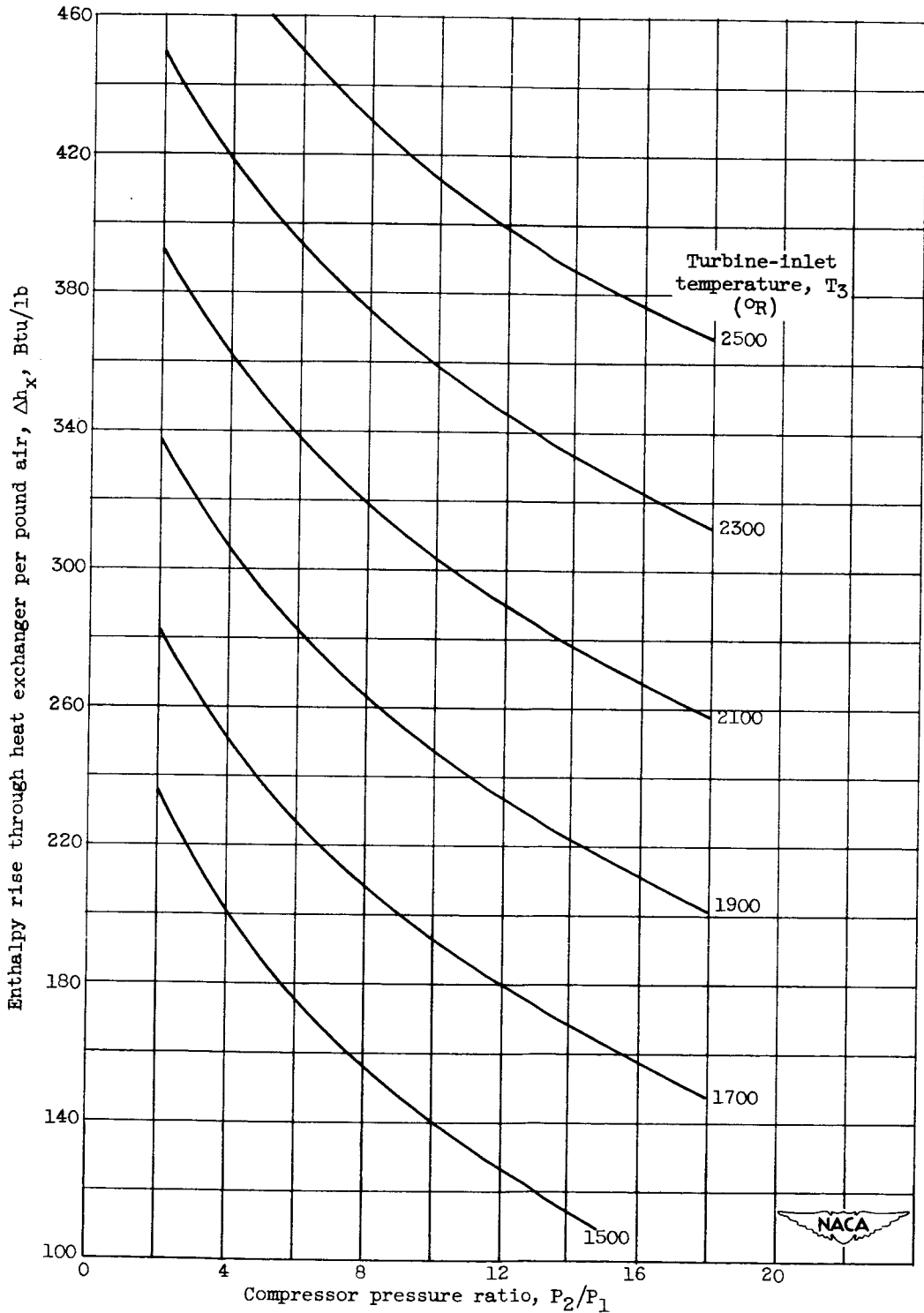
(e) Heat exchanger effective wall temperature,
 T_w , 1800 °R.

Figure 11. - Concluded. Net thrust per engine plus exchanger weight and net thrust per pound of air per second as functions of P_2/P_1 , T_w , and T_3 . Optimum M_2' ; altitude, 50,000 feet; flight Mach number, 1.5.



(a) Altitude, 30,000 feet; flight Mach number, 0.9.

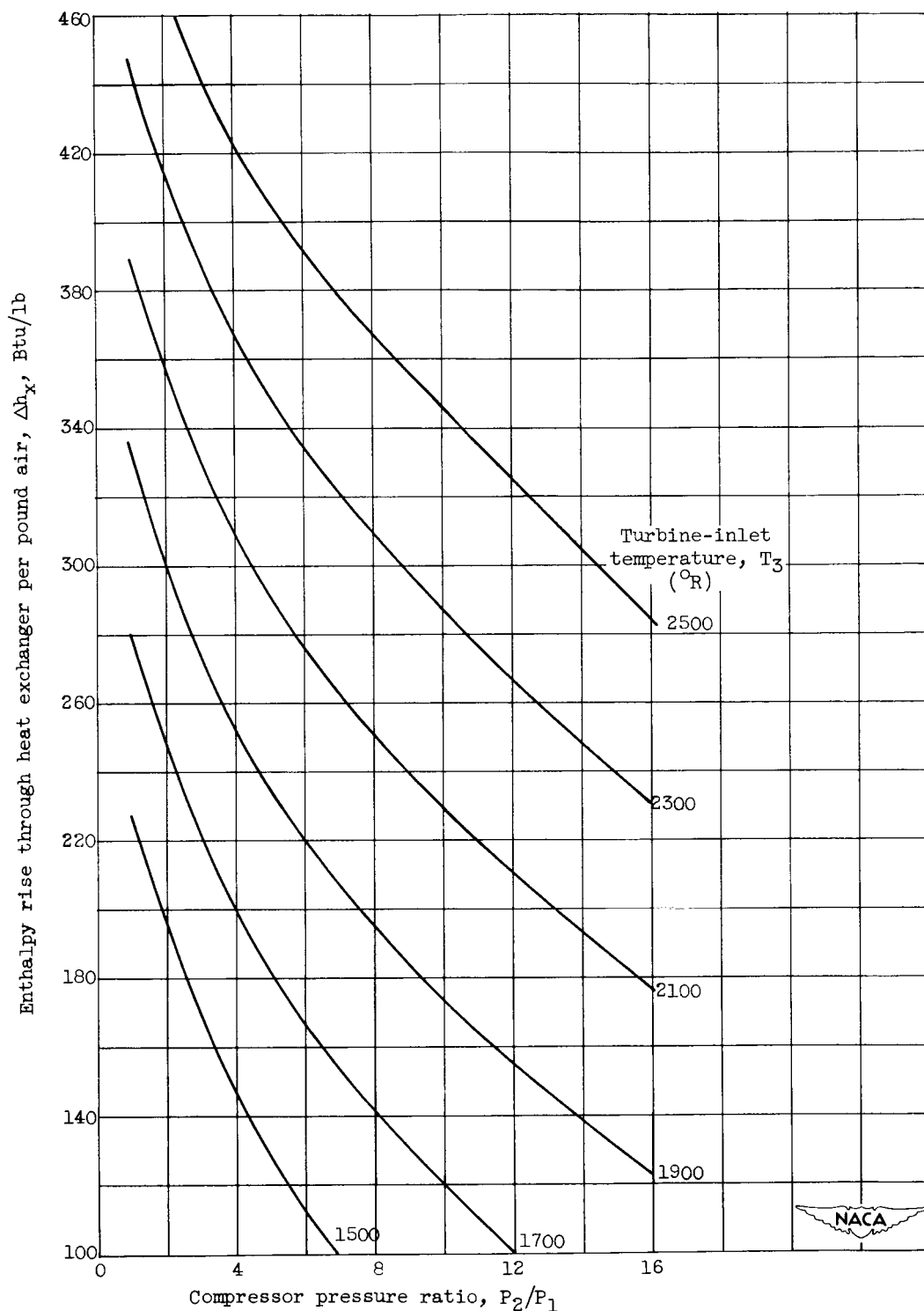
Figure 12. - Enthalpy rise of air through the heat exchanger as a function of compressor pressure ratio and turbine-inlet temperature.



(b) Altitude, 50,000 feet; flight Mach number, 0.9.

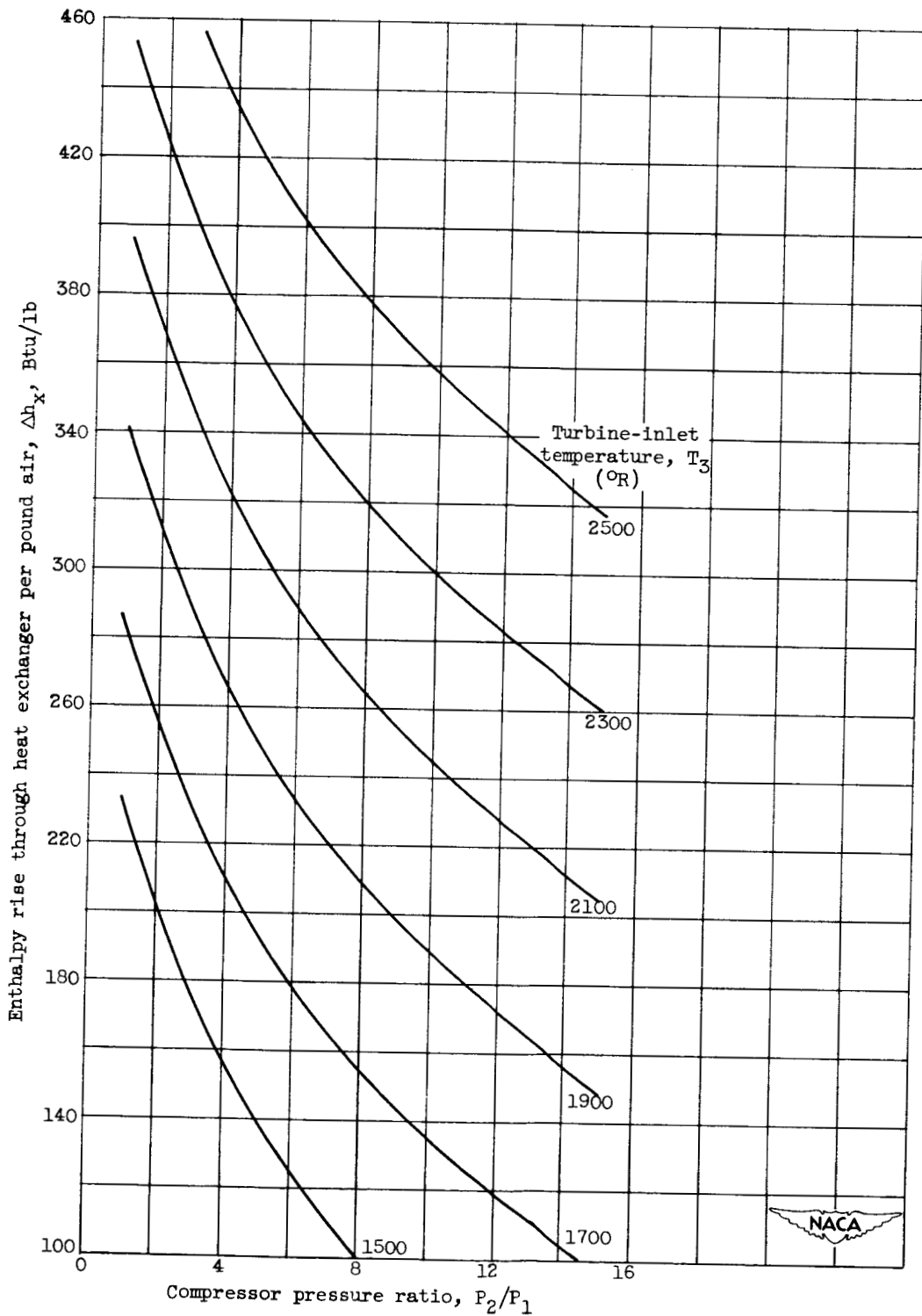
Figure 12. - Continued. Enthalpy rise of air through the heat exchanger as a function of compressor pressure ratio and turbine-inlet temperature.

0371230 1970



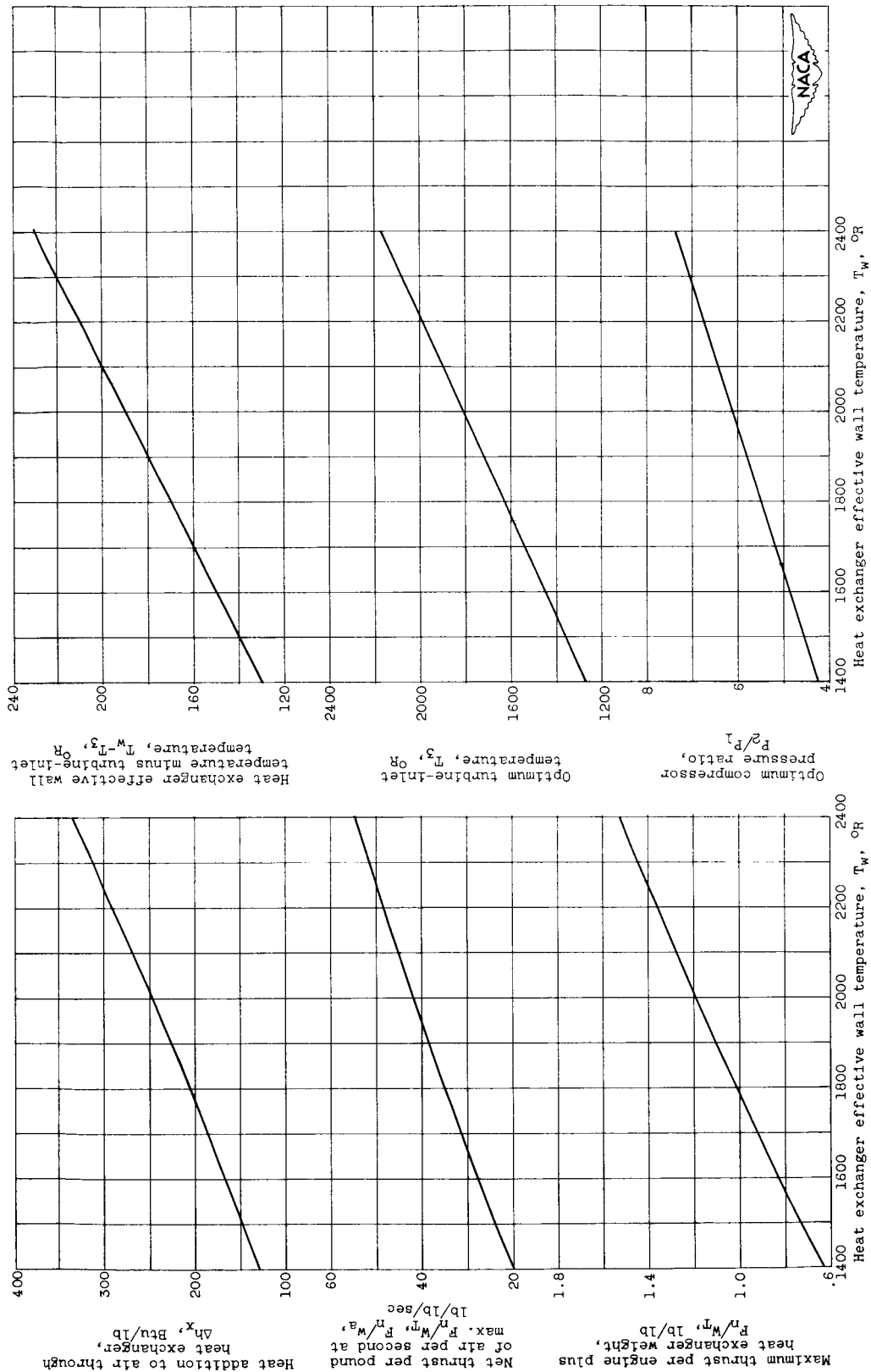
(c) Altitude, 30,000 feet; flight Mach number, 1.5.

Figure 12. - Continued. Enthalpy rise of air through the heat exchanger as a function of compressor pressure ratio and turbine-inlet temperature.



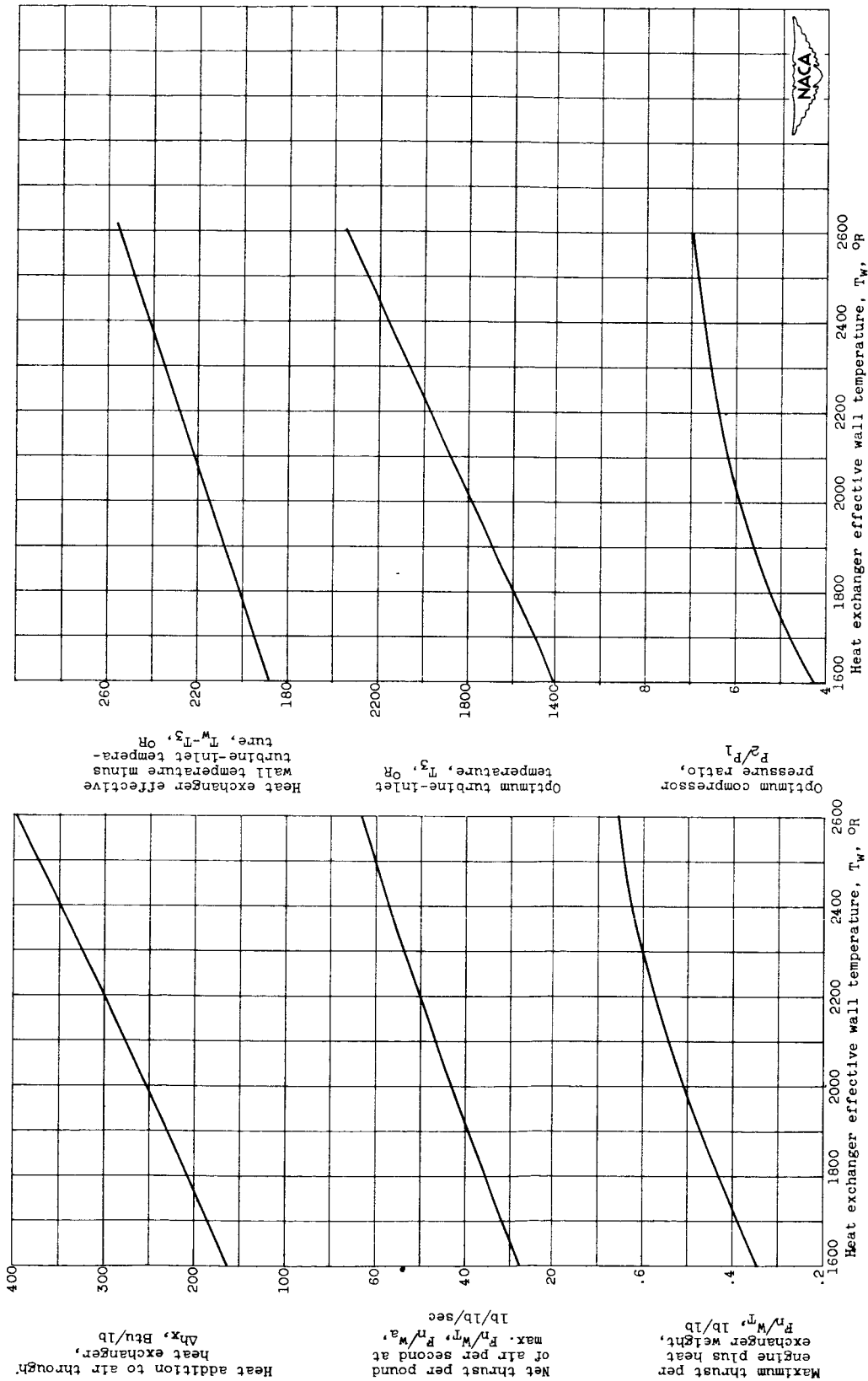
(d) Altitude, 50,000 feet; flight Mach number, 1.5.

Figure 12. - Concluded. Enthalpy rise of air through the heat exchanger as a function of compressor pressure ratio and turbine-inlet temperature.

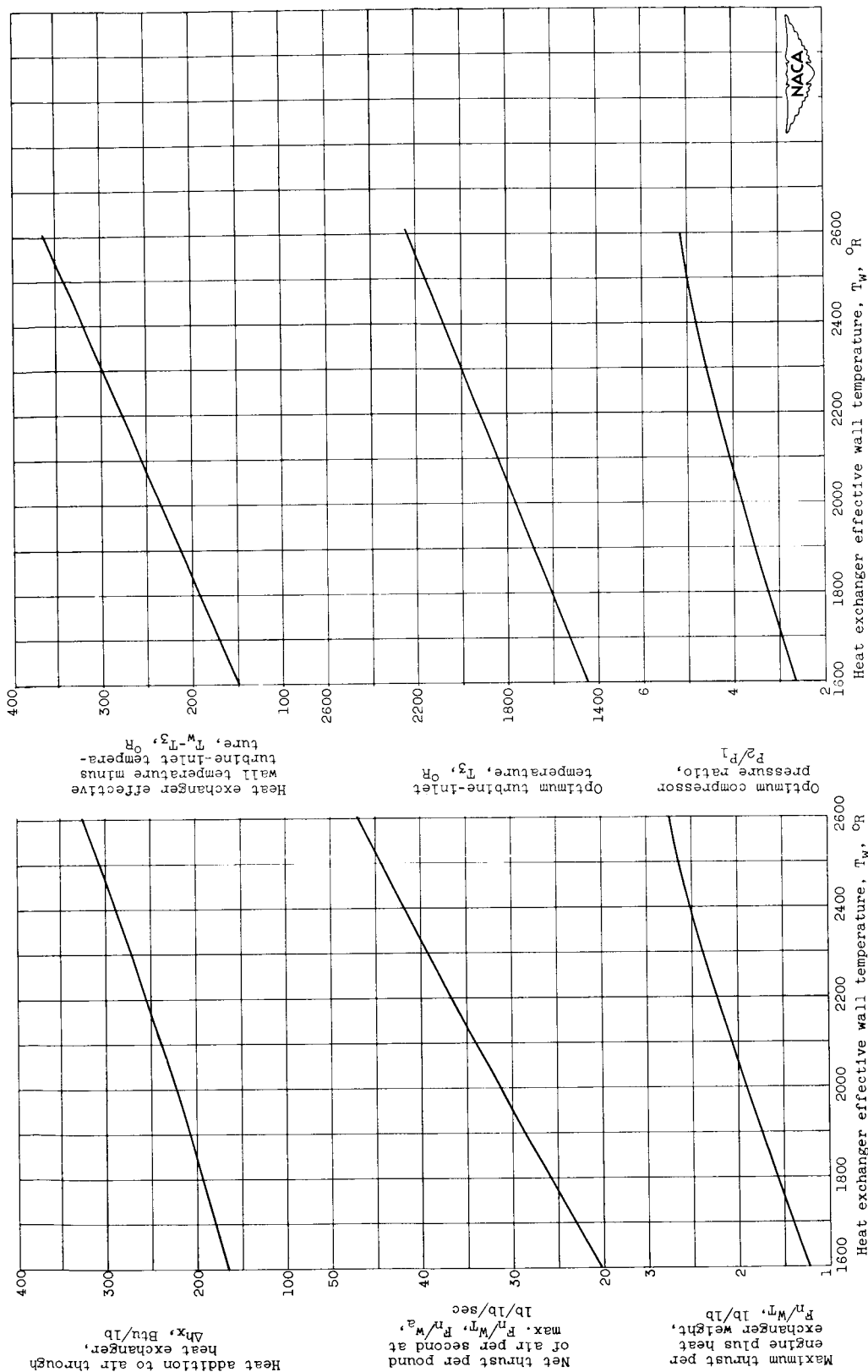


(a) Altitude, 30,000 feet; flight Mach number 0.9.

Figure 13. - Effect of heat exchanger effective wall temperature on optimum engine performance. Optimum M_2' .

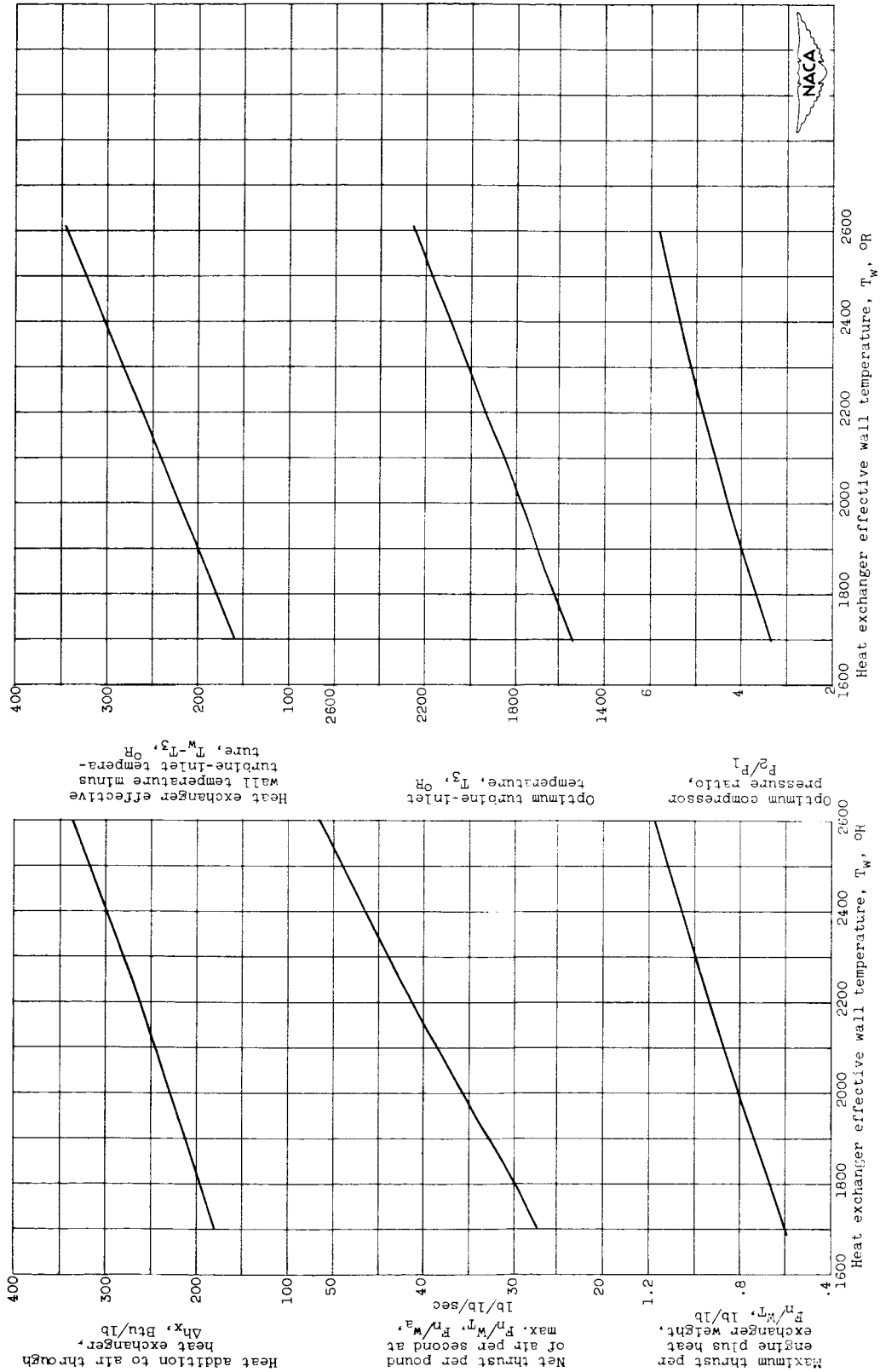


(b) Altitude 50,000 feet; flight Mach number 0.9.
Figure 13. - Continued. Effect of heat exchanger effective wall temperature on optimum engine performance. Optimum M_2 .

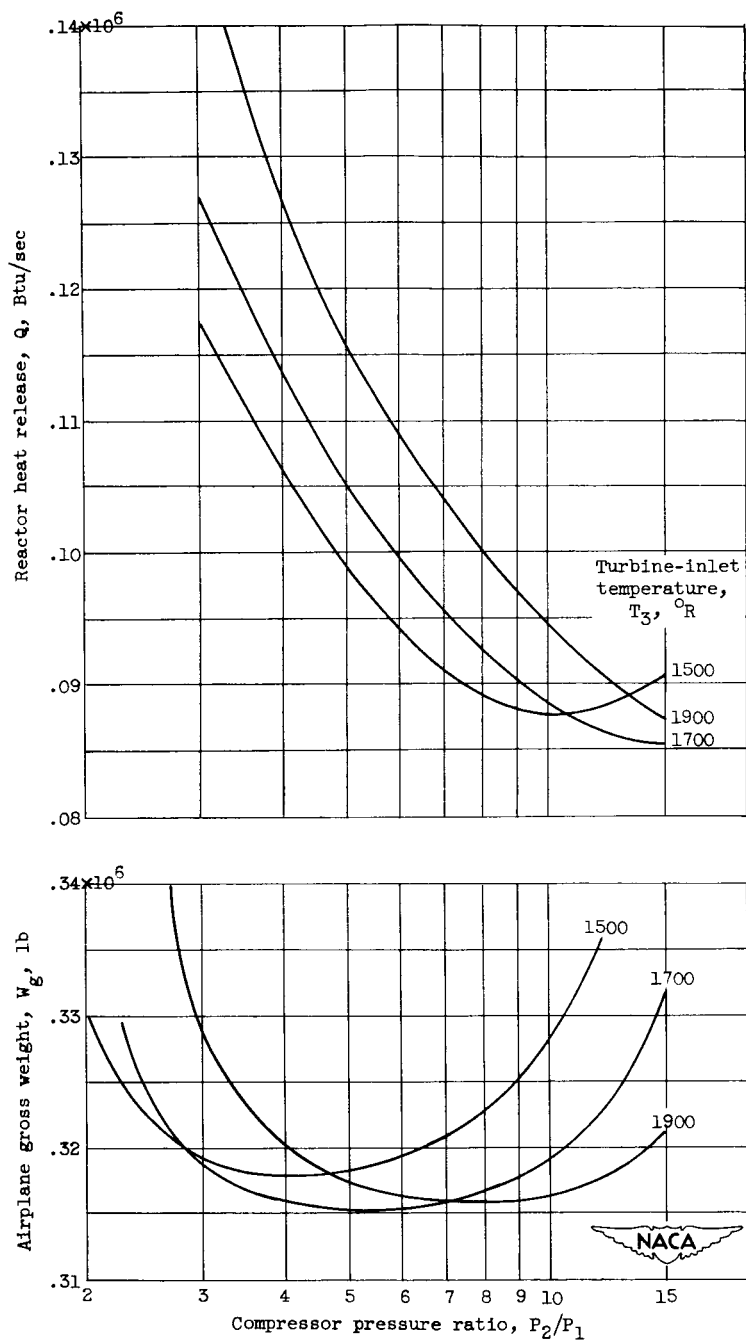


(c) Altitude 30,000 feet; flight Mach number 1.5.

Figure 13. - Continued. Effect of heat exchanger effective wall temperature on optimum engine performance. Optimum M_2 .



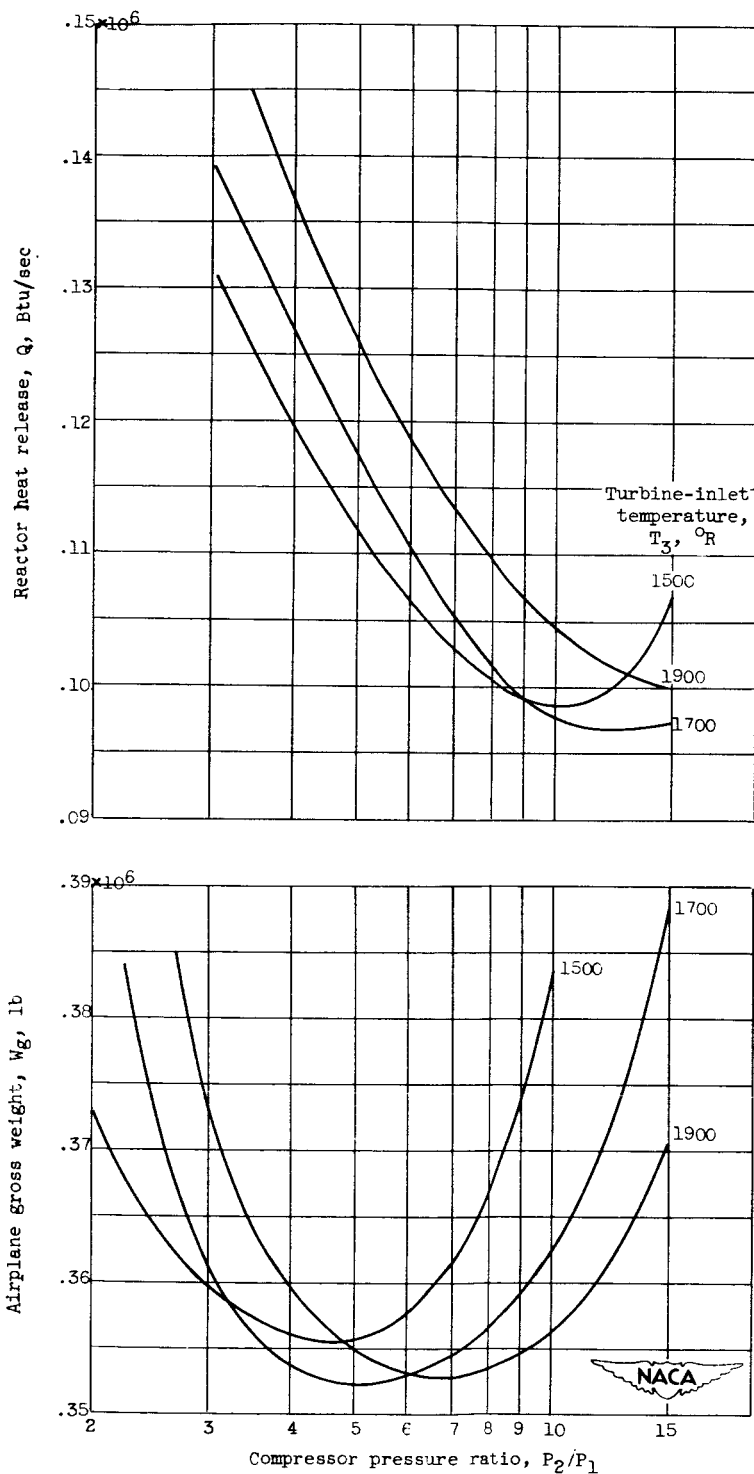
(d) Altitude 50,000 feet; flight Mach number 1.5.
Figure 13. - Concluded. Effect of heat exchanger effective wall temperature on optimum engine performance. Optimum M_2 .



(a) Reactor maximum wall temperature, 2050 $^{\circ}\text{R}$. Altitude, 30,000 feet; flight Mach number, 0.9; L/D , 18.

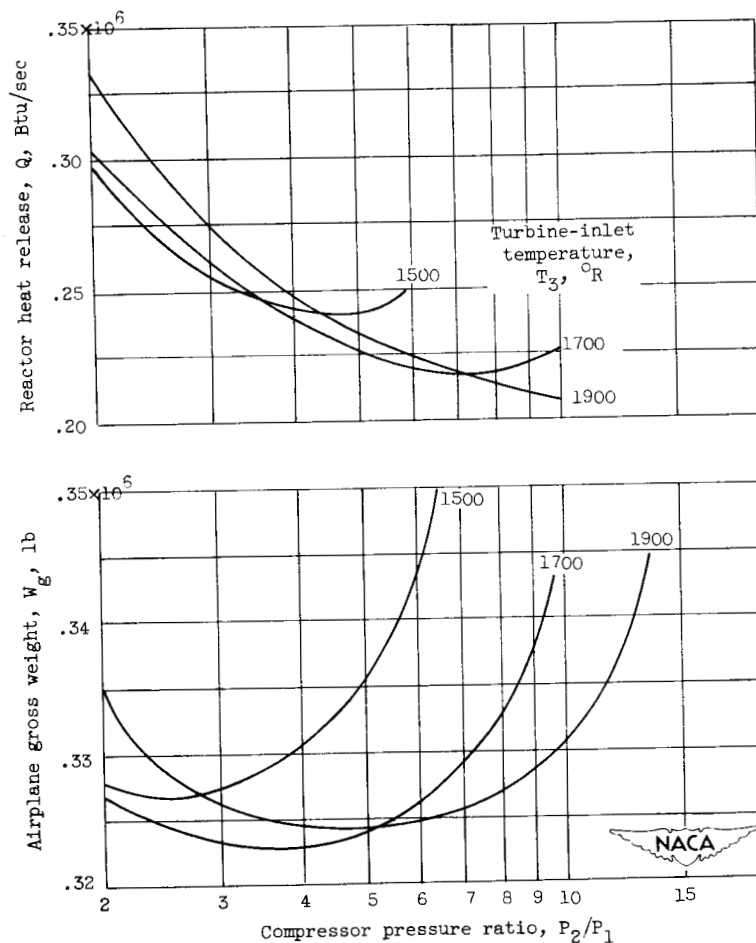
Figure 14. - Airplane gross weight and reactor heat release as a function of compressor pressure ratio and turbine-inlet temperature. T_w , 2000 $^{\circ}\text{R}$; optimum, M_2 ; W_s/W_g , 0.35; W_K , 190,000 pounds.

DECLASSIFIED



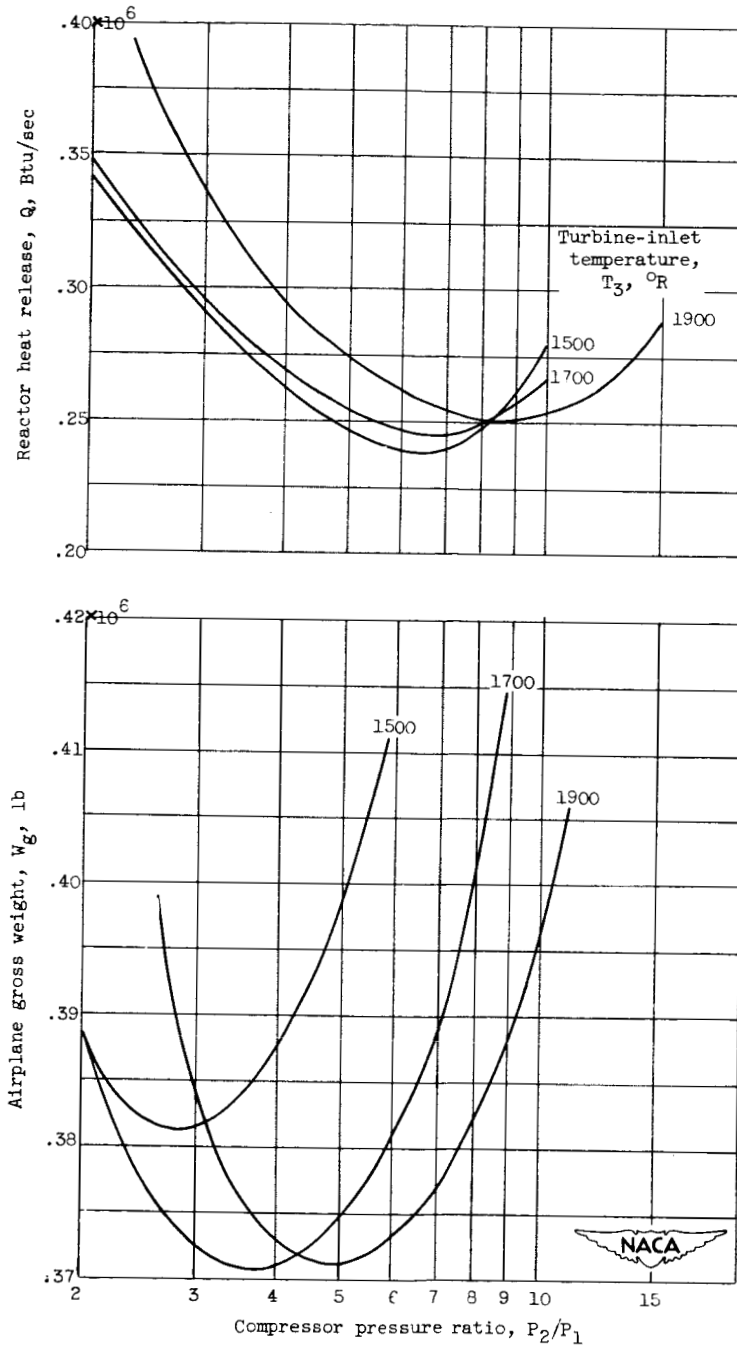
(b) Reactor maximum wall temperature, 2050 $^{\circ}\text{R}$. Altitude, 50,000 feet; flight Mach number, 0.9; L/D , 18.

Figure 14. - Continued. Airplane gross weight and reactor heat release as a function of compressor pressure ratio and turbine-inlet temperature. T_w , 2000 $^{\circ}\text{R}$; optimum, M_2' ; W_s/W_g , 0.35; W_K , 190,000 pounds.



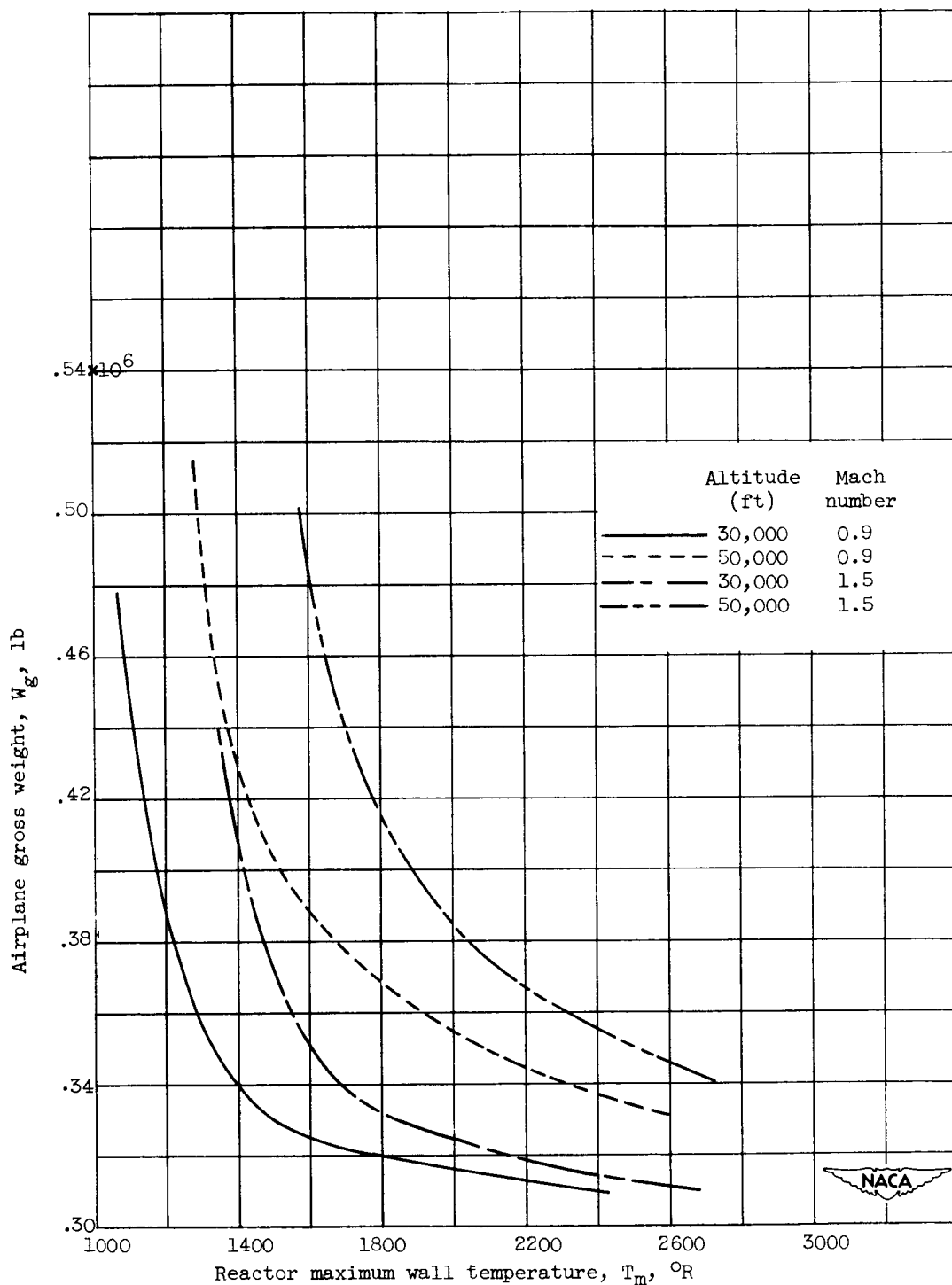
(c) Reactor maximum wall temperature, 2100 °R. Altitude, 30,000 feet; flight Mach number, 1.5; L/D , 9.

Figure 14. - Continued. Airplane gross weight and reactor heat release as a function of compressor pressure ratio and turbine-inlet temperature. T_w , 2000 °R; optimum, M_2 '; W_6/W_g , 0.35; W_K , 190,000 pounds.



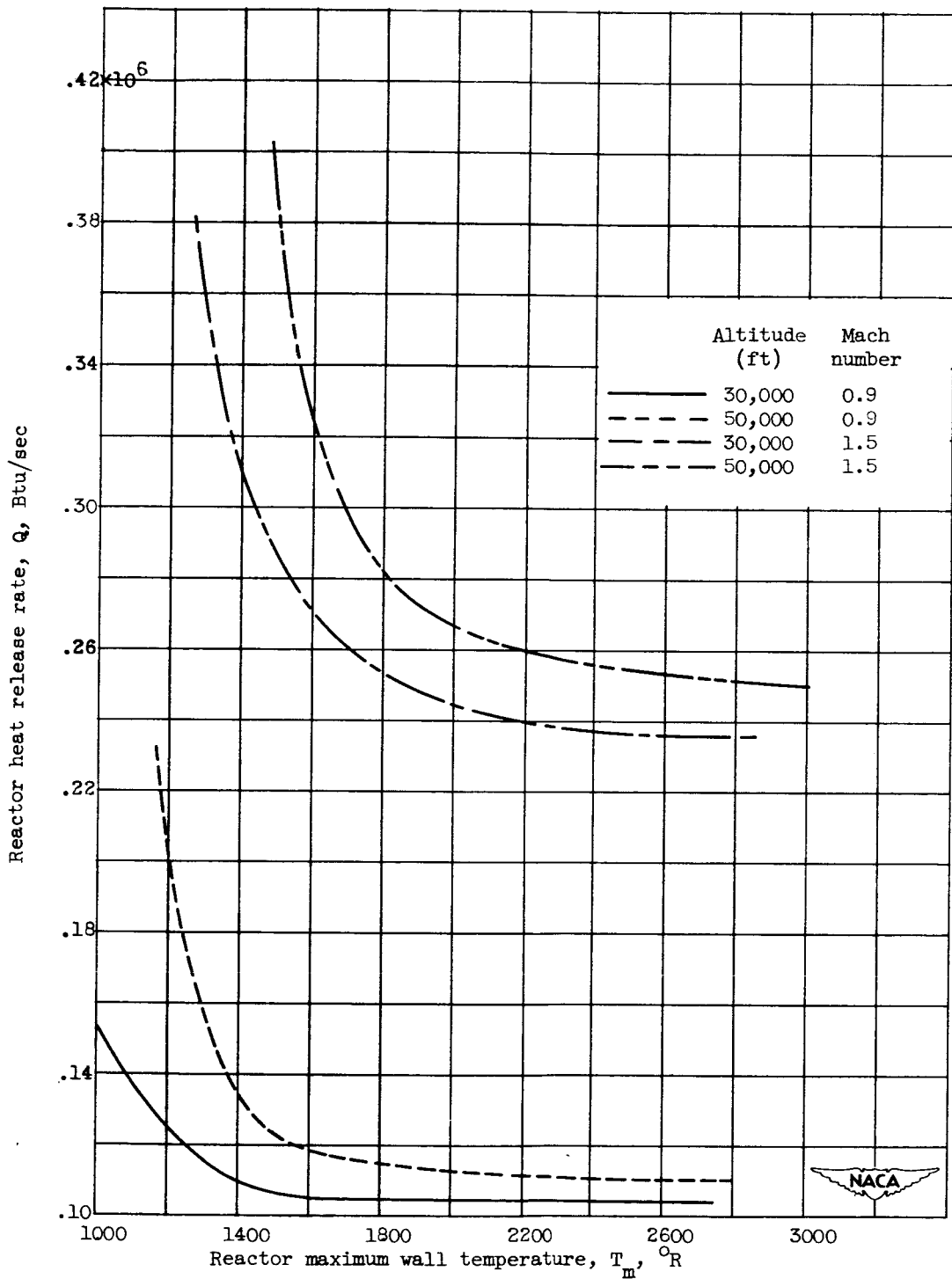
(d) Reactor maximum wall temperature, 2150 °R. Altitude, 50,000 feet; flight Mach number, 1.5; L/D , 9.

Figure 14. - Concluded. Airplane gross weight and reactor heat release as a function of compressor pressure ratio and turbine-inlet temperature. T_w , 2000 °R; optimum, M_2 ; W_s/W_g , 0.35; W_K , 190,000 pounds.



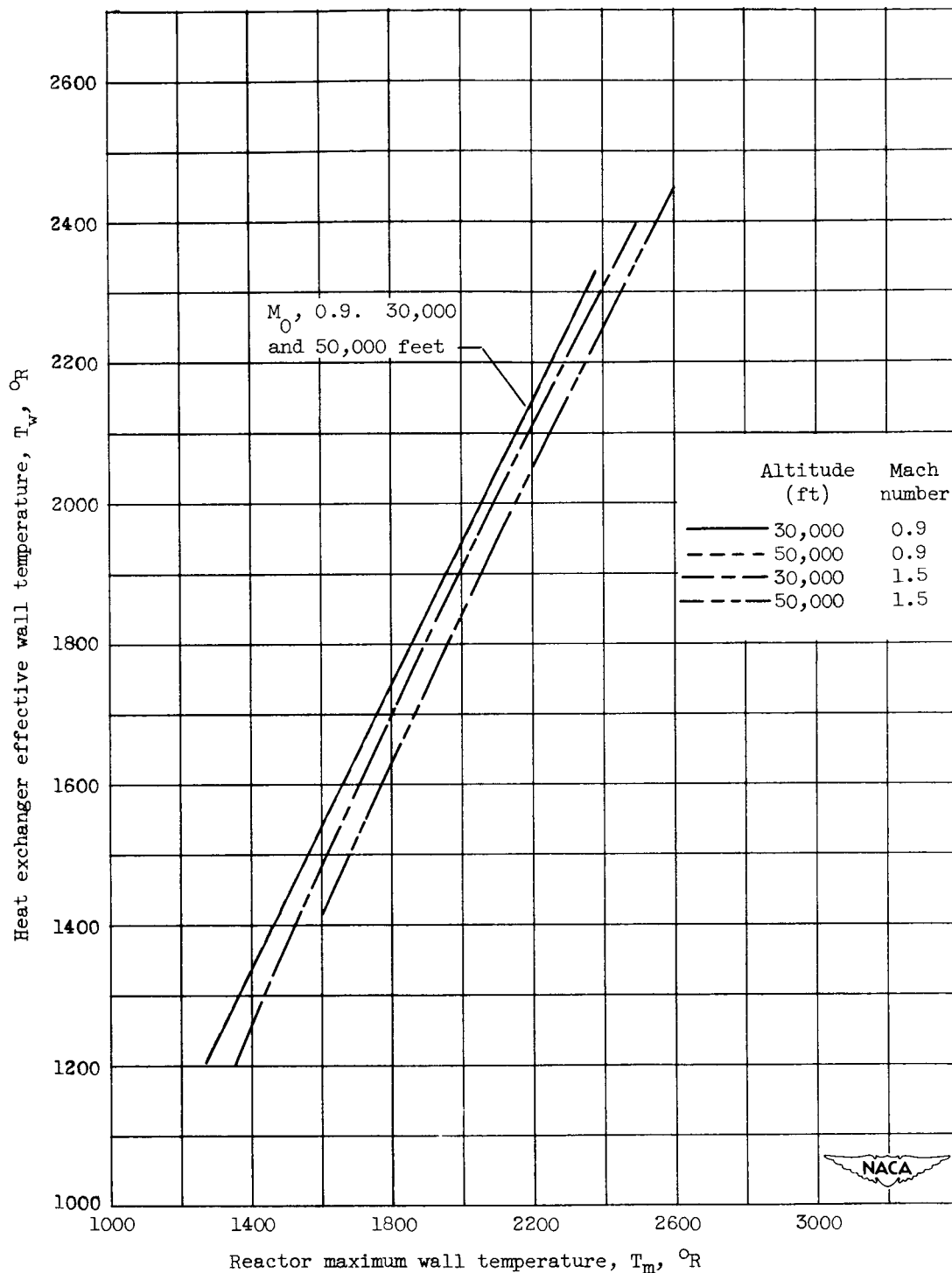
(a) Airplane gross weight.

Figure 15.- Effect of reactor maximum wall temperature on airplane gross weight, reactor heat release rate, heat-exchanger effective wall temperature. Optimum, T_3 ; optimum, P_2/P_1 ; optimum M_2' ; W_s/W_g , 0.35; W_K , 190,000 pounds.



(b) Reactor heat release rate.

Figure 15. - Continued. Effect of reactor maximum wall temperature on airplane gross weight, reactor heat release rate, heat exchanger effective wall temperature. Optimum, T_3 ; optimum, P_2/P_1 ; optimum M_2' ; W_s/W_g , 0.35; W_K , 190,000 pounds.



(c) Heat exchanger effective wall temperature.

Figure 15. - Concluded. Effect of reactor maximum wall temperature on airplane gross weight, reactor heat release rate, heat exchanger effective wall temperature. Optimum, T_3 , optimum, P_2/P_1 ; optimum M_2' ; W_s/W_g , 0.35; W_K , 190,000 pounds.

DECLASSIFIED

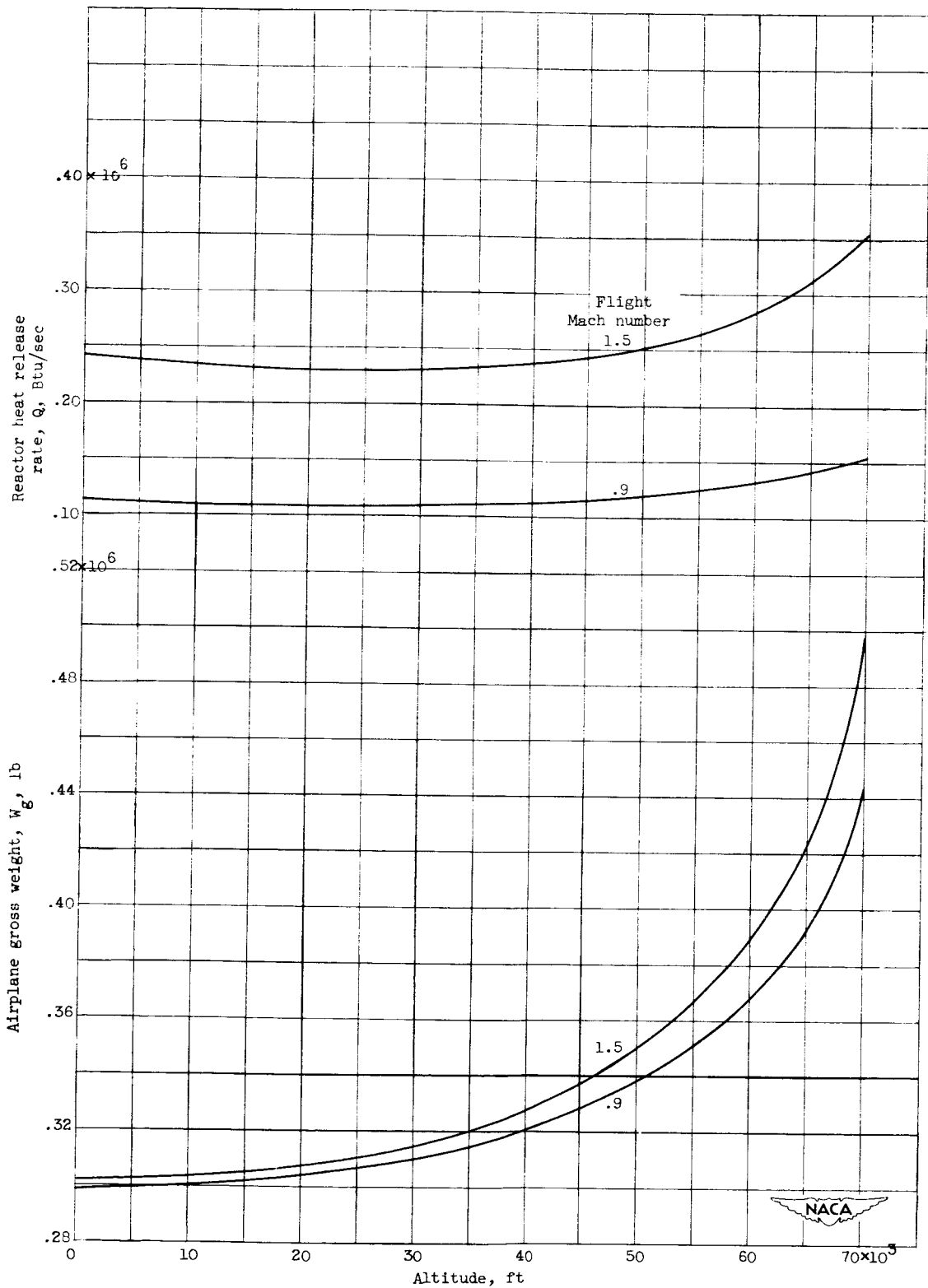


Figure 16. - Effect of altitude on airplane gross weight and reactor heat release rate. T_w , 2400 °R; T_3 , 2000 °R; P_2/P_1 , 5.0; optimum M_2' ; W_s/W_g , 0.35; W_K , 190,000 pounds.

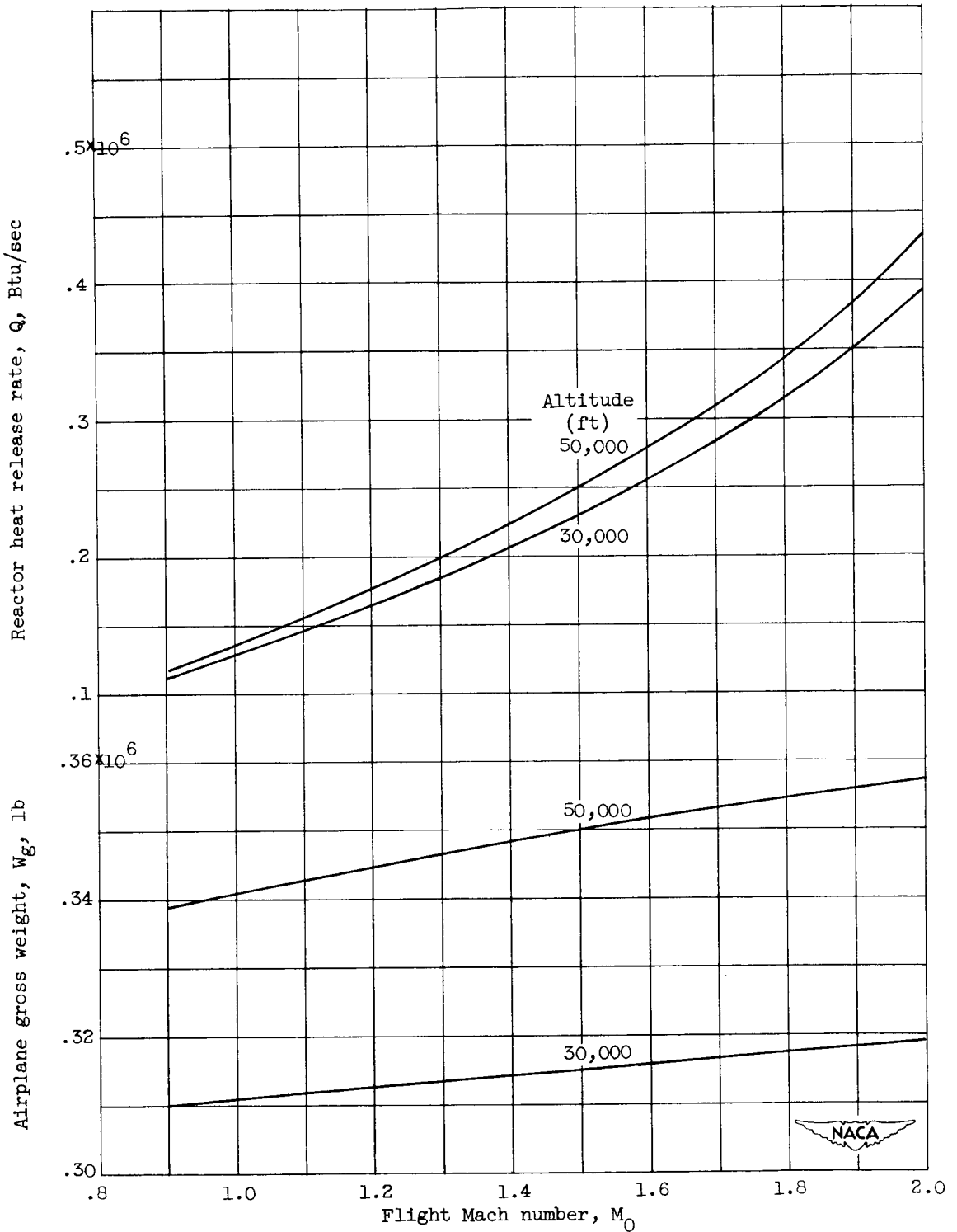


Figure 17. - Effect of flight Mach number on airplane gross weight and reactor heat release. T_w , 2400° R; T_3 , 2000° R; P_2/P_1 , 5.0; optimum M_2' ; W_s/W_g , 0.35; W_K , 190,000 pounds.

DECLASSIFIED

CONFIDENTIAL

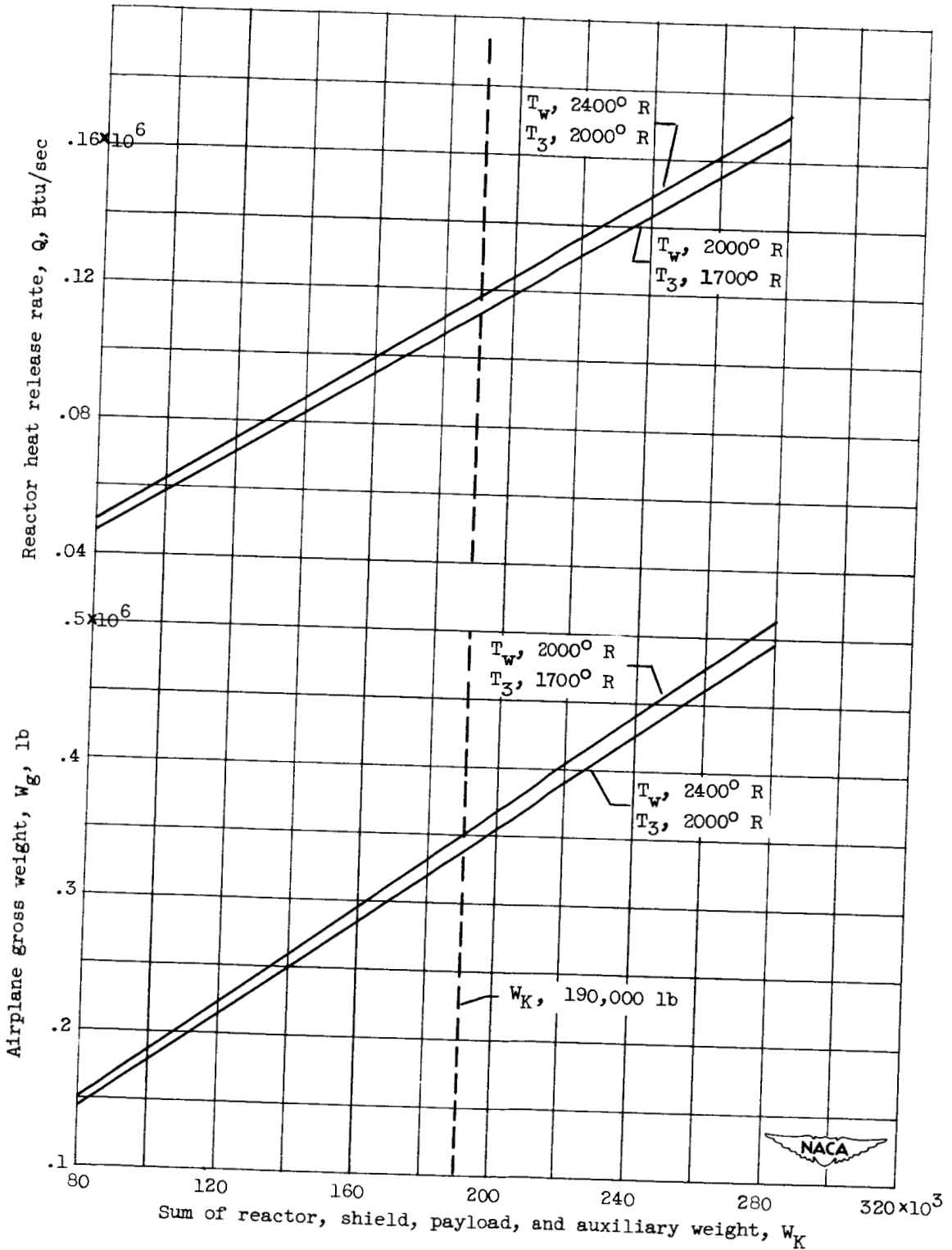


Figure 18. - Effect of the sum of reactor, shield, payload, and auxiliary weight on airplane gross weight and reactor heat release rate. Optimum P_2/P_1 ; optimum M_2' ; altitude, 50,000 feet; flight Mach number 0.9; W_s/W_g , 0.35.

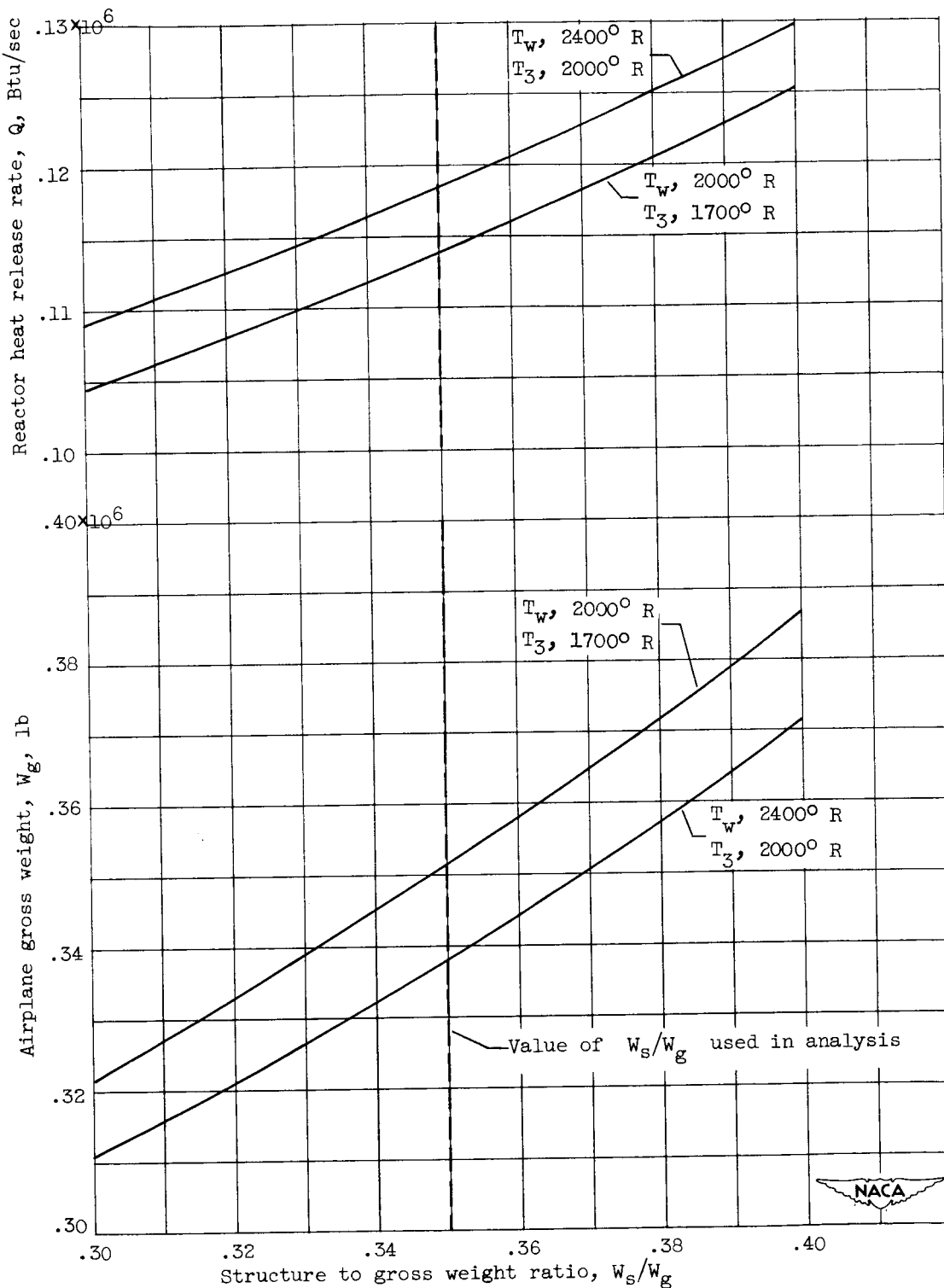
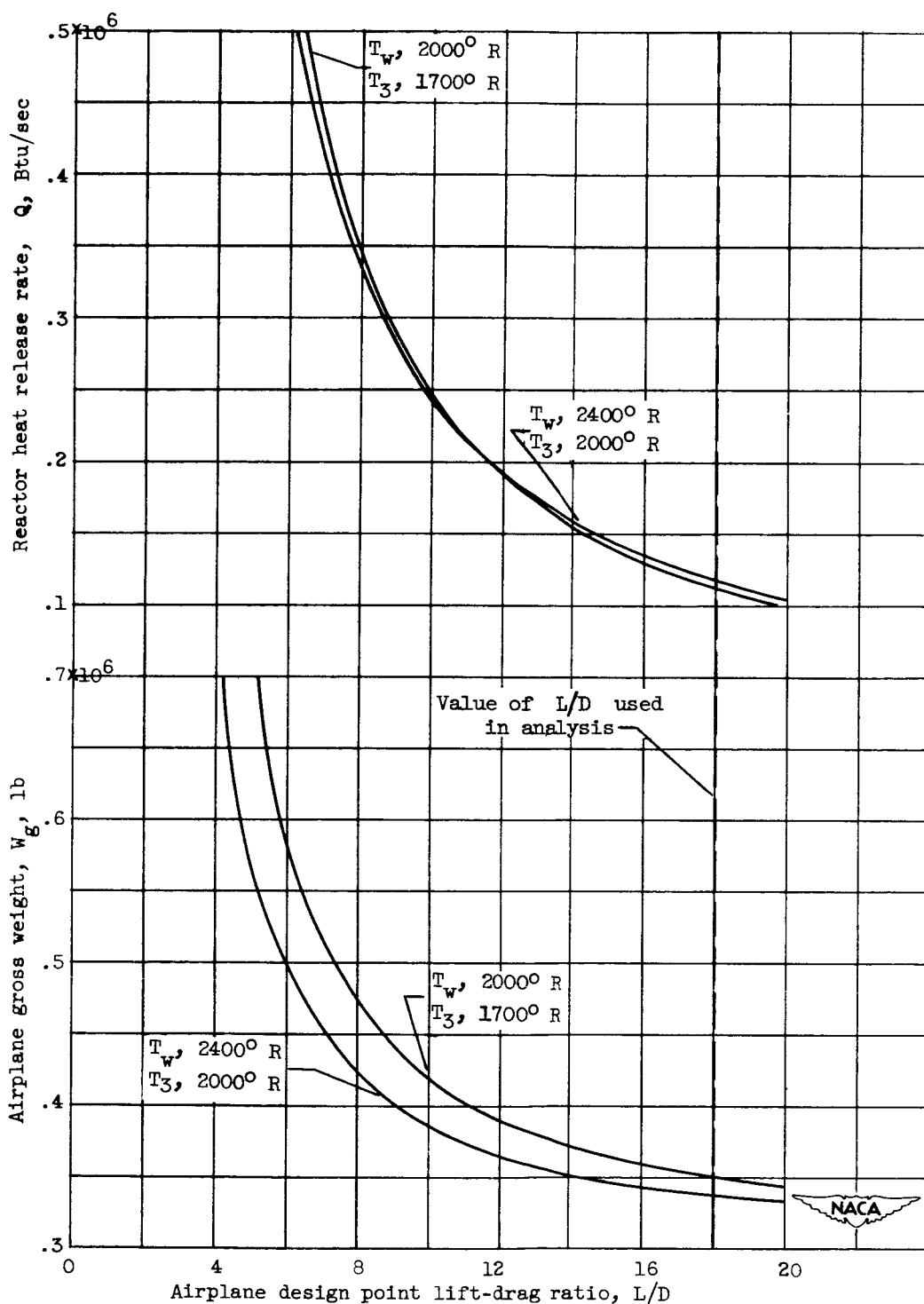
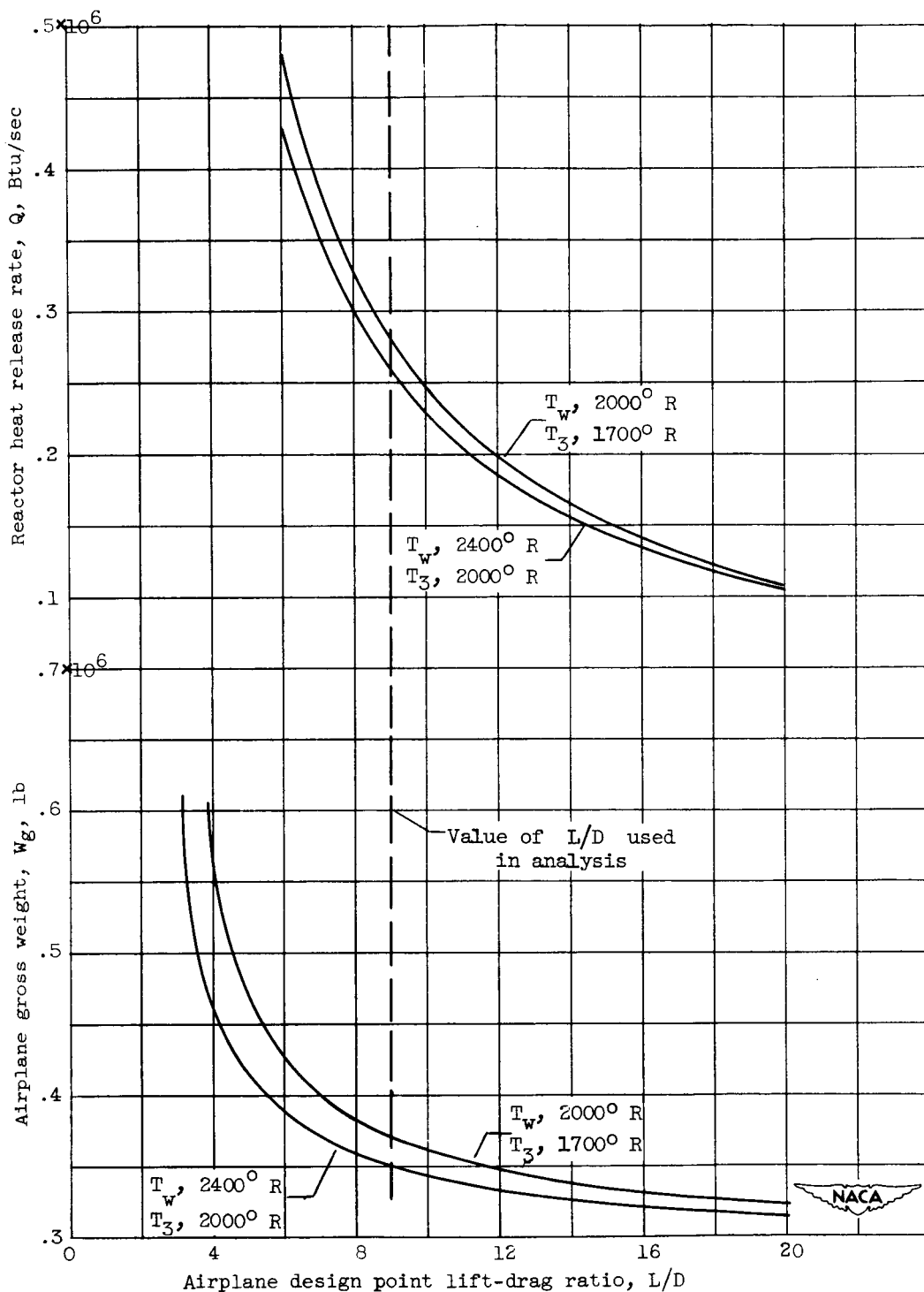


Figure 19. - Effect of structure to gross weight ratio on airplane gross weight and reactor heat release rate. Optimum P_2/P_1 ; optimum M_2' ; altitude, 50,000 feet; flight Mach number, 0.9; W_K , 190,000 pounds.



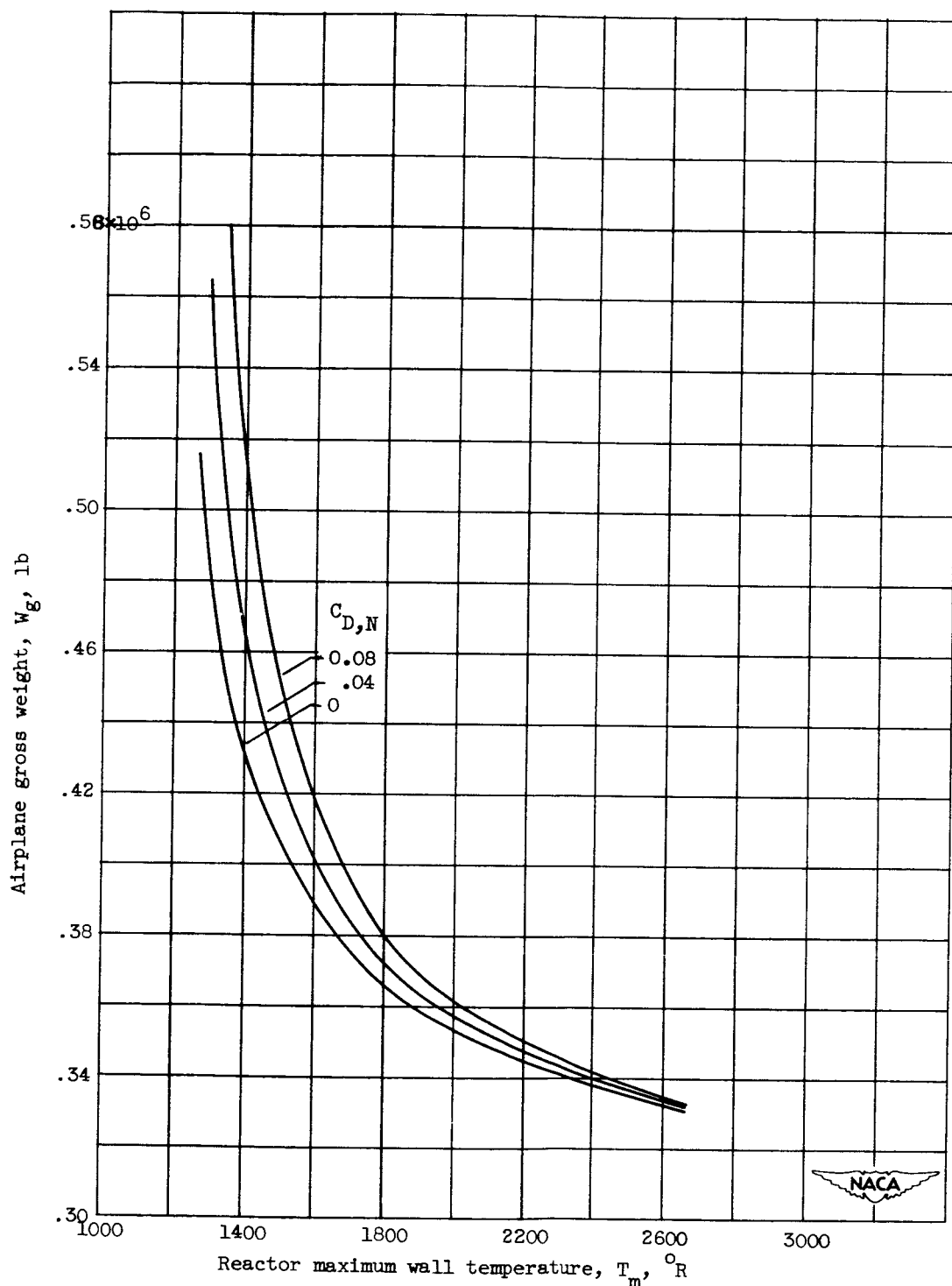
(a) Altitude, 50,000 feet; flight Mach number, 0.9.

Figure 20. - Effect of airplane design point lift-drag ratio on gross weight and reactor heat release rate. Optimum P_2/P_1 ; optimum, M_2' ; W_s/W_g , 0.35; W_K , 190,000 pounds.



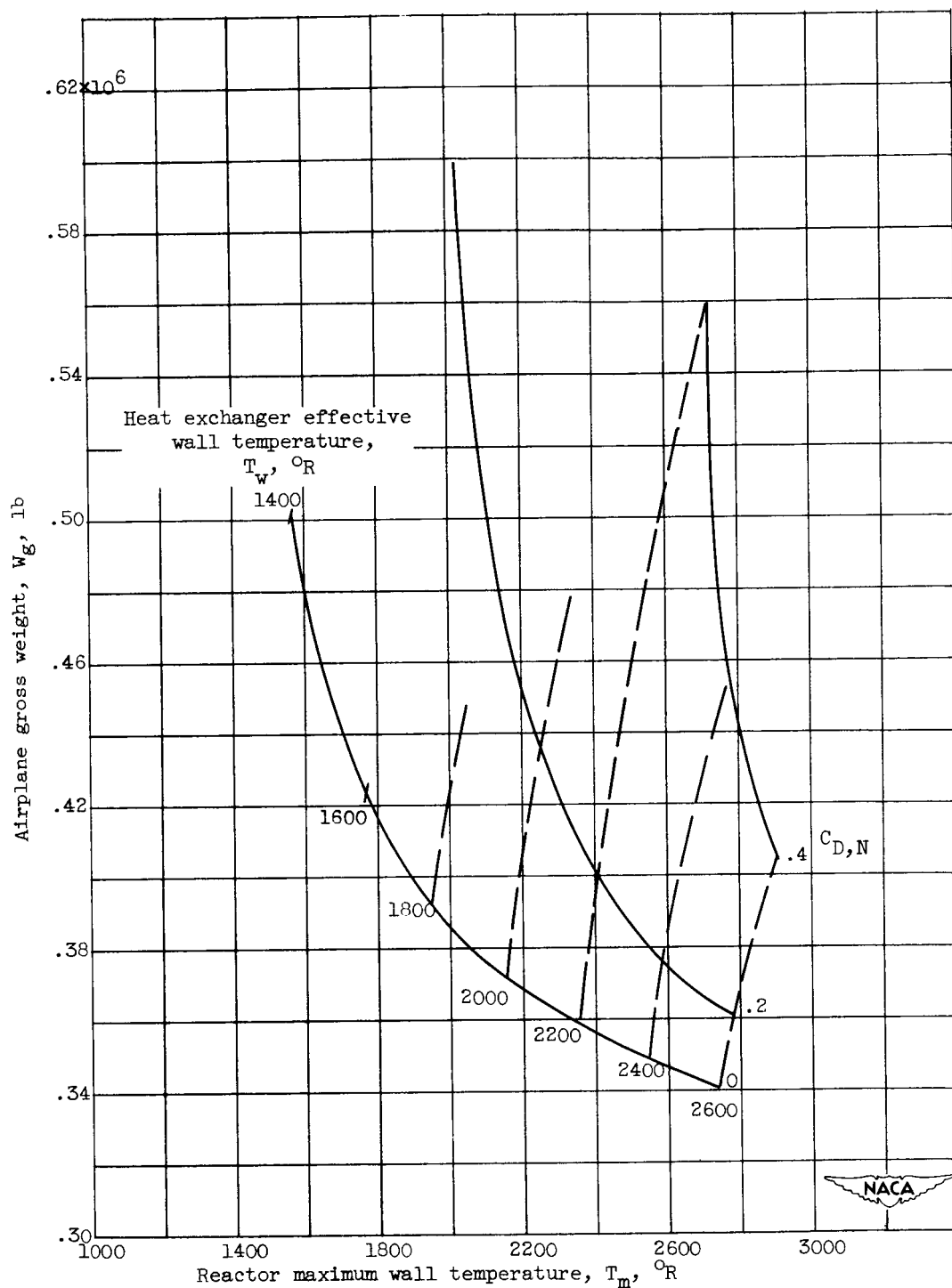
(b) Altitude, 50,000 feet; flight Mach number, 1.5.

Figure 20. - Concluded. Effect of airplane design point lift-drag ratio on gross weight and reactor heat release rate. Optimum P_2/P_1 ; optimum, M_2' ; W_s/W_g , 0.35; W_K , 190,000 pounds.



(a) Altitude, 50,000 feet; flight Mach number, 0.9.

Figure 21. - Effect of nacelle drag on airplane gross weight as a function of reactor maximum wall temperature. Optimum P_2/P_1 ; optimum M_2' ; optimum T_3 ; W_s/W_g , 0.35; W_K , 190,000 pounds.



(b) Altitude, 50,000 feet; flight Mach number, 1.5.

Figure 21. - Concluded. Effect of nacelle drag on airplane gross weight as a function of reactor maximum wall temperature. Optimum P_2/P_1 ; optimum M_2' ; optimum T_3 ; W_s/W_g , 0.35; W_K , 190,000 pounds.

DECLASSIFIED

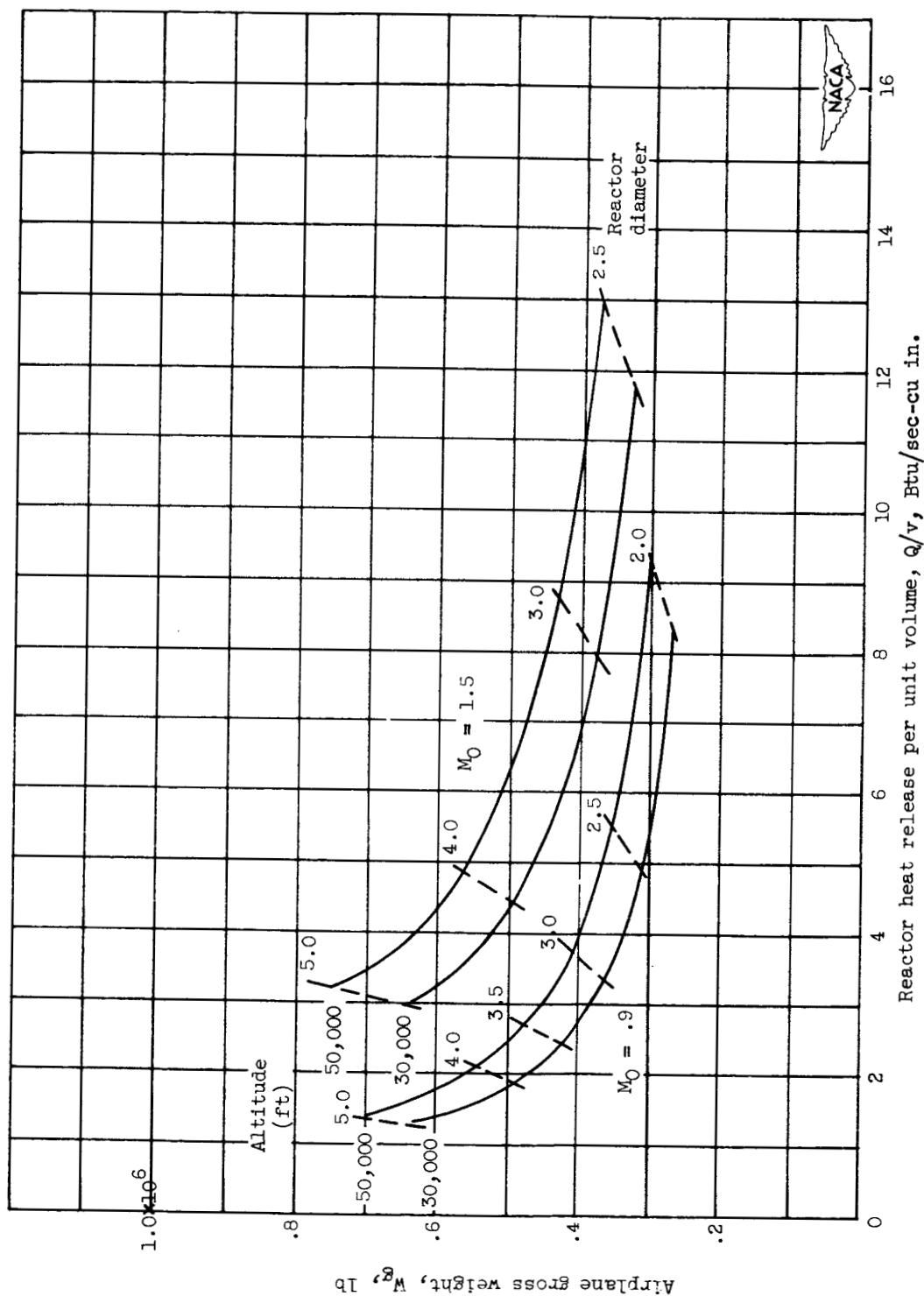


Figure 22. - Effect of reactor diameter upon airplane gross weight and reactor unit heat release. T_w , 2000 OR; T_3 , 1700 OR; optimum, P_2/P_1 ; optimum, M_2 ; W_g/W_g , 0.35; W_K , 190,000 pounds; reactor length-diameter ratio, 1.0.

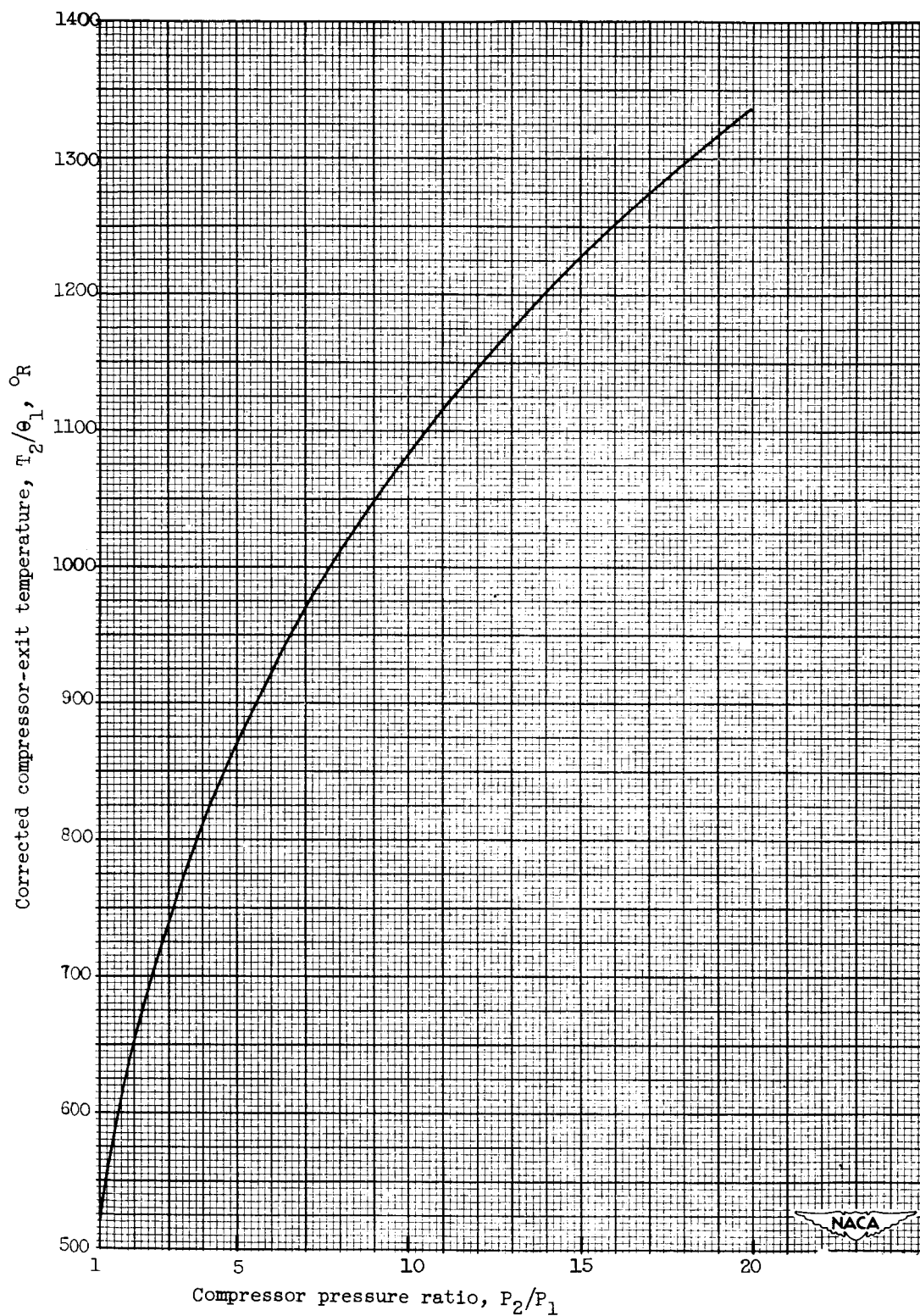


Figure 23. - Corrected compressor-outlet temperature against compressor pressure ratio. $\eta_{c,\infty} 0.88$.

~~CONFIDENTIAL~~

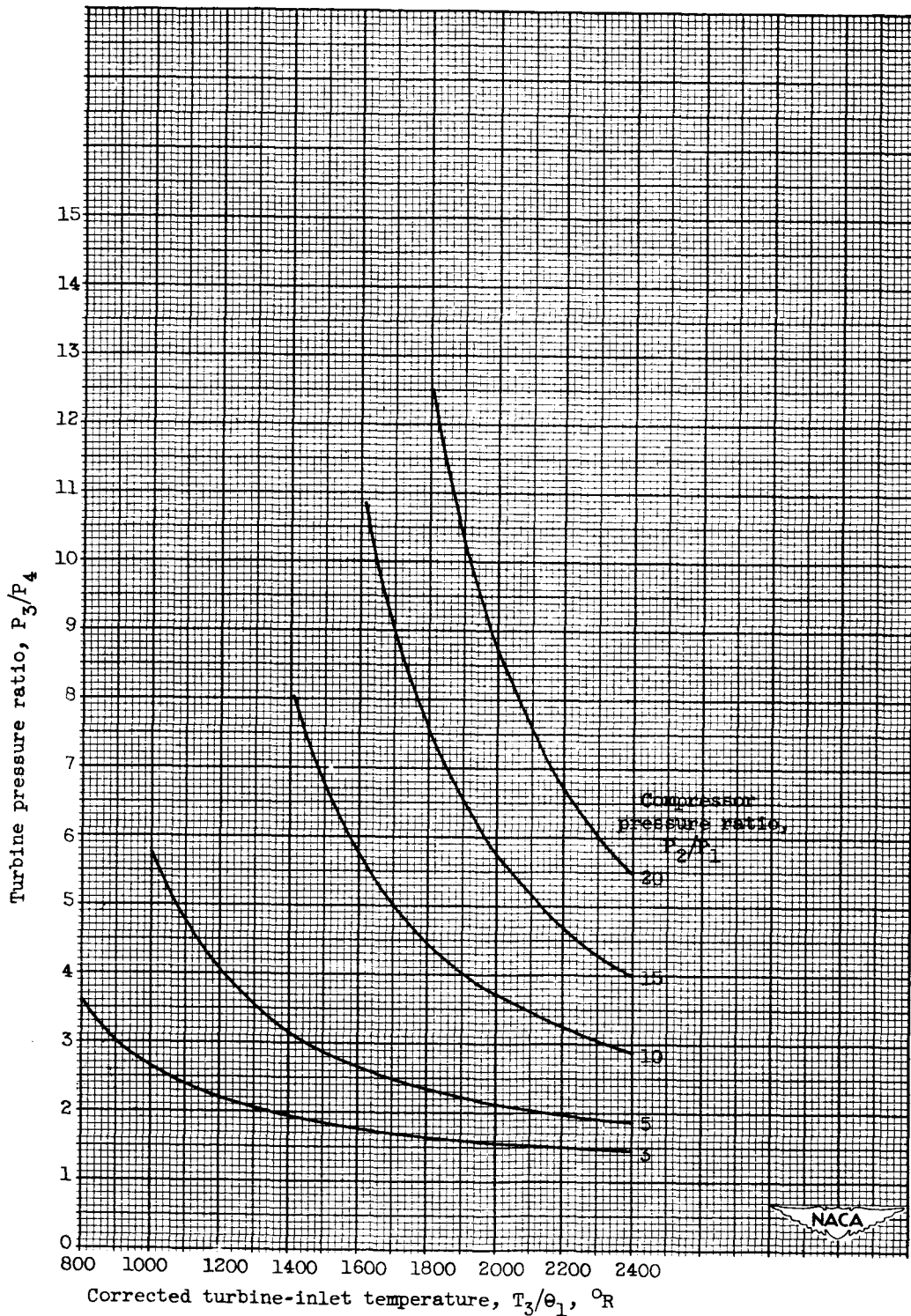


Figure 24. - Turbine pressure ratio against corrected turbine-inlet temperature for a range of compressor pressure ratios. $\eta_{c, \infty}$, 0.88; η_t , 0.90.

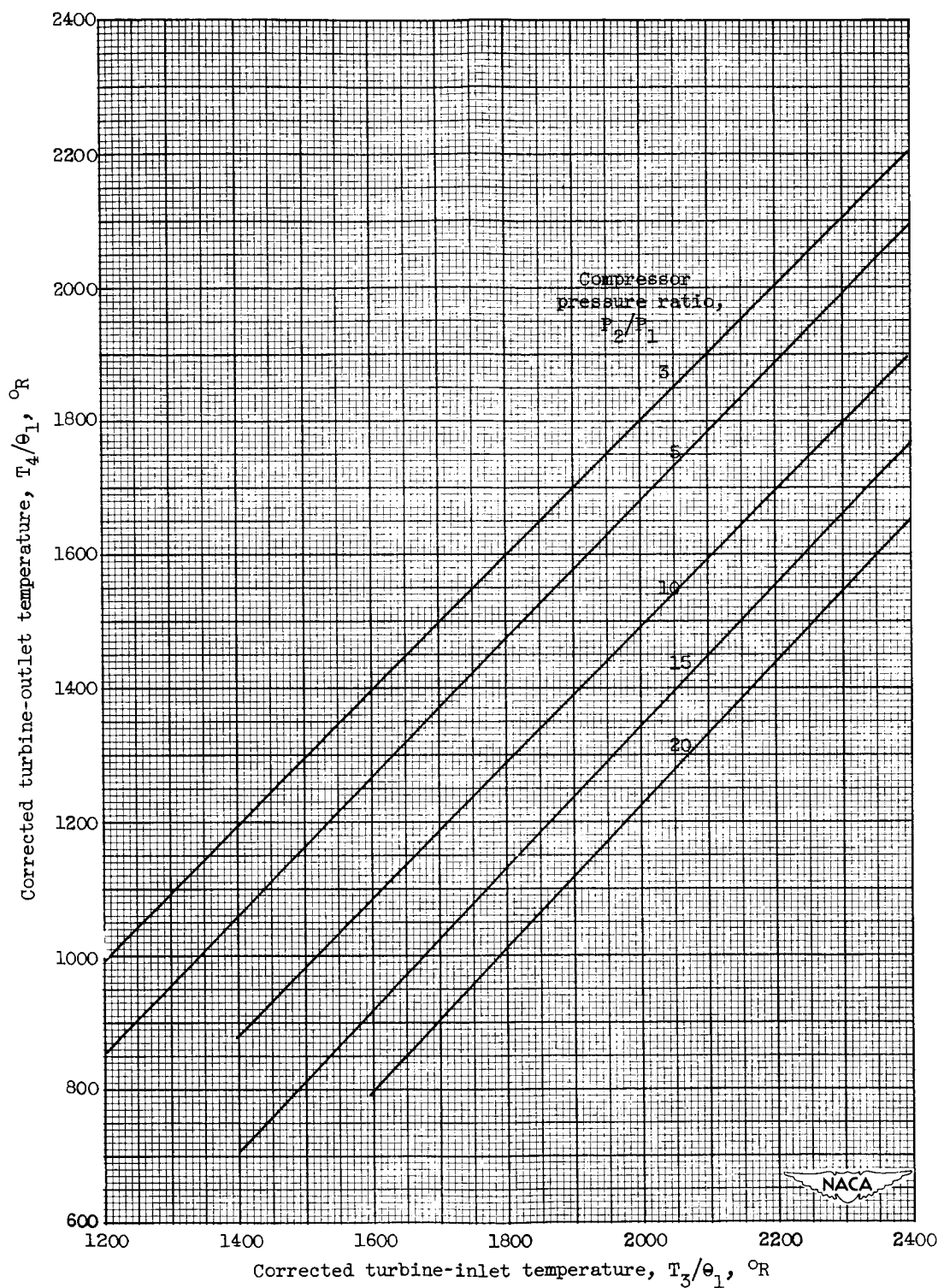
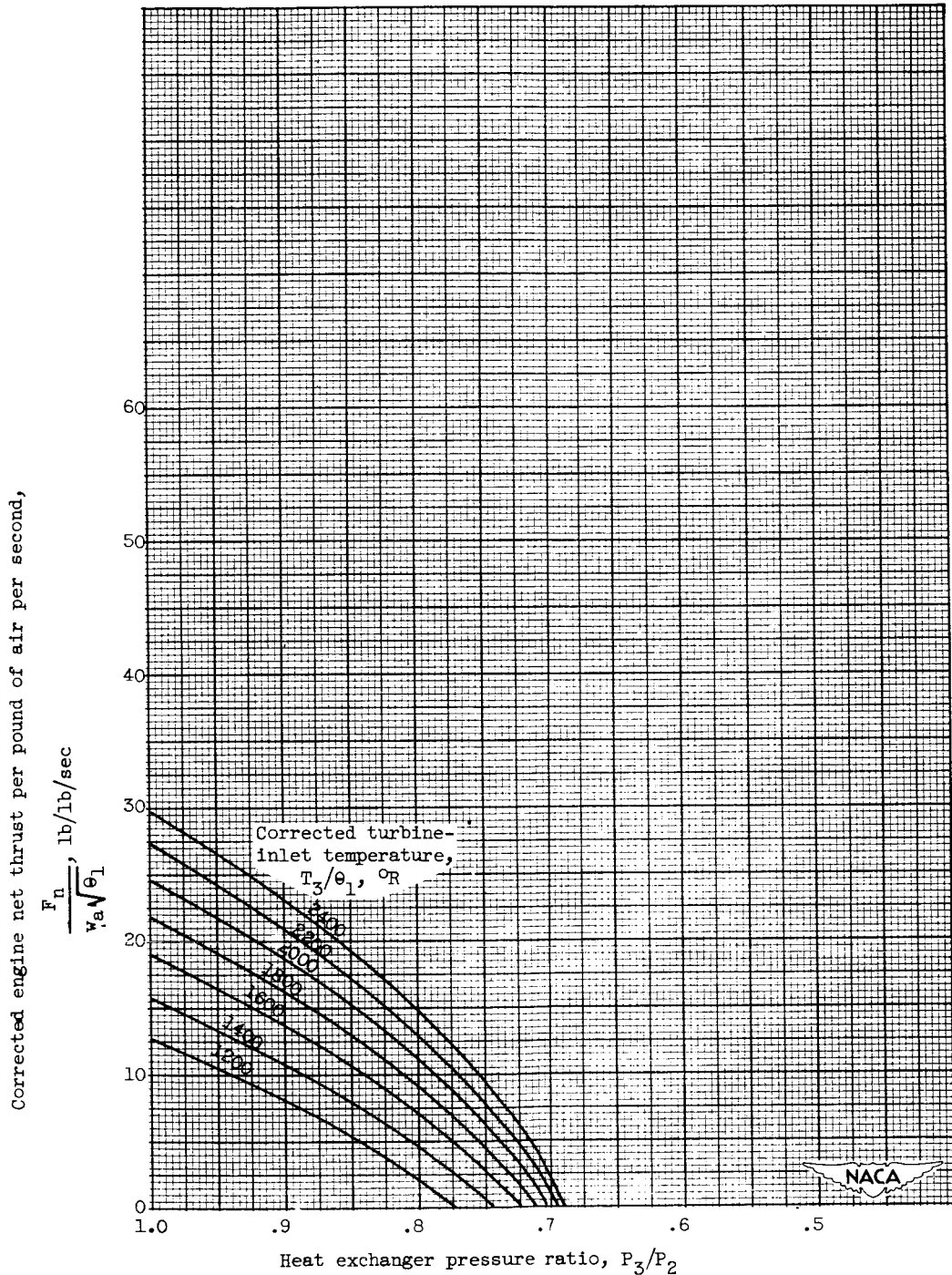


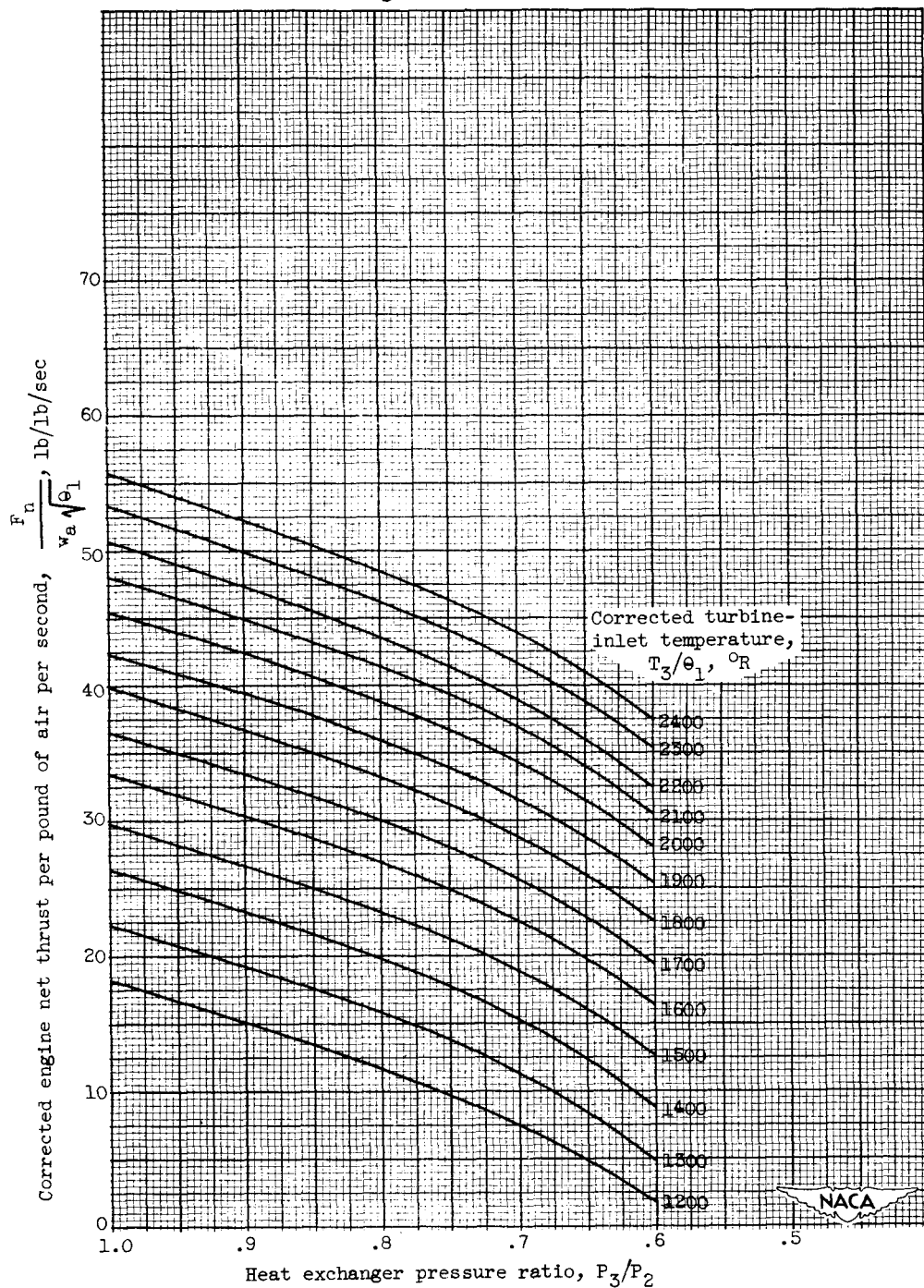
Figure 25. - Corrected turbine-outlet temperature against corrected turbine-inlet temperature for a range of compressor pressure ratios. $\eta_{c,\infty}$, 0.88; η_t , 0.90.



(a) Flight Mach number 0.9; compressor pressure ratio, 1.0.

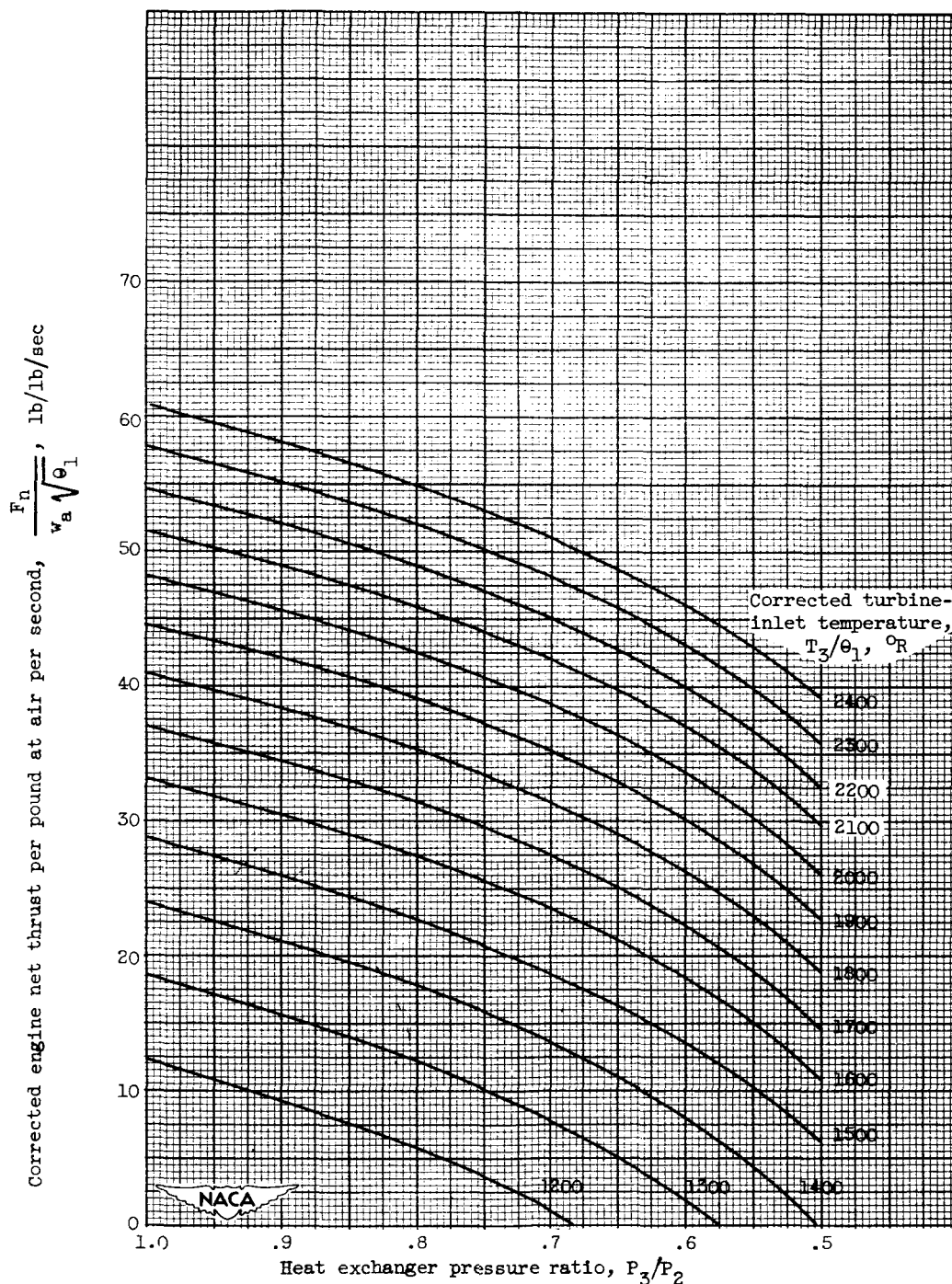
Figure 26. - Corrected engine net thrust per pound of air per second against heat exchanger pressure ratio for a range of corrected turbine-inlet temperatures. $\eta_{c,\infty}$, 0.88; η_t , 0.90; C_v , 0.97; fully expanding nozzle; $C_{D,N}$, 0.

037123a.1930



(b) Flight Mach number 0.9; compressor pressure ratio, 3.

Figure 26. - Continued. Corrected engine net thrust per pound of air per second against heat exchanger pressure ratio for a range of corrected turbine-inlet temperatures. $\eta_{c,\infty}$, 0.88; η_t , 0.90; C_v , 0.97; fully expanding nozzle; $C_{D,N}$, 0.

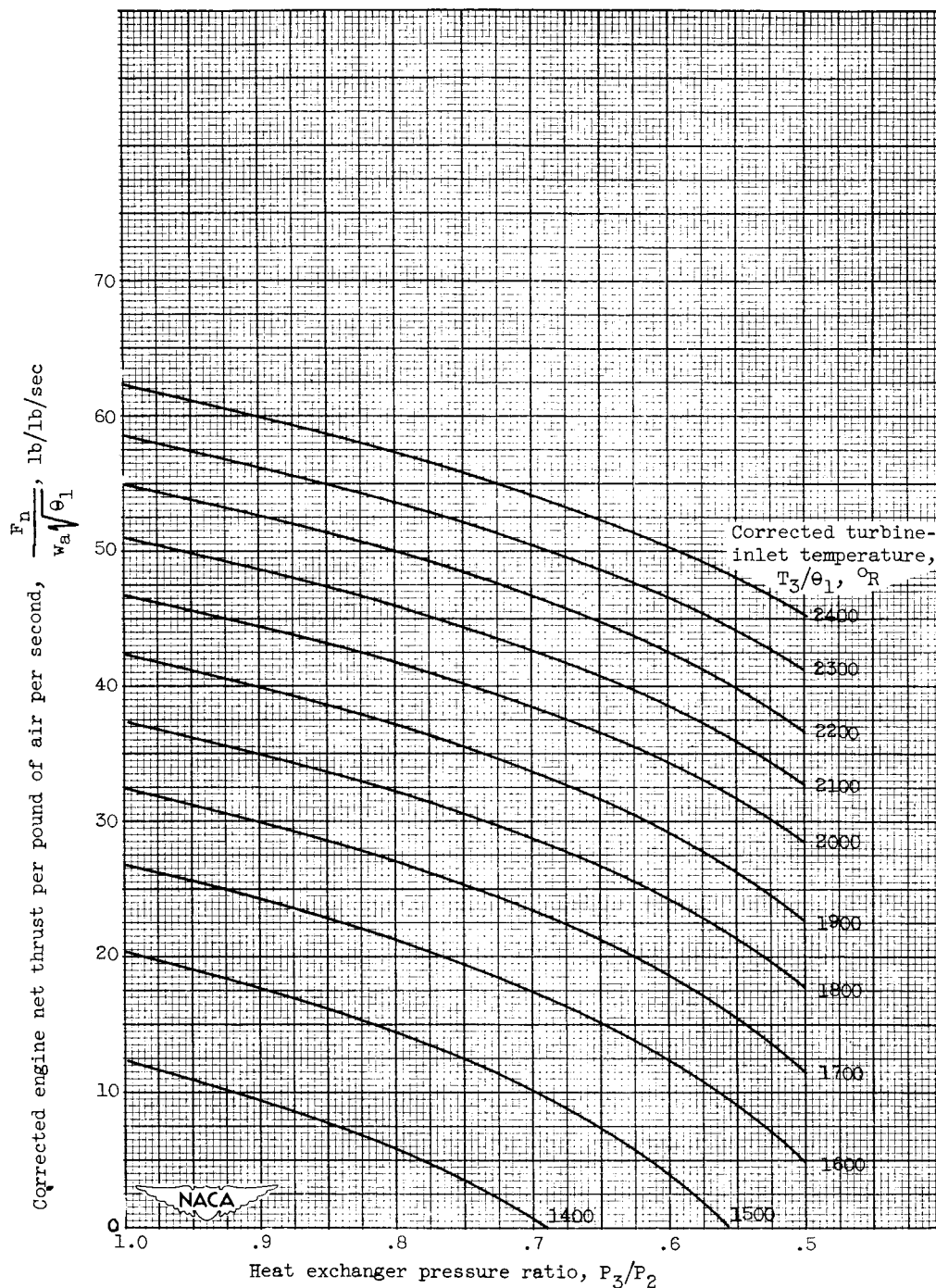


(c) Flight Mach number 0.9; compressor pressure ratio, 5.

Figure 26. - Continued. Corrected engine net thrust per pound of air per second against heat exchanger pressure ratio for a range of corrected turbine-inlet temperatures. $\eta_{c,\infty}$, 0.88; η_t , 0.90; C_v , 0.97; fully expanding nozzle, $C_{D,N}$, 0.

0371224 1030

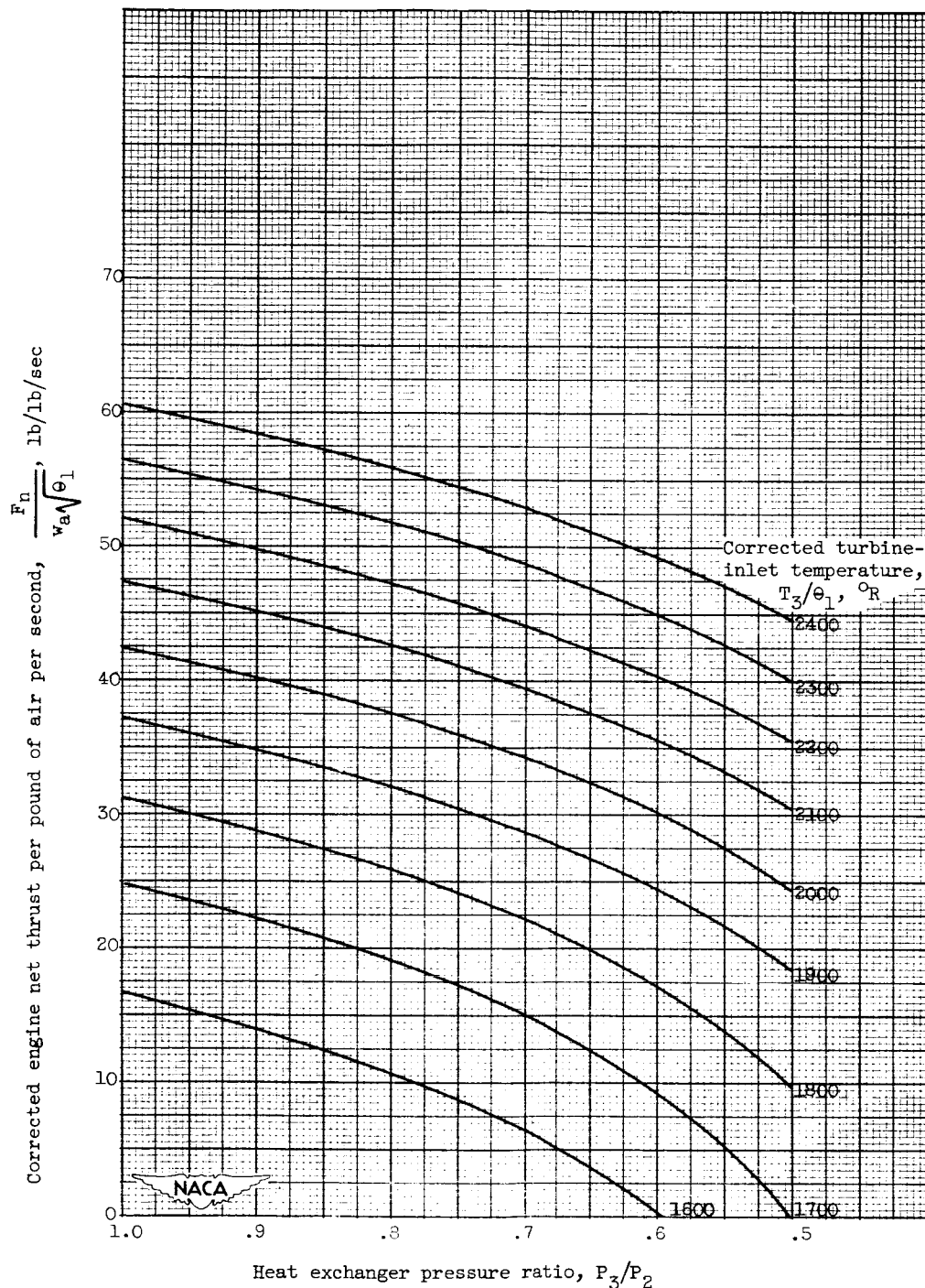
CONFIDENTIAL



(d) Flight Mach number, 0.9; compressor pressure ratio, 10.

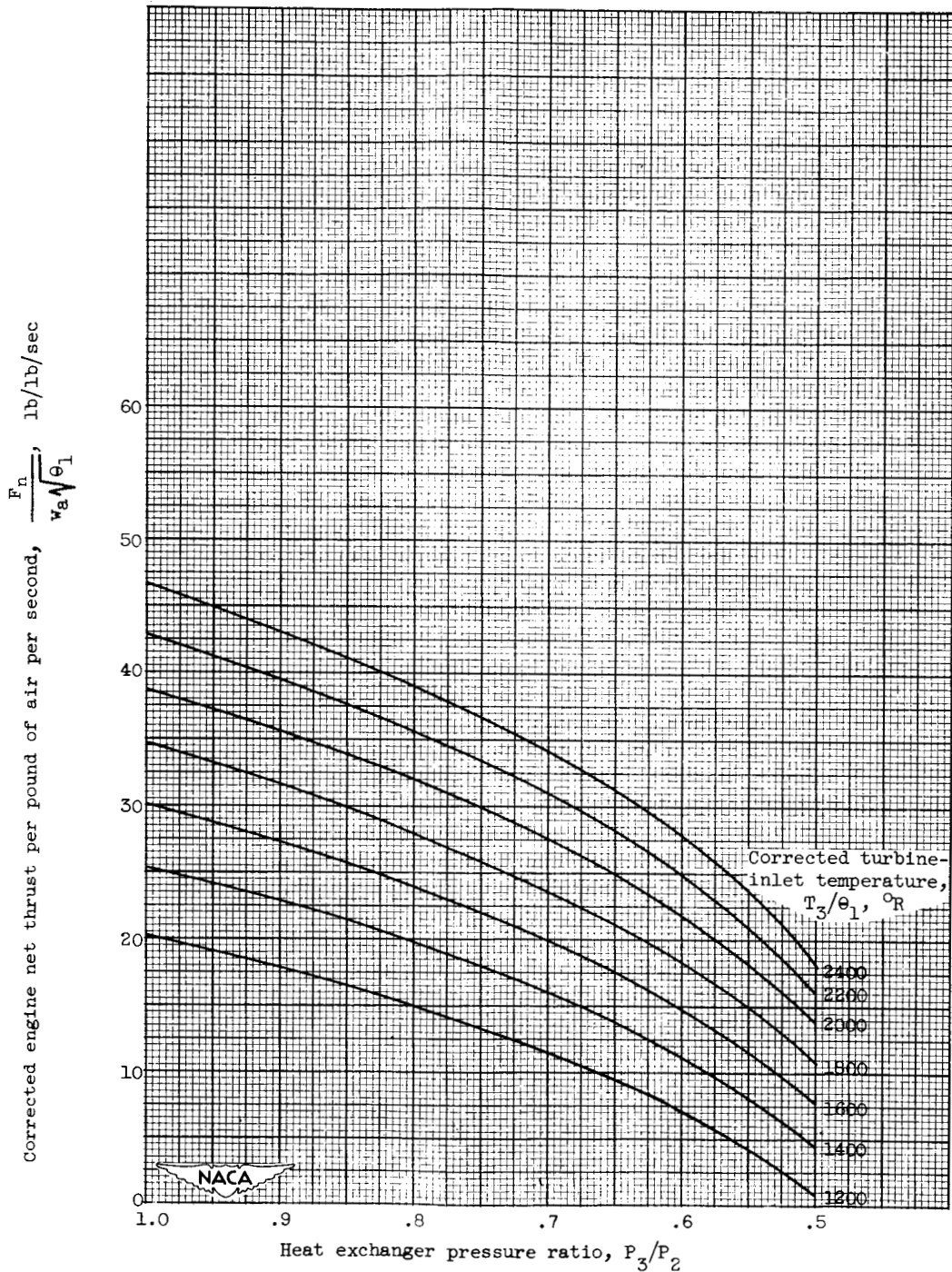
Figure 26. - Continued. Corrected engine net thrust per pound of air per second against heat exchanger pressure ratio for a range of corrected turbine-inlet temperatures. $\eta_{c,\infty}$, 0.88; η_t , 0.90; C_v , 0.97; fully expanding nozzle; $C_{D,N}$, 0.

CONFIDENTIAL



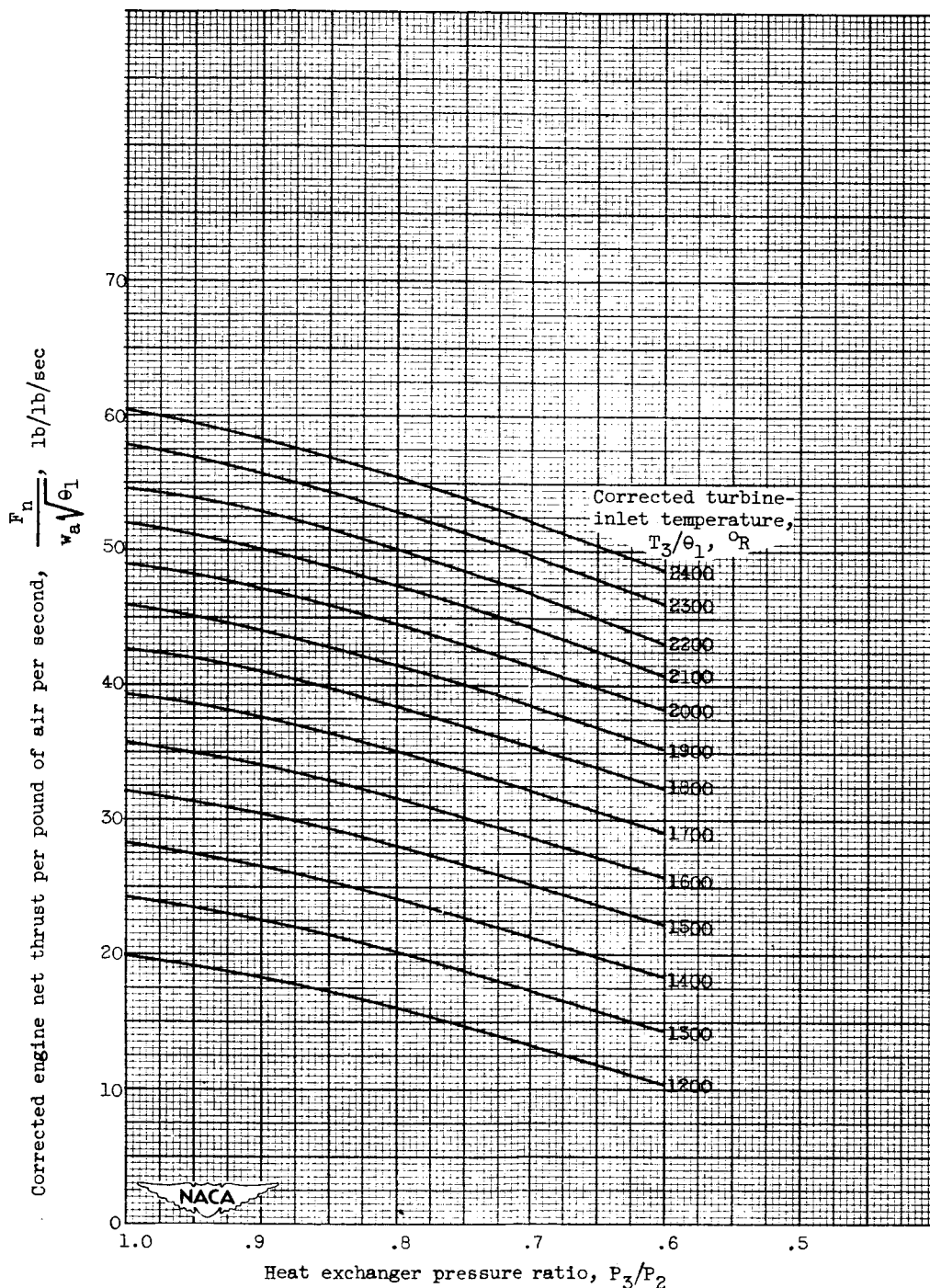
(e) Flight Mach number, 0.9; compressor pressure ratio, 15.

Figure 26. - Continued. Corrected engine net thrust per pound of air per second against heat exchanger pressure ratio for a range of corrected turbine-inlet temperatures. $\eta_{c,a}$, 0.88; η_t , 0.90; C_v , 0.97; fully expanding nozzle; $C_{D,N}$, 0.



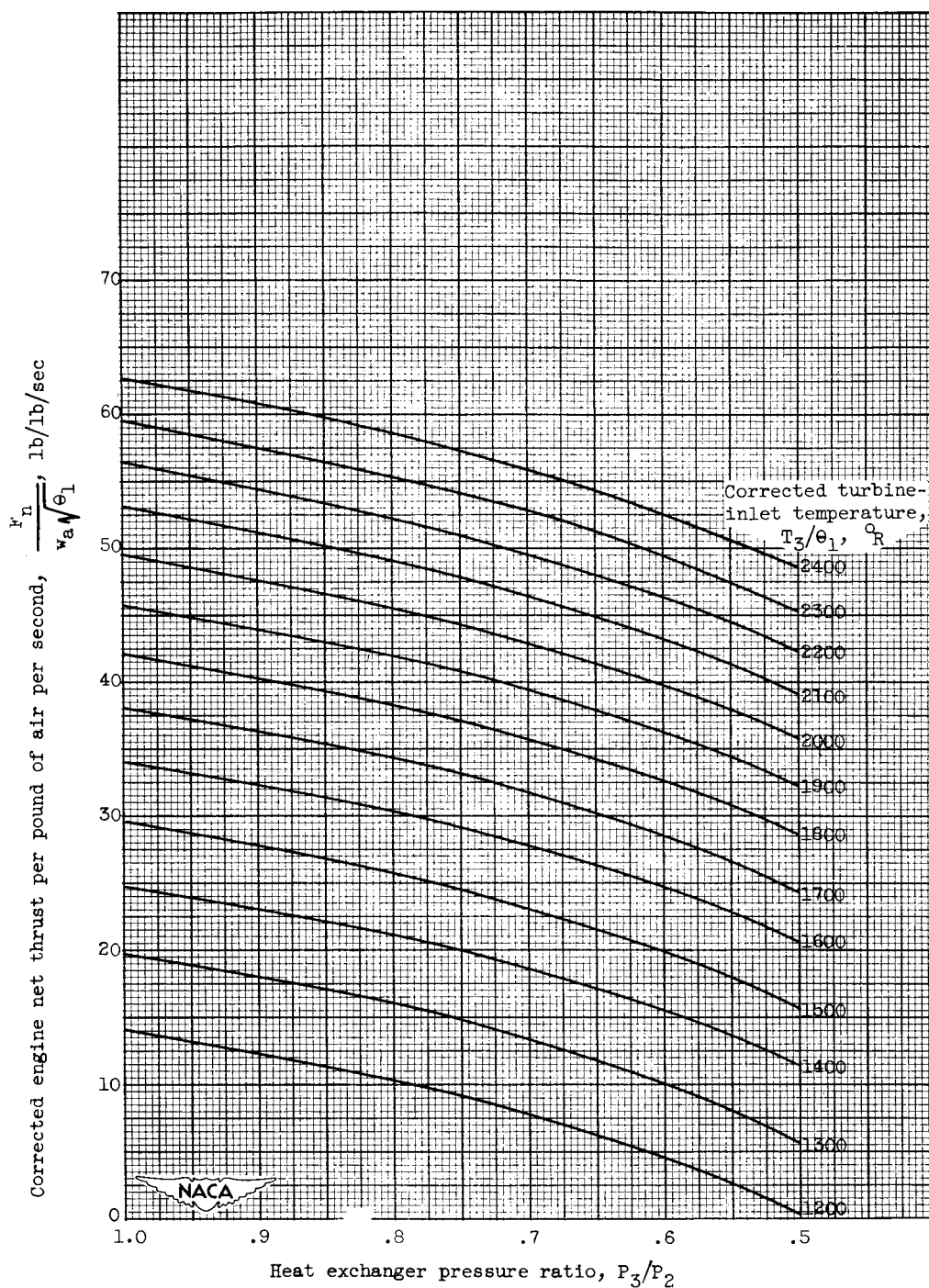
(f) Flight Mach number 1.5; compressor pressure ratio, 1.

Figure 26. - Continued. Corrected engine net thrust per pound of air per second against heat exchanger pressure ratio for a range of corrected turbine-inlet temperatures. $\eta_{c,\infty}$, 0.88; η_t , 0.90; C_v , 0.97; fully expanding nozzle; $C_{D,N}$, 0.



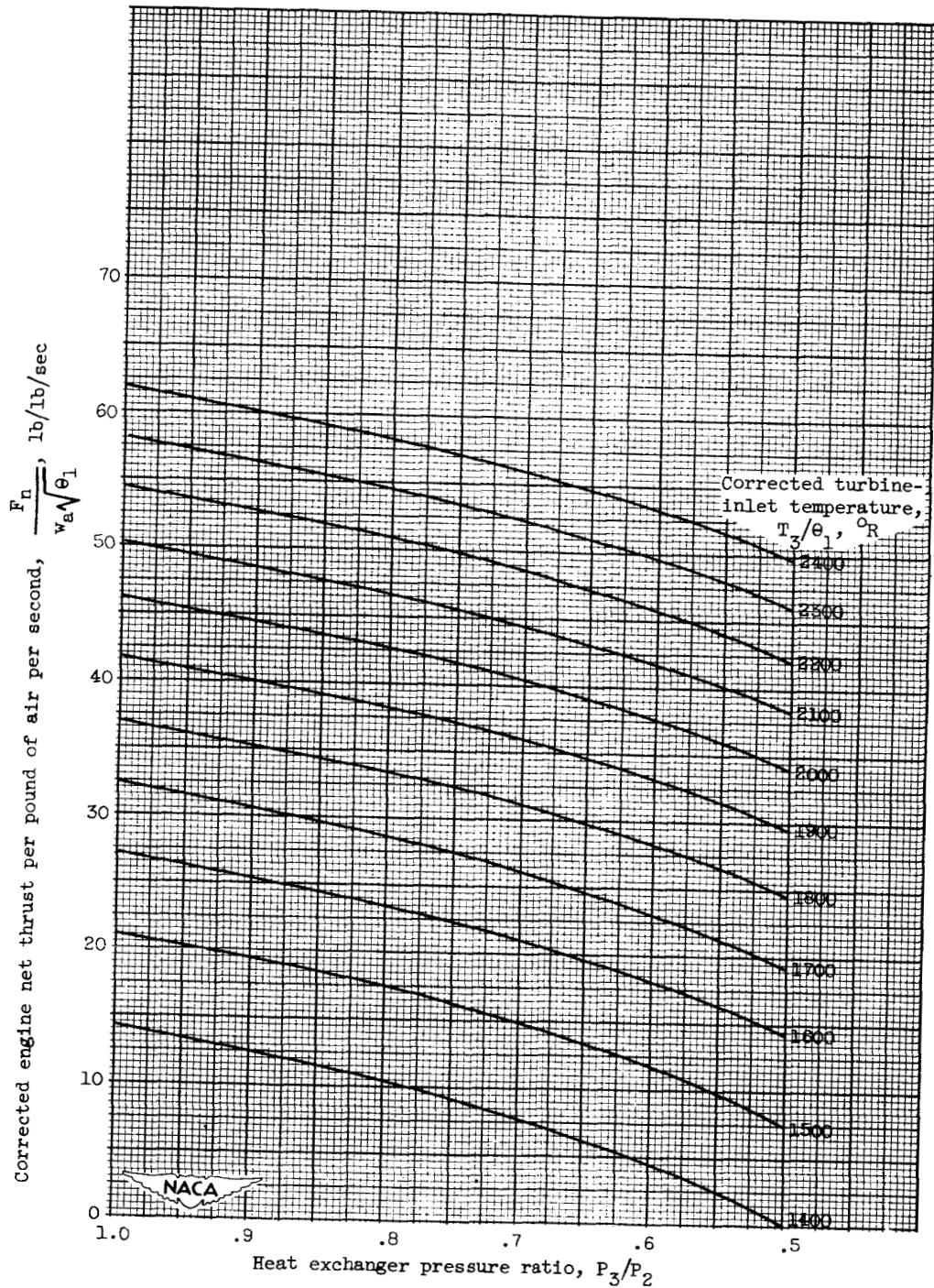
(g) Flight Mach number 1.5; compressor pressure ratio, 3.

Figure 26. - Continued. Corrected engine net thrust per pound of air per second against heat exchanger pressure ratio for a range of corrected turbine-inlet temperatures. $\eta_{c,\infty}$, 0.88; η_t , 0.90; C_v , 0.97; fully expanding nozzle; $C_{D,N}$, 0.



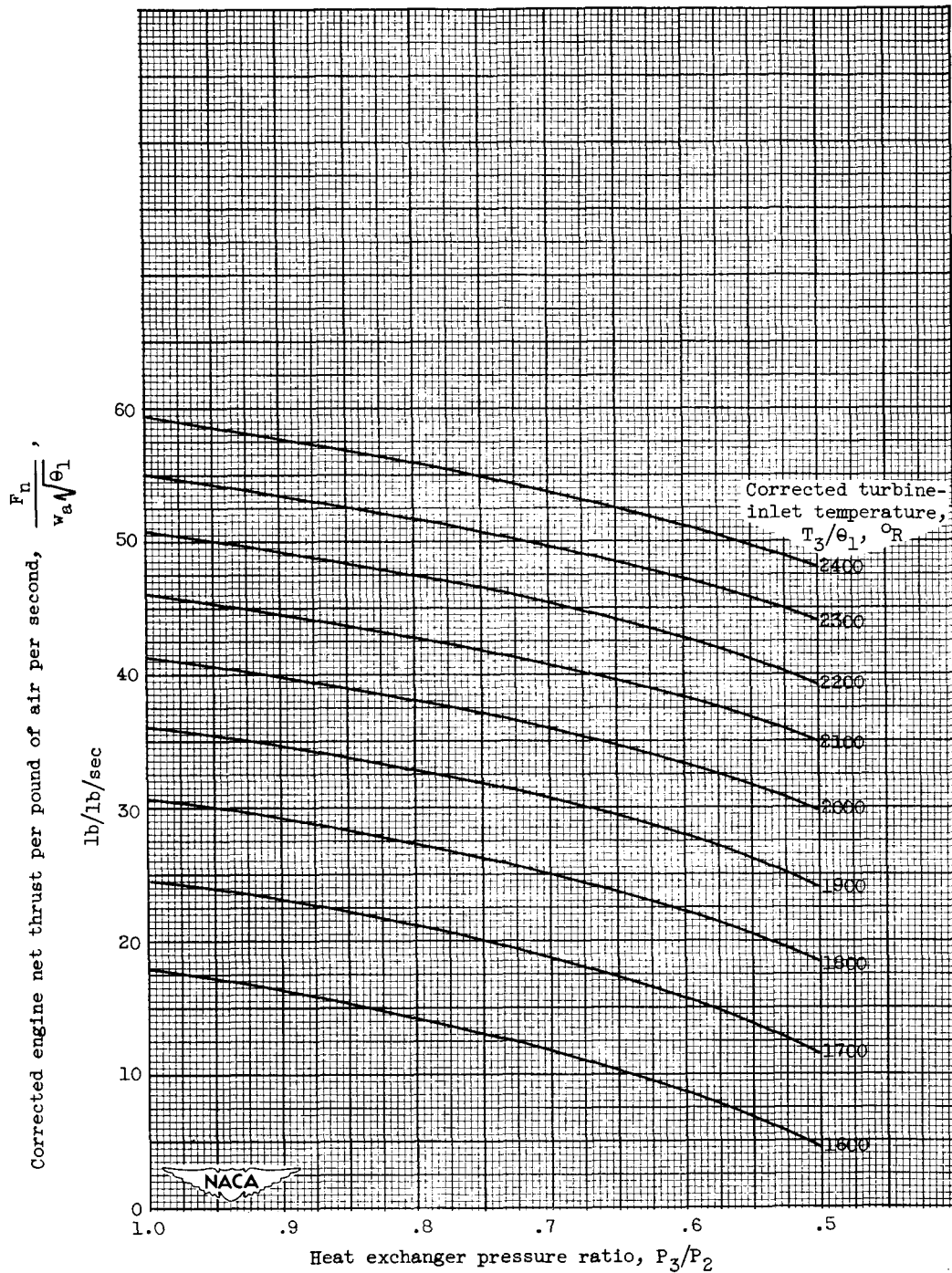
(h) Flight Mach number 1.5; compressor pressure ratio, 5.

Figure 26. - Continued. Corrected engine net thrust per pound of air per second against heat exchanger pressure ratio for a range of corrected turbine-inlet temperatures. $\eta_{c,\alpha}$, 0.88; η_t , 0.90; C_v , 0.97; fully expanding nozzle; $C_{D,N}$, 0.



(i) Flight Mach number, 1.5; compressor pressure ratio, 10.

Figure 26. - Continued. Corrected engine net thrust per pound of air per second against heat exchanger pressure ratio for a range of corrected turbine-inlet temperatures. $\eta_{c,a}$, 0.88; η_t , 0.90; C_v , 0.97; fully expanding nozzle; $C_{D,N}$, 0.



(j) Flight Mach number, 1.5; compressor pressure ratio, 15.

Figure 26. - Concluded. Corrected engine net thrust per pound of air per second against heat exchanger pressure ratio for a range of corrected turbine-inlet temperatures. $\eta_{c,\infty}$, 0.88; η_t , 0.90; C_v , 0.97; fully expanding nozzle; $C_{D,N}$, 0.